Development of Rhodium-Catalyzed Stitching Polymerization for the Synthesis of Ethylene- or Silicon-Bridged π-Conjugated Polymers

Sho Ikeda

March 2022

Development of Rhodium-Catalyzed Stitching Polymerization for the Synthesis of Ethylene- or Silicon-Bridged π-Conjugated Polymers

A dissertation submitted to
THE GRADUATE SCHOOL OF ENGINEERING SCIENCE
OSAKA UNIVERSITY
in partial fulfillment of the requirements for the degree of
DOCTOR OF PHILOSOPHY IN ENGINEERING

by

Sho Ikeda

March 2022

Abstract

Polyacetylenes obtained by transition metal-catalyzed polymerization of substituted acetylenes are potentially useful class of π-conjugated polymers as functional materials. In particular, rhodium-catalyzed polymerizations have been widely explored to effectively catalyze polymerization of terminal alkyne monomers. To date, a lot of well-defined rhodium-catalysts have been developed that allow for living and stereo-controlled alkyne polymerization. On the other hand, the reported polymerization patterns were limited to simple coordination insertion of monoynes or cyclopolymerization of diynes, which leads to limitation of the accessible structures.

Bridged π-conjugated polymers have received much attention as potential candidates for optoelectronic materials owing to the restriction of C–C single bond rotation by the bridged moiety of the π-conjugated unit. In general, these polymers are synthesized by polycondensation of the corresponding bridged π-conjugated monomers. This method is powerful and reliable if applicable, but accessible polymer structures are currently still limited to those consisting of repeating units that can be prepared as stable monomers beforehand.

In this context, the author developed a novel mode of polymerization, rhodium-catalyzed stitching polymerization, for the synthesis of π-conjugated polymers with bridged repeating units from non-conjugated monomers containing both terminal alkyne and internal alkyne moieties. This polymerization method allowed for the synthesis of polymers consisting of a repeating unit that is difficult to prepare as a stable monomer.

Chapter 1 provides an overview of the pioneering works and the recent development on rhodium-catalyzed polymerizations of alkyne monomers and the synthesis of bridged π-conjugated polymers.

Chapter 2 describes the development of a rhodium-catalyzed stitching polymerization of non-conjugated 1,5-hexadiynes containing both terminal and internal alkynes as monomers for the synthesis of ethylene-bridged π-conjugated polymers as realization of the concept. It was found that the polymerization proceeded smoothly with high degree of stitching efficiency. Investigation on the optical properties of the obtained polymers revealed the effective extension of π-conjugation by introduction of rigid bridged structures.

To expand the scope of this mode of polymerization, Chapter 3 describes a synthesis of silicon-bridged π-conjugated polymers by the rhodium-catalyzed stitching polymerization of alkynylsilylacetylenes possessing terminal and internal alkynes that are connected by a silicon atom. This is the first successful chain-growth polymerization of heteroatom-substituted alkynes under rhodium catalysis and it was found that the diyne structure as monomers was important for the polymerization of silylacetylenes. The solubility of the polymers could be tuned by introduction of appropriate functional groups on the silicon atoms.

Contents

Chapter 1

General Introduction

1.1 Metal-catalyzed polymerization of alkyne monomers

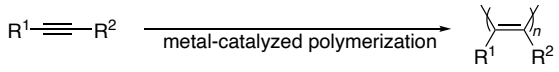

Scheme 1. Metal-catalyzed polymerization of alkyne monomers

Polyacetylenes,[1] possessing the structure composed of alternating double bonds and single bonds in the main chain, have been widely explored as functional materials with semiconductivity,[2] liquid crystallinity,[3] gas permeability,[4] helix-induced chirality[5] or fluorescent characters.[6] Since Natta *et al*. obtained insoluble polyacetylene by the reaction of acetylene in the presence of $AlEt_3$ and $Ti(OPr)_4$,[7a] and Shirakawa, MacDiarmid and Heerger *et al*. found that iodine-doped polyacetylene films showed high conductivity,[7b-7e] a lot of synthetic methods of polyacetylenes have been reported. To date, a large number of transition-metal catalysts including Ti,[8] Fe,[9] W,[10,11] Mo,[11,12] Ta,[13] Nb,[13g-i] Rh,[14] Pd,[15] Ru,[16] and Ni[17] are known to polymerize acetylenic monomers (Scheme 1). In the early studies, early transition-metal salts such as W, Mo, and Ta were intensively investigated as living polymerization catalysts of both internal alkynes[10d,12a] and terminal alkynes.[12b,12c,12d] Masuda and Katz proposed that these polymerizations proceed by the metathesis mechanism via metal carbenes (Scheme 2-(a)),[10a,10b,12f] but Maeda *et al.* recently revised the polymerization mechanism with WCl_6/Ph_4Sn[10e] or $TaCl_5/n Bu_4Sn$[13f] as insertion mechanism via a metal-carbon single bond instead of metathesis mechanism. On the other hand, rhodium complexes are often used to effectively catalyze

polymerization of terminal alkyne monomers and they exhibit high tolerance towards functional groups compared to early transition metal catalysts. To date, a lot of well-defined rhodium-catalysts have been developed that allow for living and stereo-controlled alkyne polymerization via a 2,1-insertion mechanism (Scheme 2-(b)). In this section, selected pioneering works and recent developments on rhodium-catalyzed polymerization of acetylenic monomers are described.

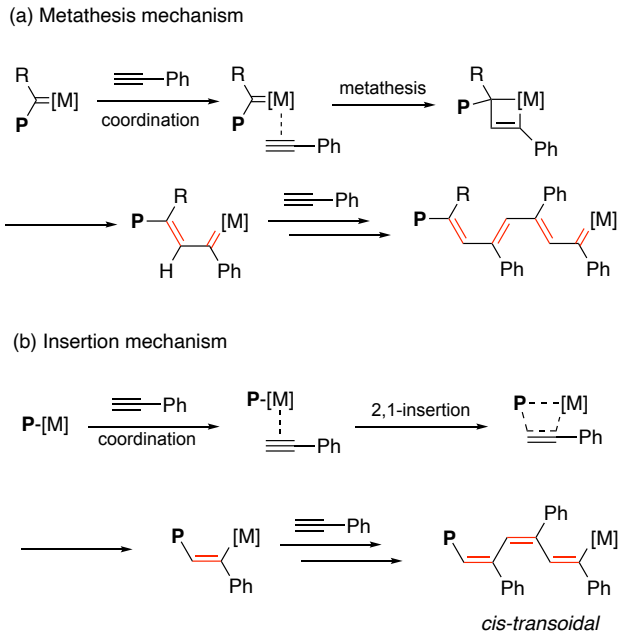

Scheme 2. Polymerization mechanisms of phenylacetylene

1.1.1 Rhodium-catalyzed polymerization of phenylacetylene

In 1969, Kern *et al.* reported the first rhodium-catalyzed polymerization of phenylacetylene by using $RhCl_3$-$LiBH_4$ or $RhCl(PPh_3)_3$ (Scheme 3).[18] However, the polymerization resulted in either a low yield or low molecular weight.

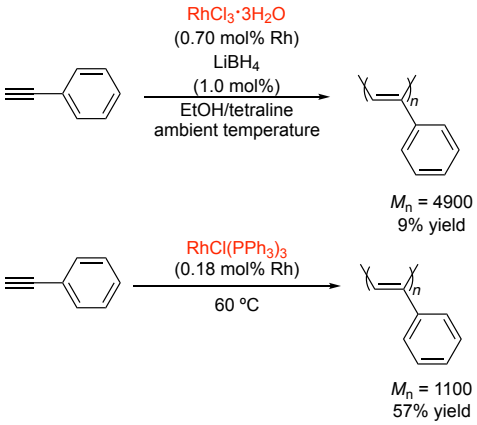

Scheme 3. Polymerization of phenylacetylene with $RhCl_3 \cdot 3H_2O$ or $RhCl(PPh_3)_3$

In 1986, Furlani *et al.* found that rhodium catalysts with diene ligands, such as $[Rh(cod)bipy]PF_6$, $[Rh(nbd)bipy]PF_6$, and $[RhCl(cod)]_2$, polymerized phenylacetylene effectively.[19] When polymerization was conducted using $[RhCl(cod)]_2$ in MeOH in a monomer to catalyst molar ratio of 273:1, highly *cis-transoidal* stereoregulated polyphenylacetylene with M_n of 100000 was produced as a yellow powder (Scheme 4).

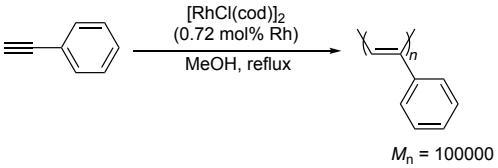

Scheme 4. Polymerization of phenylacetylene with a Rh(diene) catalyst

Subsequently, Tabata *et al*. investigated the effect of Et_3N as base in the polymerization of *m*-chlorophenylacetylene with $[RhCl(nbd)]_2$ in chloroform (Scheme 5-(a)).[20] It was observed that the number average molecular weights of the obtained polymers were decreased as a ratio of Et_3N to Rh-catalyst was increased. Furthermore, when the relationship between molecular weight and the amount of added monomer was investigated, molecular weights were almost constant regardless of the amount of added

monomers. These results indicated that Et_3N worked as a promoter for dissociation to [RhCl(nbd)-Et_3N] from $[RhCl(nbd)]_2$ and the monomeric species, not the dimer, initiated polymerization. The propagation rate would be much higher than the initiation rate in this polymerization (Scheme 5-(b)).

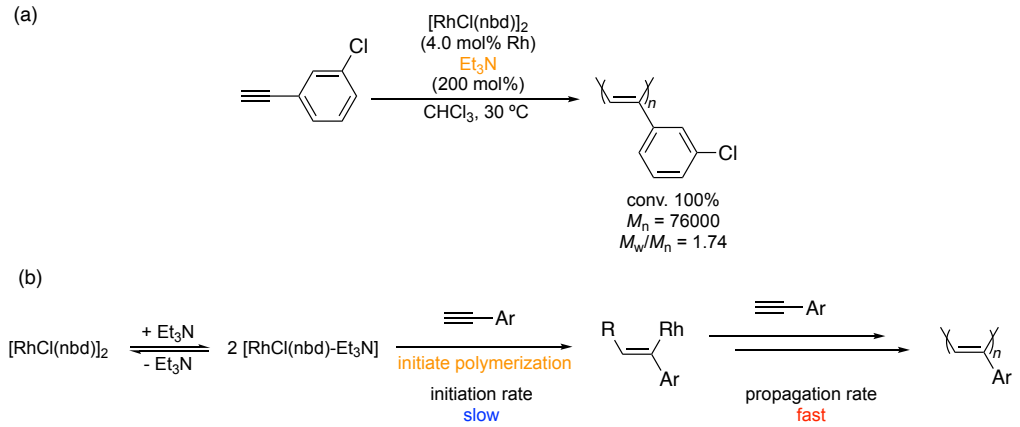

Scheme 5. (a) Polymerization of *m*-chlorophenylacetylene with $[RhCl(cod)]_2/Et_3N$ (b) The proposed effect of Et_3N in the polymerization of arylacetylene

In 1994, Noyori *et al*. reported the well-defined catalyst $[Rh(C{\equiv}CPh)(nbd)(PPh_3)_2]$, which was isolated by the reaction of $[RhCl(nbd)]_2$, PPh_3, and $LiC{\equiv}CPh$ in Et_2O, and this catalyst gave polyphenylacetylene with a very narrow molecular weight distribution.[21] Polymerization of phenylacetylene with this catalyst in the presence of 4-(dimethylamino)pyridine (DMAP) proceeded well in a living manner to give red-brown precipitates with an M_n of 14900 and M_w/M_n of 1.15 in a monomer to catalyst ratio of 50:1 (Scheme 6). In the absence of DMAP, the molecular weight distribution became higher to 1.31.

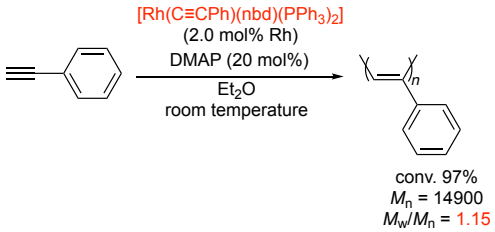

Scheme 6. Polymerization of phenylacetylene using [Rh(C≡CPh)(nbd)(PPh_3)$_2$] complex

The same group reported that the polymerization of phenylacetylene with [Rh(OCH_3)(nbd)]$_2$/PPh_3/DMAP in a ratio of 1:2:20 gave polyphenylacetylene with M_n of 6900 and M_w/M_n of 1.11 (Scheme 7).[22] Initiation efficiency in this system was estimated to be 0.72, which was higher than their previous report in the system of [Rh(C≡CPh)(nbd)(PPh_3)$_2$]/DMAP. These two catalyst systems differ in terms of the amount of PPh_3 against rhodium, and it was revealed that the initiating species of polymerization was tetracoordinate complex [Rh(C≡CPh)(nbd)(PPh_3)]. This complex was generated by dissociation of one PPh_3 ligand from pentacoordinate complex [Rh(C≡CPh)(nbd)(PPh_3)$_2$] according to the NMR analysis of the reaction of [Rh(OCH_3)(nbd)]$_2$, PPh_3, and phenylacetylene in a molar ratio of 1:2:10 at –30 ºC (Scheme 8).[23]

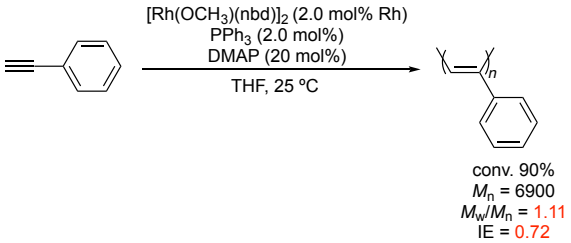

Scheme 7. Synthesis of polyphenylacetylene with very narrow molecular weight distribution

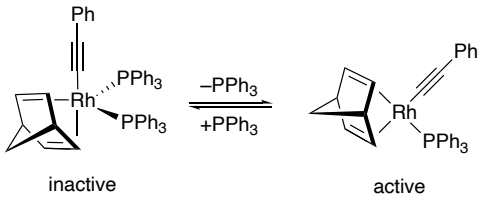

Scheme 8. Initiating species in polymerization of phenylacetylene with $[Rh(OCH_3)(nbd)]_2/PPh_3$

Jiménez *et al.* also observed the Rh(C≡CPh)(diene) species using the $[Rh(cod)(PPh_2(CH_2)_3NMe_2)]BF_4$ having a hemilabile bidentate ligand.[24] When the reaction of phenylacetylene and the rhodium catalyst in a molar ration of 20:1 was conducted, $[Rh(C{\equiv}CPh)(cod)(Ph_2P(CH_2)_3NHMe_2)]BF_4$ was observed as an initiation species, which was generated through the deprotonation of phenylacetylene by the hemilabile amido ligand (Scheme 9). These results implied that initiating species generated from $[RhX(diene)]_2$ and base in the polymerization of phenylacetylene would be [Rh(C≡CPh)(diene)(sol)] and this was supported by DFT, ONIOM and ONIOM-MD calculations by Morokuma *et al.* (Scheme 10).[25]

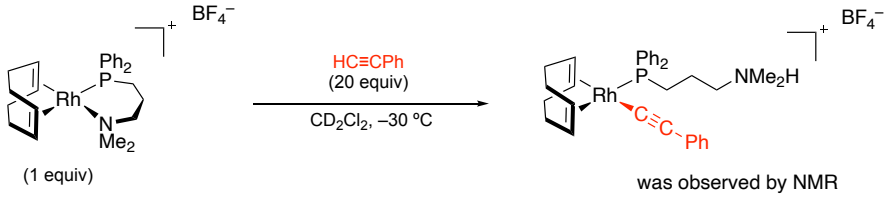

Scheme 9. Initiation species in the reaction of phenylacetylene with $[Rh(cod)(Ph_2P(CH_2)_3NMe_2)]BF_4$

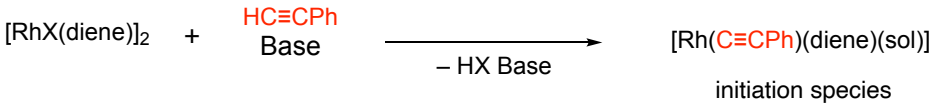

Scheme 10. Initiation mechanism in polymerization of phenylacetylene with $[RhX(diene)]_2$/base

Based on Noyori's works, Masuda *et al.* reported the novel rhodium(I) complex $[Rh(nbd)(CPh{=}CPh_2)(PPh_3)]$, which was generated by the reaction of $[RhCl(nbd)]_2$, PPh_3, and $LiCPh{=}CPh_2$ in a molar ratio of 1:4:6 (Scheme 11).[26] This vinylrhodium(I) catalyst possessing an identical structure to that of propagating species enabled the living polymerization with high initiation efficiency and the initiation-end-functionalization of polyphenylacetylene.

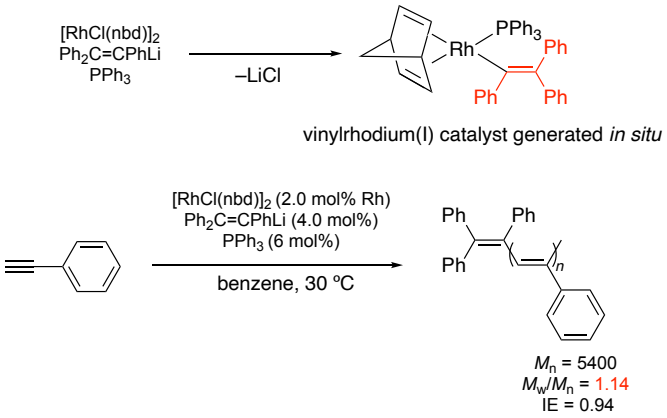

Scheme 11. Polymerization of phenylacetylene with vinylrhodium complex

The same group isolated vinylrhodium complex $[Rh(CPh{=}CPh_2)(nbd)(P(4\text{-}FC_6H_4)_3)]$, which was generated by the reaction of $[RhCl(nbd)]_2$, $LiCPh{=}CPh_2$, and $P(4\text{-}FC_6H_4)_3$ in benzene and it showed more controlled living polymerization.[27] When polymerization of phenylacetylene was conducted with isolated vinylrhodium complex in the presence of $P(4\text{-}FC_6H_4)_3$ in a phosphine to rhodium catalyst ratio of 5:1, narrower molecular weight

distribution (M_w/M_n = 1.05) and higher initiation efficiency were accomplished compared to the previous ternary system of [RhCl(nbd)]$_2$, PPh_3, and $LiCPh{=}CPh_2$ (Scheme 12).

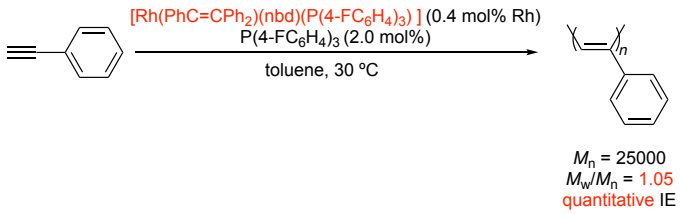

Scheme 12. Polymerization of phenylacetylene using isolated vinylrhodium complex

In 2006, Masuda *et al.* reported an effective new diene ligand, tetrafluorobenzobarrelene (tfb) for polymerization of phenylacetylene.[28] The tfb ligand has high π-acidity compared to conventional diene ligands such as nbd and cod. Owing to the strong π-back donation from 4d orbitals of Rh to LUMO of tfb, the coordination ability of alkyne monomer to the rhodium center and stability of the rhodium catalyst were improved, which led to acceleration of the propagation rate. For example, the polymer obtained in the [RhCl(tfb)]$_2$/Et_3N system showed a higher molecular weight (M_n = 281000) compared to that in the system of [RhCl(nbd)]$_2$/Et_3N (M_n = 118000) (Scheme 13).

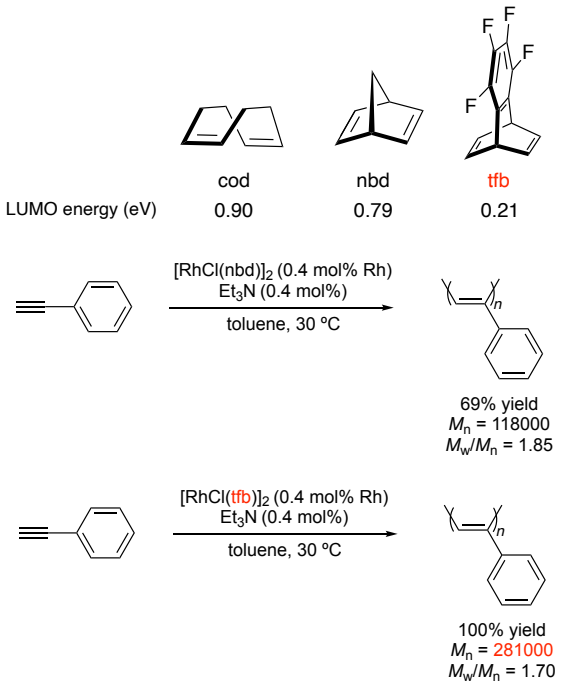

Scheme 13. Effect of tfb diene ligand

Recently, Maeda *et al.* reported initiation-end-functionalization of polyphenylacetylene in the system of $[RhCl(nbd)]_2$/arylboronic acid/diphenylacetylene/50% aqueous KOH (Scheme 14).[29] By adding diphenylacetylene, stabilized complexes were formed, which led to fast initiation of polymerization because dissociation of PPh_3 from rhodium center was promoted by η^2- or η^1-coordination of the phenyl group.[30] This method enabled introduction of various functional substituents such as halogen, amino, vinyl, and ethynyl groups at the initiation-end of polyphenylacetylene via well-controlled living polymerization.

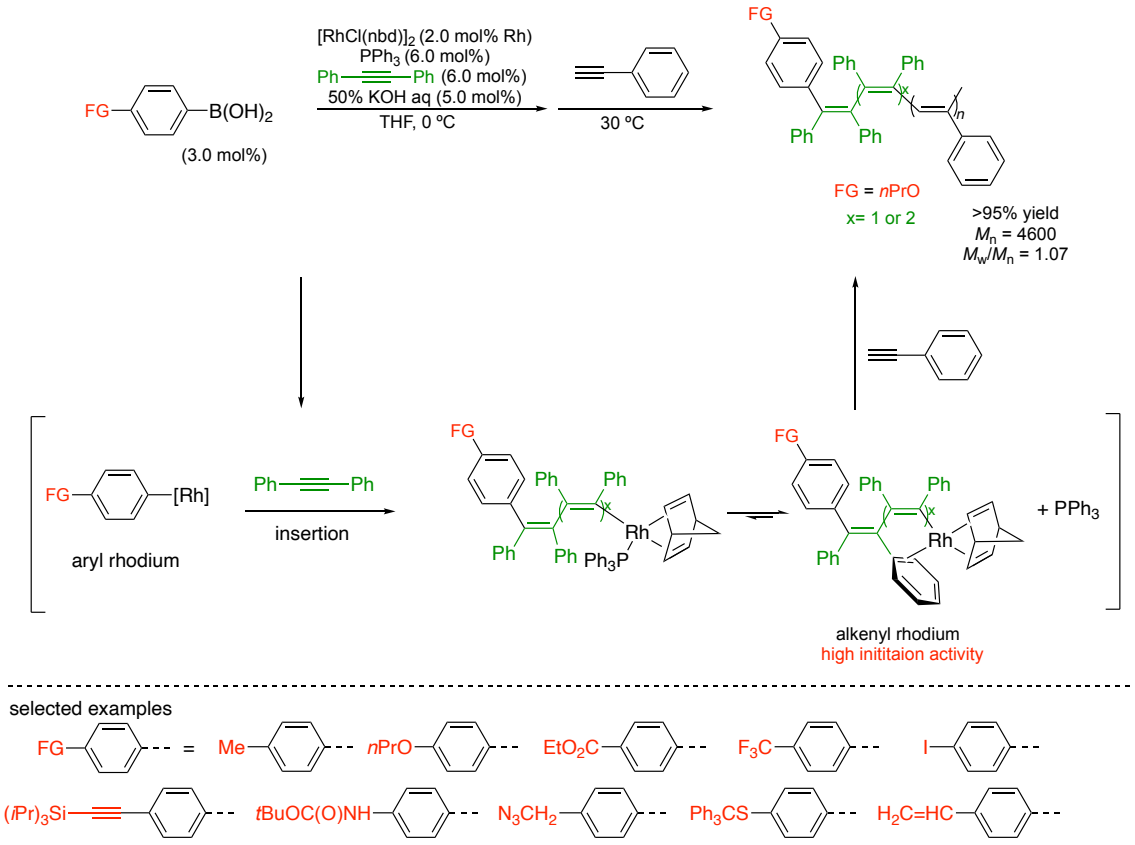

Scheme 14. Initiation-end-functionalization of polyphenylacetylene

Subsequently, the same group reported the preparation of termination-end-functionalized polyphenylacetylene by rhodium-catalyzed conjugate addition to α,β-unsaturated carbonyl compounds after living polymerization (Scheme 15).[31] A wide range of functional groups, such as halogen, fluorous, epoxide, and hydroxy groups, could be introduced at the termination-end by this method. These works enabled the synthesis of telechelic polyphenylacetylene with functional groups at both ends and the development of novel functional materials would be expected.

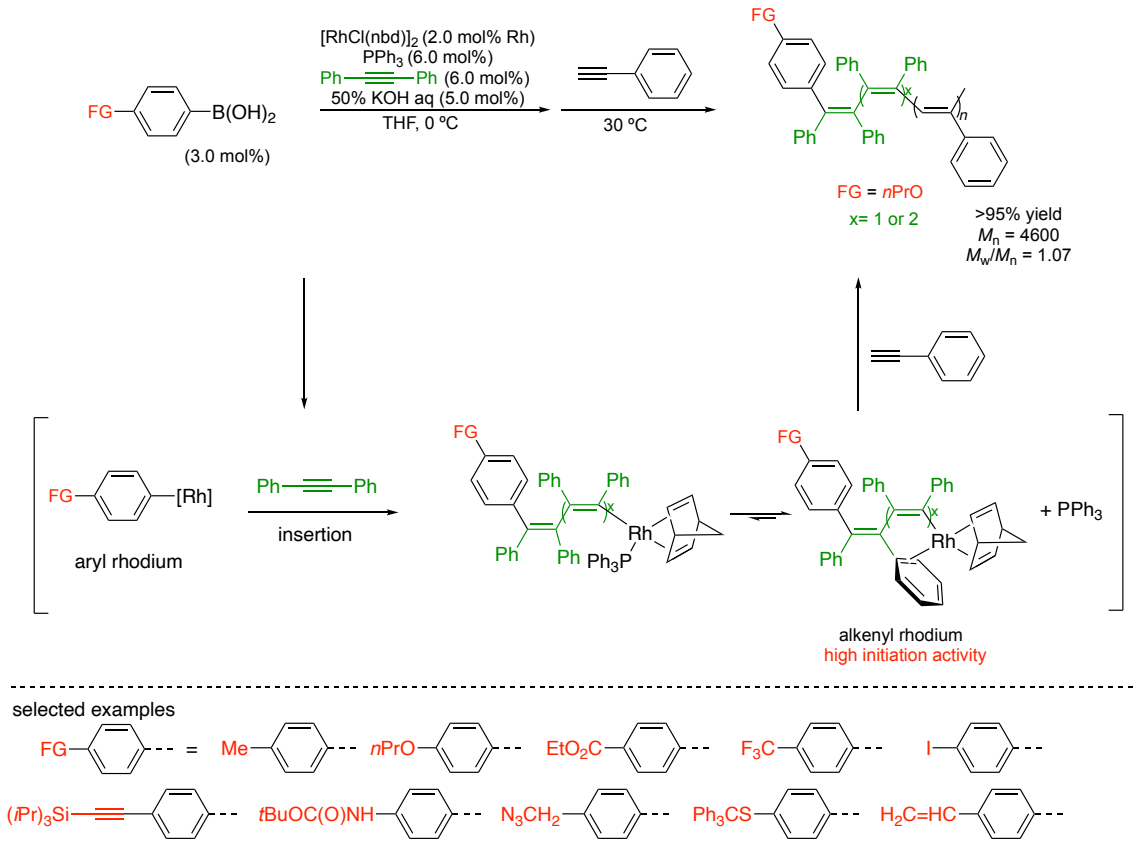

Scheme 15. Synthesis of telechelic polyphenylacetylene

1.1.2 Applicable monomers by rhodium-catalyzed alkyne polymerization

Rh(diene)-complexes effectively catalyze polymerization of phenylacetylene, but applicable alkyne monomers are limited. In particular, monomers possessing a less electrophilic alkyne such as alkylacetylenes and silylacetylenes are difficult to polymerize with rhodium-catalysts. In 1994, Ogawa *et al.* reported that $[Rh(SC_6H_5)(cod)]_2$ catalyst was not effective for polymerization of 1-hexyne although polymerization of phenylacetylene proceeded by this catalyst.[32] Similarly, Sedláček[33] *et al.* and Noyori[23] *et al.* also reported that poly-*n*-butylacetylene and poly-*t*-butylacetylene were obtained only in low yields using neutral rhodium-diene catalysts. Ozawa *et al.* reported that a cationic rhodium(I) tris(pyrazolyl)borate complex $Tp^{Me2}Rh(cod)$ showed high catalytic activity

for polymerization of arylacetylenes possessing an electron-withdrawing group or an electron-donating group without additives, but polymers were not produced in the case of *tert*-butylacetylene, trimethylsilylacetylene, and (methoxycarbonyl)acetylene as monomers (Scheme 16).[34]

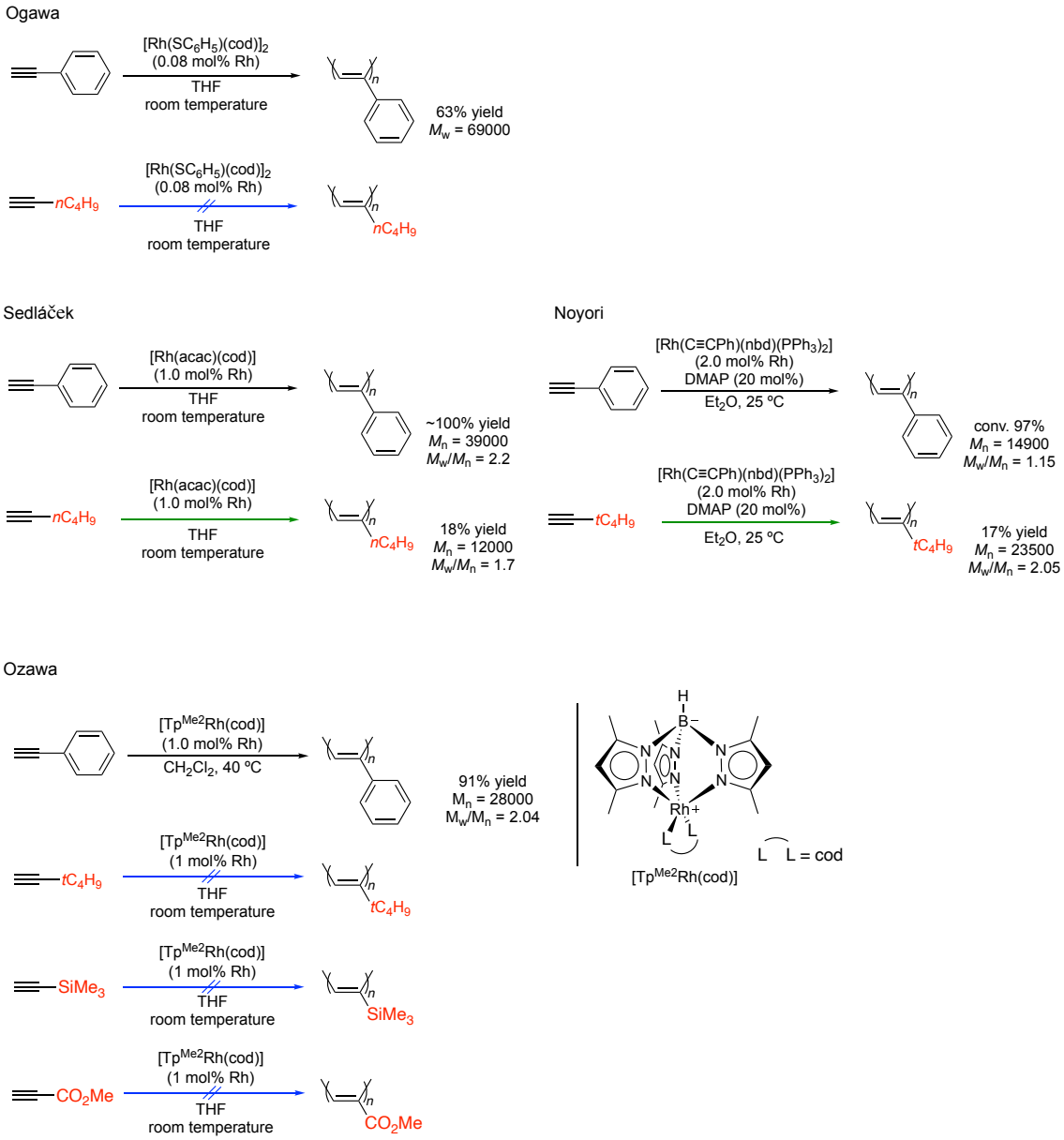

Scheme 16. Polymerizations of several alkyne monomers

Russo *et al*. also found that polymerization of *N*-benzylpropargylamine possessing a slightly electrophilic alkyne compared to alkylacetylene proceeded moderately in the presence of cationic [Rh(cod)(bpz)]PF_6 (Scheme 17).[35]

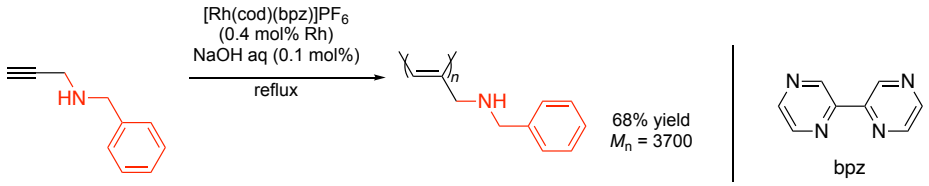

Scheme 17. Polymerization of *N*-benzylpropargylamine

In 1995, Noyori *et al.* discovered that cationic [Rh(nbd){η^6-$(C_6H_5)B(C_6H_5)_3$}] catalyst initiated the polymerization of alkylacetylenes such as *tert*-butylacetylene, 3-ethyl-1-pentyne and cyclohexylacetylene in THF at 19–21 ºC in a monomer to rhodium ratio of 50:1 to produce polyalkylacetylenes in quantitative yields (Scheme 18).[36] However, even with this catalyst, no polymerization took place for trimethylsilylacetylene, methyl propiolate and *N*,*N*-dimethylpropargylamine.

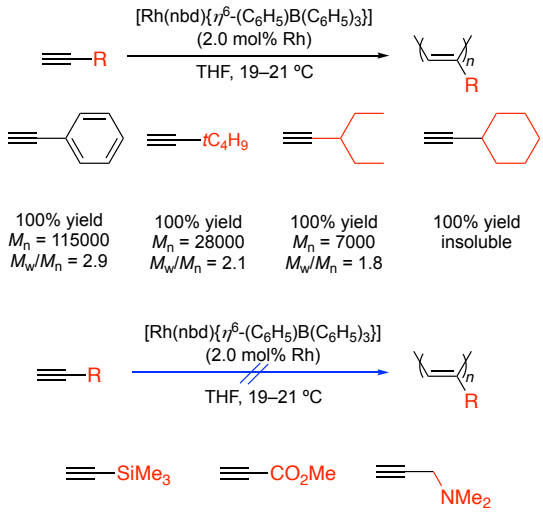

Scheme 18. Polymerizations of several monomers with [Rh(nbd){η^6-$(C_6H_5)B(C_6H_5)_3$}]

Masuda *et al.* subsequently reported that [Rh(nbd){η^6-$(C_6H_5)B(C_6H_5)_3$}] efficiently catalyzed polymerization of *N*-propargylamide,[37] propargyl ester,[37] and 1-methylpropargyl alcohol[38] as monomers (Scheme 19). These polymers had helical structures by stabilized hydrogen bonds or bulky substituents.

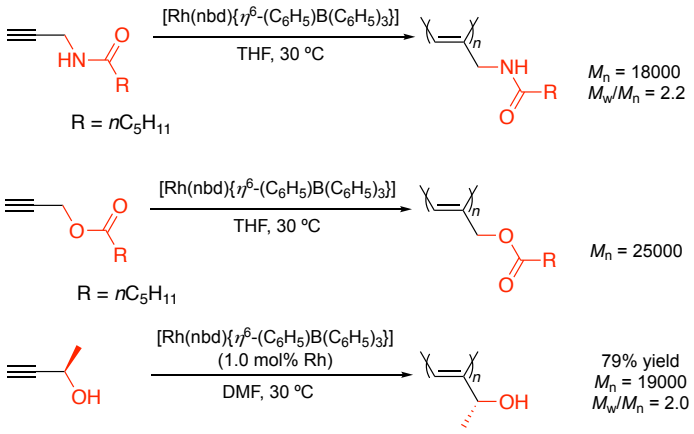

Scheme 19. Polymerizations of *N*-propargylamide, propargyl ester and 1-methylpropargyl alcohol with [Rh(nbd){η^6-$(C_6H_5)B(C_6H_5)_3$}]

In 1994, Tabata *et al.* found that the polymerizations of alkyl propiolates proceeded well in the presence of $[RhCl(nbd)]_2$ in MeOH although the polymer was obtained in low yields in the case of $[RhCl(cod)]_2$ (Scheme 20).[39] This result indicates the decomposition of $[RhCl(cod)]_2$ catalyst owing to the lower π-acidity of COD ligand and higher electrophilicity of alkyl propiolates.

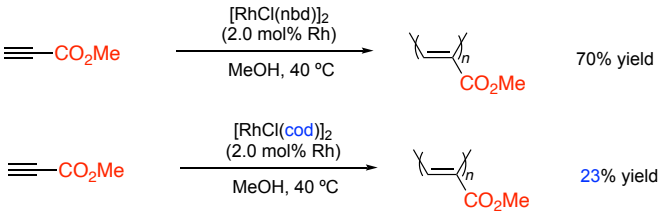

Scheme 20. Polymerizations of alkyl propiolates with Rh(diene)-catalyst

There are only a few reports on polymerization of internal alkynes with rhodium catalysts because of large steric hindrance although W,[10c,10d,10e] Ta,[12a,12e] and Pd[15d] catalysts can be effectively employed. Masuda *et al.* reported that polymerization of highly strained cyclooctyne as a disubstituted alkyne monomer proceeded with $[RhCl(nbd)]_2$ catalyst and Et_3N additive in toluene (Scheme 21).[40] Cyclooctyne exhibited higher polymerization activity than phenylacetylene according to the result of copolymerization of cyclooctyne and phenylacetylene. The obtained polycyclooctyne homopolymer showed higher thermal stability compared to polyphenylacetylene homopolymer.

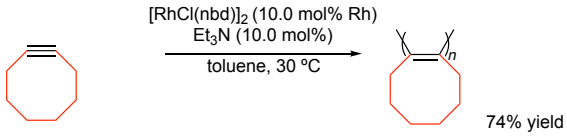

Scheme 21. Polymerization of cyclooctyne as internal alkyne

1.1.3 Rhodium-catalyzed polymerization of diynes

As described above, a lot of rhodium-catalyzed polymerizations of monoyne monomers were reported, but there are only a few reports on polymerizations of monomers possessing two alkynes.

In 2003, Masuda *et al*. reported copolymerization of phenylacetylene and 1,4-diethynylbenzene as a crosslinker (Scheme 22).[41] When phenylacetylene was polymerized in the presence of $[RhCl(nbd)]_2/Ph_2C{=}CPhLi/PPh_3$ and then diethynylbenzene was added to this solution, cross-linked polymer was given by intermolecular reaction of both alkynes of 1,4-diethynylbenzene with termination-end of polyphenylacetylene. The cross-linking reaction could be controlled by concentration of the crosslinker, temperature, and molecular weight of linear polymer.

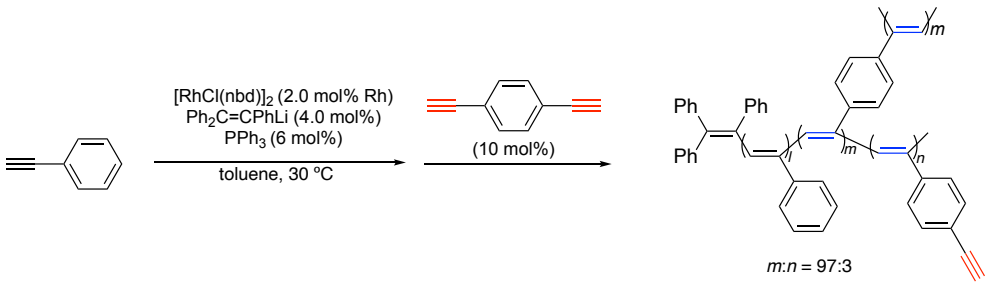

Scheme 22. Copolymerization of phenylacetylene and 1,4-diethnylbenzene.

Sedláček *et al.* described homopolymerization of 1,4-diethnylbenzene and 1,3-diethynylbenzene in the presence of [Rh(acac)(cod)] (Scheme 23).[42] According to ^{13}C NMR spectra, poly-1,4-diethynylbenzene contained 56% of remaining terminal alkynes and poly-1,3-diethynylbenzene contained 61% of terminal alkynes. These polymers are expected to be applied as gas adsorption materials.

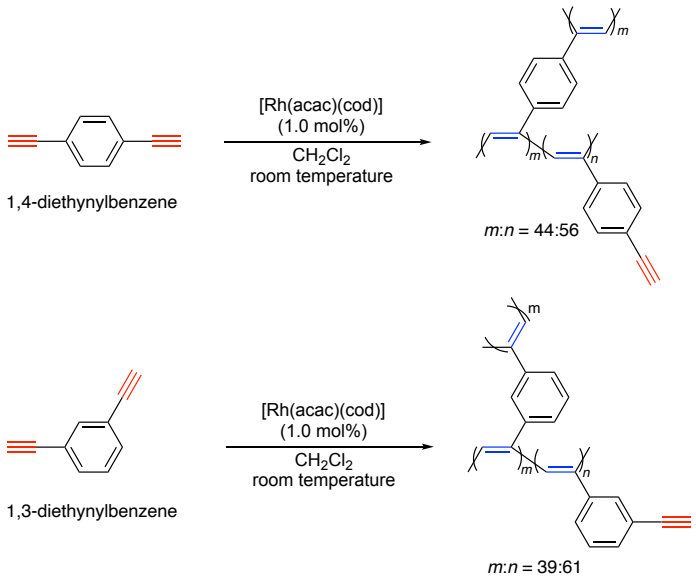

Scheme 23. Rhodium-catalyzed homopolymerizations of 1,4-diethynylbenzene or 1,3-diethynylbenzene

Masuda *et al.* described that polymerization of 1,2-diethynylbenzene with $[RhCl(nbd)]_2/Et_3N$ gave a polymer with 61% of remaining alkynes (Scheme 24).[43] According to the pyrolysis GC-MS analysis of the obtained polymer, a small amount of indene derivatives were observed, which indicated that the obtained polymer structure was estimated to contain partially arylene-bridged architecture generated by intramolecular cyclization.

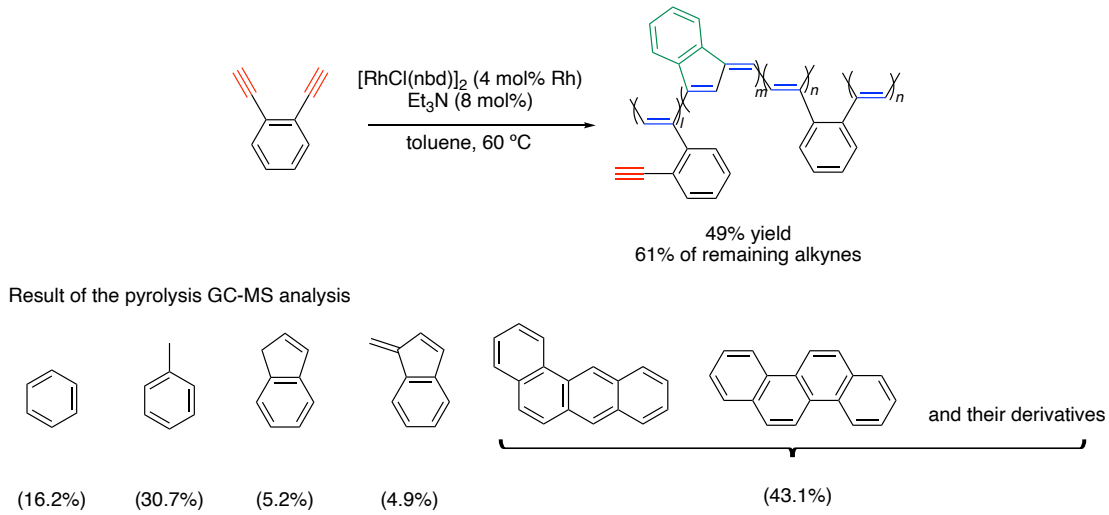

Scheme 24. Rhodium-catalyzed polymerization of 1,2-diethynylbenzene

Hayashi *et al.* reported rhodium-diene catalyzed asymmetric cyclopolymerization of 1,8-diynes containing terminal and internal alkynes to afford helix-sense-selective π-conjugated polymers (Scheme 25).[44] According to the ^{13}C NMR analysis, almost all the internal alkynes were incorporated into the main chain, which indicated that this polymerization effectively proceeded through intermolecular insertion of the terminal alkyne and intramolecular insertion of the internal alkyne alternately to form seven-membered ring in a repeating unit.

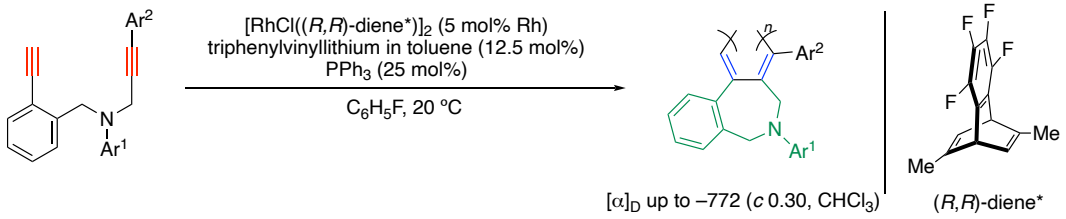

Scheme 25. Asymmetric cyclopolymerization of achiral 1,8-diynes

1.2 Bridged and ladder π-conjugated polymers

Bridged π-conjugated polymers[45] represented by poly(fluorene), poly(dibenzosilole), and poly(dibenzothiophene) have rigid π-conjugated repeating units (Figure 1-(a)). Owing to the restriction of C–C single bond rotation by the bridged moiety of the π-conjugated unit, these polymers exhibit longer conjugation lengths and have been intensively investigated as functional materials such as organic light-emitting diodes (OLED),[46] organic field-effect transistors (OFET),[47] and organic photovoltaics (OPV).[48] Generally, bridged π-conjugated polymers are synthesized by polycondensation of the corresponding bridged π-conjugated monomers.[49] This method is powerful and reliable if applicable, but accessible polymer structures are currently still limited. In this section, representative synthetic methods of carbon- or silicon-bridged π-conjugated polymers are summarized along with some synthetic methods of related ladder π-conjugated polymers (Figure 1-(b)).[50] In addition, as a new and complementary method for the synthesis of bridged π-conjugated compounds, the stitching reaction developed in our group is also described.

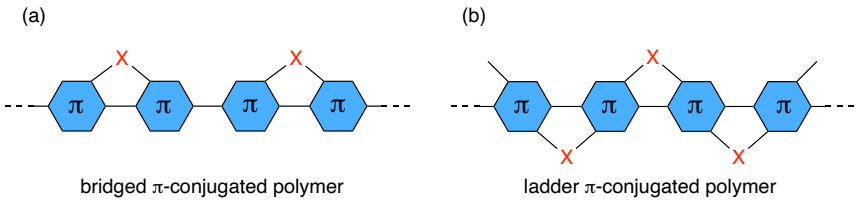

Figure 1. Structures of (a) bridged and (b) ladder π-conjugated polymer

1.2.1 Synthesis of carbon- or silicon-bridged π-conjugated polymers

In 1989, Fukuda *et al.* reported the first synthesis of poly(fluorene), the most representative carbon-bridged π-conjugated polymer, by the reaction of 9,9-

dialkylfluorene with $FeCl_3$ as a catalyst (Scheme 26).[51] It was found that this oxidative coupling polymerization gave a polymer with a low molecular weight and it partially contained irregular structures according to the NMR analysis.[52]

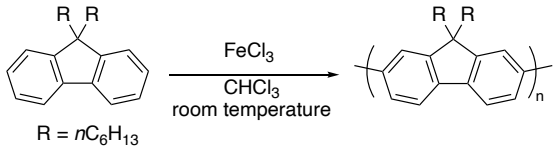

Scheme 26. Synthesis of poly(fluorene) by oxidative coupling with $FeCl_3$

Pei *et al.* reported the synthesis of poly(2,7-fluorene)s with a high molecular weight by the reductive coupling reaction in the presence of a Ni catalyst (Scheme 27-(a)).[53] This polymer showed an absorption maximum at ca. 380 nm, and photoluminescence was observed at 430 nm.[54] The bis(3,6-dioxaheptyl) side chains could dissolve lithium salts and it is expected to be applied to an ionic conductor. Leclerc *et al.* also described a palladium-catalyzed Suzuki-Miyaura coupling copolymerization of 9-carboxylated-2,7-dibromofluorene and 2,7-bis(dioxaboranyl)fluorene (Scheme 27-(b)).[55] Treatment of this polymer by base gave deprotonated polymers that showed conductivities of 10^{-6}–10^{-5} S cm^{-1}.

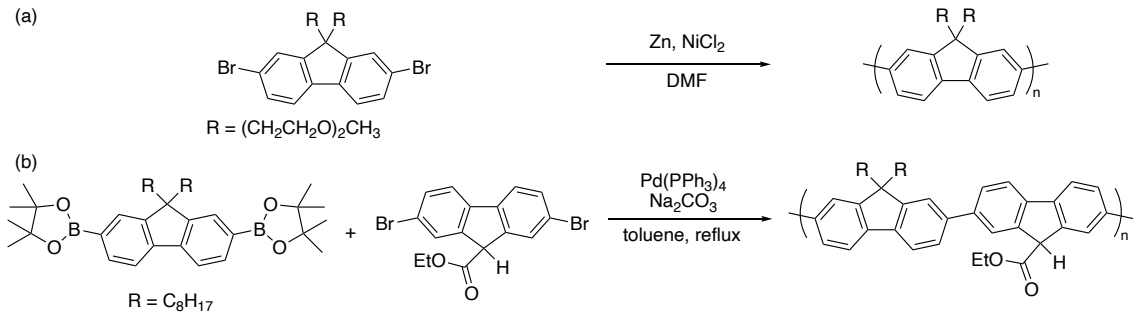

Scheme 27. Metal-catalyzed (a) coupling and (b) cross-coupling polymerizations

Jin *et al.* synthesized poly(fluorene vinylene)s by the Heck reaction between 2,7-divinylfluorene and 2,7-dibromofluorene (Scheme 28-(b)).[56] The absorption maximum of this polymer showed red shift (λ_{max} = 416 nm) compared to poly(2,7-fluorene), and this polymer emitted blue-greenish light ($\lambda_{max,PL}$ = 470 nm), which indicated the effective π-extension by the introduction of vinylene units.

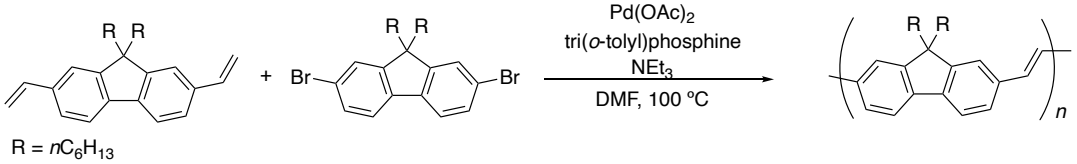

Scheme 28. Synthesis of poly(fluorene vinylene) by the Heck reaction

Kim *et al.* synthesized poly(fluorene ethynylene)s by the Sonogashira coupling reaction in the presence of Pd/Cu catalyst (Scheme 29).[57] According to the UV-vis spectrum, the absorption maximum was observed at 380 nm and the emission peak was shown at 475 nm.

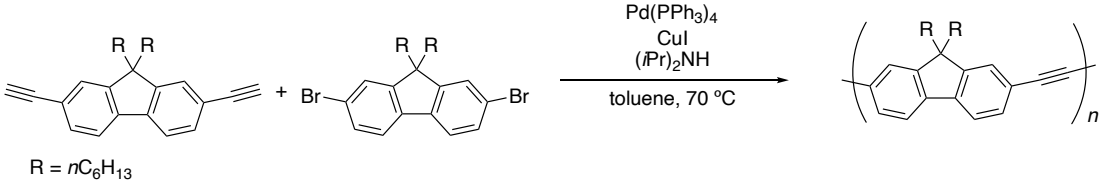

Scheme 29. Synthesis of poly(fluorene ethynylene) by the Sonogashira coupling reaction

As synthesis of carbon-bridged π-conjugated polymers other than poly(2,7-fluorene), in 2007, Cao *et al*. reported the first synthesis of poly(3,6-fluorene) by a Ni-catalyzed reductive coupling polymerization.[58] This polymer showed a hypsochromic shift (λ_{max} = 260 nm) in the UV-vis absorption spectrum compared to poly(2,7-fluorene), and it

showed an emission maximum at 347 nm, which was much shorter than poly(2,7-fluorene).

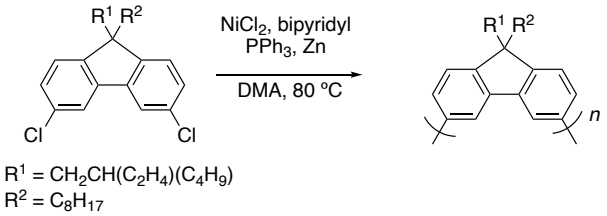

Scheme 30. Synthesis of poly(3,6-fluorene) in the presence of Ni catalyst

Yamamoto *et al.* synthesized poly(2,7-dihydrophenanthrene) by a Ni-mediated coupling reaction (Scheme 31-(a)).[59] The obtained polymer showed low solubility in $CHCl_3$ even though this polymer had ethylene-bridged moieties. To improve the solubility, Müllen *et al.* reported the synthesis of poly(2,7-tetrahydropyrene) with two octyl groups at the ethylene-bridged moieties (Scheme 31-(b)).[60] Polymerization of 4,9-dialkylated 4,5,9,10-tetrahydropyrenes in the presence of excess Ni complexes produced a soluble polymer with a higher molecular weight.

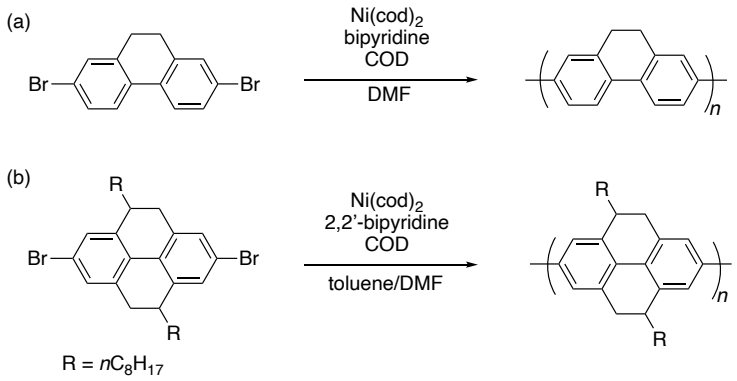

Scheme 31. Synthesis of (a) poly(2,7-dihydrophenanthrene) and (b) poly(2,7-tetrahydropyrene)

Suh *et al.* synthesized carbon-bridged poly(dihydroindeno[2,1-*a*]indene) in the presence of excess Ni complexes (Scheme 32).[61] By inclusion of one additional vinylene unit between the two phenylene units, this polymer with a rigid planar structure exhibited strong and uniform absorbance at the longer wavelength region (λ_{max} = 440 nm). This polymer also possessed good processability due to the introduction of four alkyl groups.

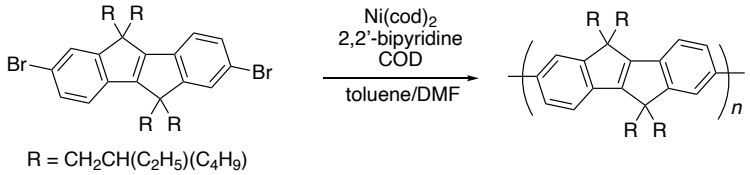

Scheme 32. Synthesis of poly(dihydroindeno[2,1-*a*]indene)

Müllen *et al.* synthesized poly(2,8-indenofluorene), which exhibited high thermal stability and good solubility (Scheme 33).[62] The absorption maximum of this polymer was located at 416 nm, which is intermediate between those of poly(fluorene) and ladder poly(*p*-phenylene) (λ_{max} = 438 nm).[63]

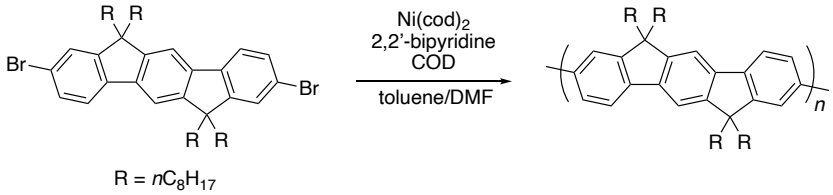

Scheme 33. Synthesis of poly(2,8-indenofluorene)

Bo *et al*. synthesized poly(spirobifluorene) by the Suzuki-Miyaura coupling reaction (Scheme 34).[64] Although poly(2,7-fluorene) showed a blue band emission, a low energy green band emission appeared during annealing under air due to the keto defects or

excimer formation.[65] On the other hand, the thermal treatment of poly(spirobifluorene) had no effect on the photoluminescence and only blue emission was shown.

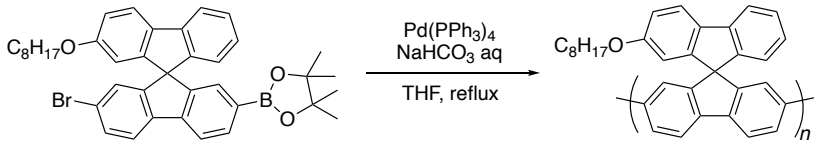

Scheme 34. Synthesis of poly(spirobifluorene)

In 1994, Zotti *et al.* described the first electrochemical synthesis of poly(cyclopentadithiophene), which can be regarded as a structural analogue of poly(fluorene).[66] Scherf *et al.* also synthesized poly(cyclopentadithiophene) by a Ni-mediated coupling reaction (Scheme 35).[67] Dialkyl-substituted poly(cyclopentadithiophene) was shown to be highly conjugated (λ_{max} = 560~590 nm)[68] with a relatively narrow band gap, and exhibited red photoluminescence at 639 nm.

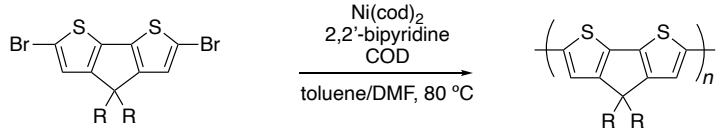

R = $CH_2CH(C_4H_9)(C_2H_5)$

Scheme 35. Synthesis of poly(cyclopentadithiophene)

The physical properties of bridged π-conjugated polymers can be tuned by changing elements on the bridged moiety. Among them, silicon-bridged π-conjugated polymers exhibit optoelectronic properties based on σ*–π* conjugation between the σ* orbital resulting from the two exocyclic substituents on silicon and π* orbital of the alkene moieties. Owing to their unique properties, they are intensively investigated for potential applications as electronic devices such as OLED[69] and OFET,[70] and various silicon-

bridged π-conjugated polymers have been developed to date (Figure 2).[71] As an example of simple silicon-bridged π-conjugated polymers, poly(2,7-dibenzosilole) was synthesized by the Suzuki-Miyaura coupling polymerization (Scheme 36).[71a] This polymer exhibited higher thermal stability compared to poly(fluorene).

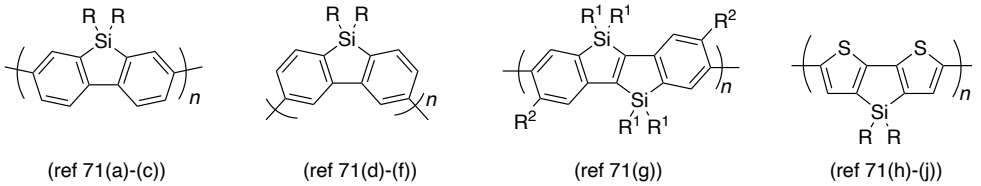

Figure 2. Examples of silicon-bridged π-conjugated polymers

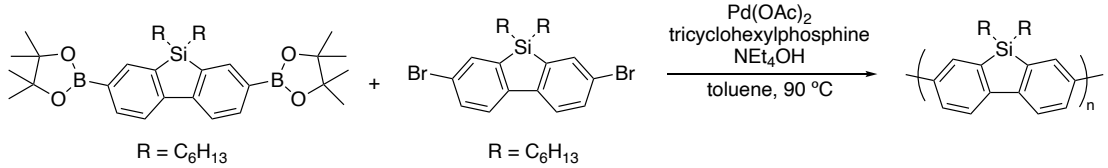

Scheme 36. Synthesis of poly(2,7-dibenzosilole)

There are only a few synthetic methods of bridged π-conjugated polymers except for polycondensation. For example, cyclopolymerization of 1,6-heptadiynes gave propylene-bridged π-conjugated polymers.[72] In 1961, Frey *et al.* reported the first metal-catalyzed cyclopolymerization of 1,6-heptadiyne via metathesis mechanism in the presence of triisobutylaluminum and titanium tetrachloride catalysts to give a dark red or black π-conjugated polymer partially containing propylene-bridged moiety (Scheme 37).[73] The proposed pathway is that the α-addition of a metal-alkylidene complex with terminal alkyne produces intermediate **A**, which undergoes cyclization by the intramolecular reaction of another alkyne to form a five-membered ring. When the β-addition of metal-alkylidene proceeds, a six-membered ring is formed (Scheme 38).[74]

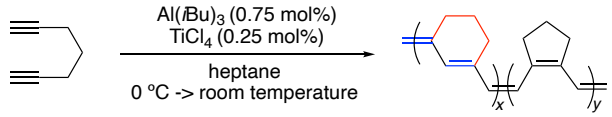

Scheme 37. Synthesis of propylene-bridged π-conjugated polymer by cyclopolymerization of 1,6-heptadiyne

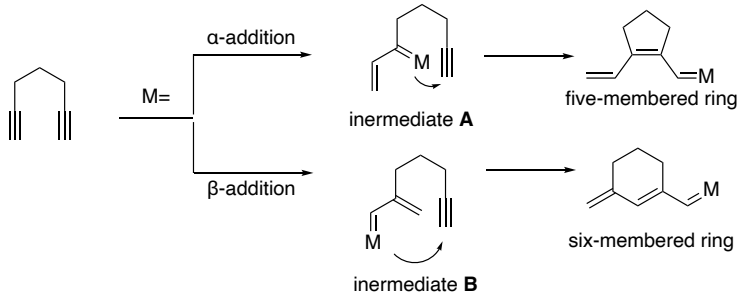

Scheme 38. Proposed pathway of cyclopolymerization of 1,6-heptadiyne

In 2016, Choi *et al*. described cyclopolymerization of 1,6-heptadiynes possessing bulky R substituents in the presence of *Z*-selective Grubbs catalyst containing a chelating *N*-heterocyclic carbene (NHC) ligand. The reaction selectively produced a propylene-bridged conjugated polymer having six-membered rings with up to 95% selectivity (Scheme 39).[75] The α-addition was suppressed by steric repulsion between the R substituent of 1,6-heptadiyne and the adamantyl NHC ligand of the Ru-catalyst.

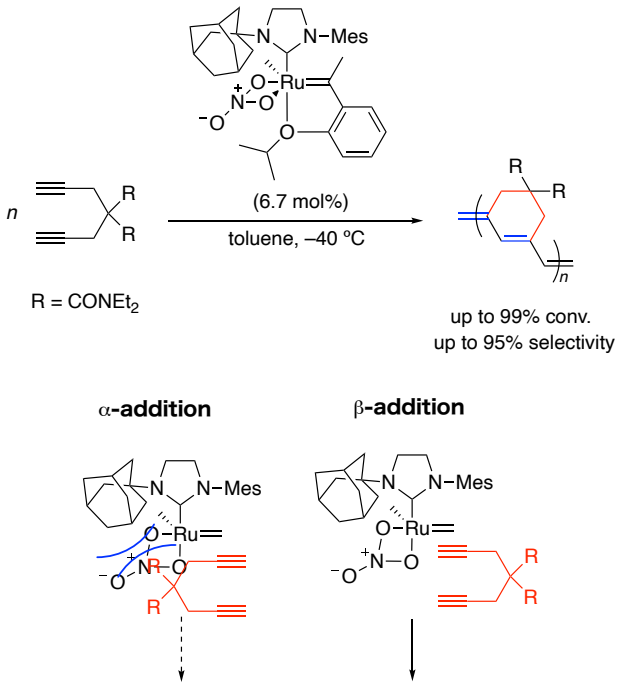

Scheme 39. Highly β-selective cyclopolymerization of 1,6-heptadiyne

Tang *et al.* reported cyclopolymerization of 1-phenyl-7-aryl-1,6-heptadiyne possessing two internal alkynes in the presence of WCl_6/Ph_4Sn.[76] According to the ^{13}C NMR analysis, it was estimated that only a propylene-bridged π-conjugated polymer having six-membered rings was obtained without the formation of the five-membered rings (Scheme 40). This polymer showed high thermal stability and processability due to the bulky aromatic groups.

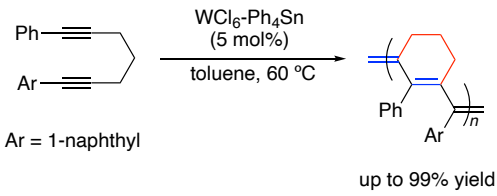

Scheme 40. W-catalyzed cyclopolymerization of disubstituted 1,6-heptadiyne monomer

1.2.2 Synthesis of ladder π-conjugated polymer

Bridged π-conjugated units also appear in the ladder π-conjugated polymers, which have fully ring-fused polycyclic skeletons. Ladder π-conjugated polymers have been used for a wide range of applications such as OLED[77] and OFET[78] owing to the optoelectronic properties derived from the restriction of torsional motion between the repeating units. A few representative examples are briefly described here.

In 1991, Müllen *et al.* synthesized a methylene-bridged ladder poly(*p*-phenylene) by electrophilic aromatic substitution by the Friedel–Crafts reaction of the hydroxymethyl-substituted poly(*p*-phenylene) precursor (Scheme 41).[63] In the UV-vis spectrum of this ladder polymer, absorption maximum was observed at 438 nm and emission was shown at 447 nm. These values indicated a very small Stokes shift due to the rigid geometry.

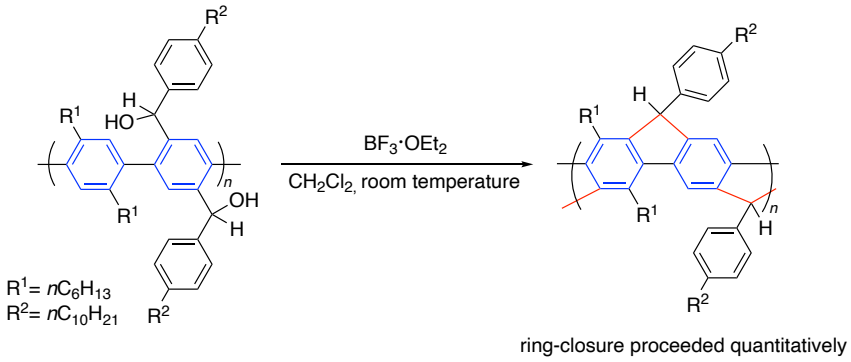

Scheme 41. Synthesis of ladder poly(*p*-phenylene) by the Friedel–Crafts reaction

Swager *et al.* developed a synthetic method to give an angular poly(acene) based on a Brønsted acid-promoted alkyne benzannulation of a linear poly(2,5-diethynyl-*p*-phenylene) (Scheme 42).[79] A peak corresponding to the alkyne stretch was not observed by the IR spectrum and a smaller effective volume of the ladder polymer compared to the linear precursor polymer was observed according to the GPC analysis. These results

indicated that Brønsted acid-promoted alkyne benzannulation quantitatively proceeded. Recently, peropyrene- and teropyrene-based ladder polymers were also synthesized by using this method.[80]

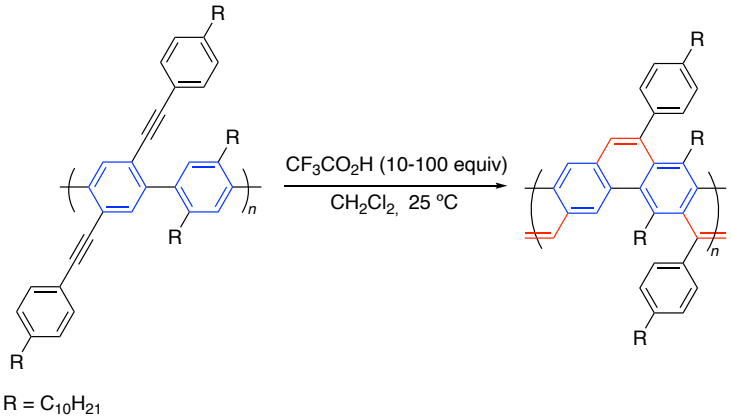

Scheme 42. Synthesis of ladder π-conjugated polymer by alkyne benzannulation

In 2006, Müllen *et al.* reported that an oxidative cyclodehydrogenation reaction in the presence of $FeCl_3$ and $MeNO_2$ (Scholl reaction) gave polycyclic aromatic hydrocarbons like graphene nanoribbons,[81] and they applied this method to synthesize ladder π-conjugated polymers like angular poly(acene) (Scheme 43).[82] According to the IR spectra of the obtained polymers, the peaks corresponding to the freely rotating phenyl rings were not observed, which indicated the absence of non-fused aromatic rings although the structure was not fully clarified.

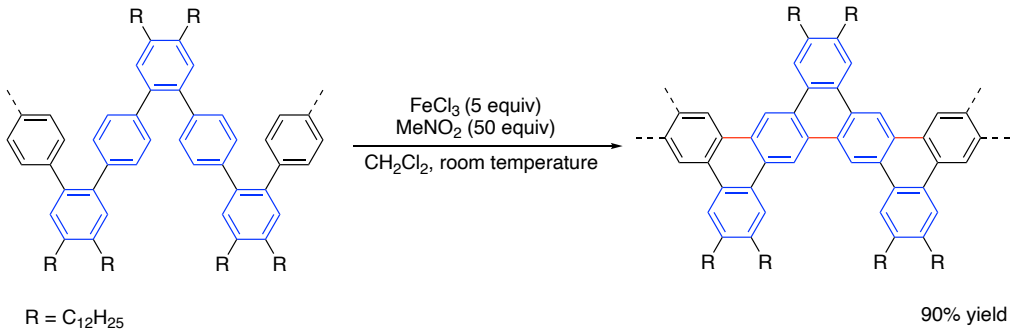

Scheme 43. Synthesis of ladder π-conjugated polymer by the Scholl reaction

1.2.3 Stitching reaction for the synthesis of bridged π-conjugated compound

Our group developed a rhodium-catalyzed stitching reaction as a new method for the synthesis of bridged π-conjugated compounds.[83] Unlike the conventional stepwise approaches, this method allows for the construction of a bridged structure and extension of π-conjugation at the same time from non-conjugated linear precursors. As shown in Scheme 44, two oligo(silylene-ethynylene)s (**1** and **2**), one of which contains an arylmetal moiety on one end and a haloarene moiety on the other end, undergo a multiple carbon–carbon bond-forming reaction in a stitching manner to give silicon-bridged ladder-type π-conjugated compounds **8** in the presence of a rhodium/cyclooctadiene catalyst. Initial transmetalation of the arylmetal moiety of **1** to rhodium(I) generates arylrhodium **3**, which undergoes intermolecular carborhodation to the alkyne at the terminal position of **2** to give alkenylrhodium **4**. This intermediates undergoes five-membered ring-forming carborhodation to the nearest alkyne to give new alkenylrhodium species **5**. Repeating the five-membered ring-formimg carborhodation arrives at alkenylrhodium **6**. Oxidative addition of aryl–X bond to alkenylrhodium gives **7** and reductive elimination leads to quinoidal fused oligosilole **8** with regeneration of rhodium(I).

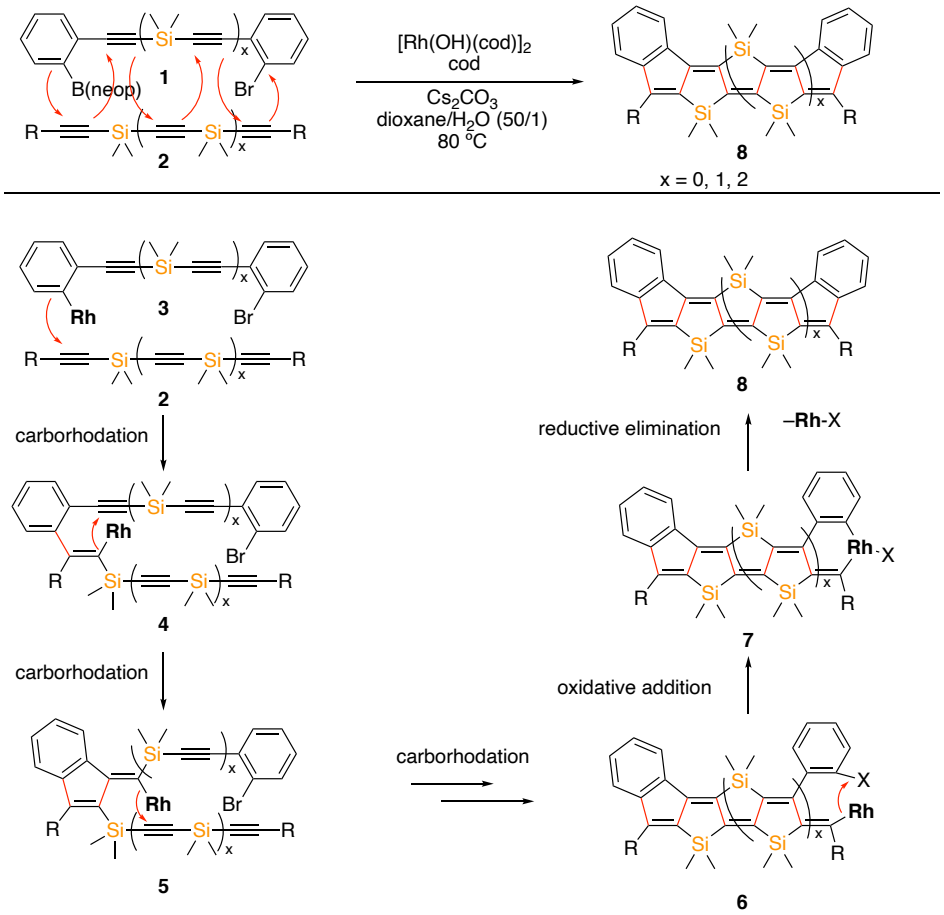

Scheme 44. Mechanism of the stitching reaction

Our group also found that a series of bridged dibenzofulvalenes having C, Ge, S, and P as the bridging elements were readily accessible from simple precursors by using the stitching reaction, which allowed for the facile structural tuning of bridged dibenzofulvalenes (Scheme 45).[84]

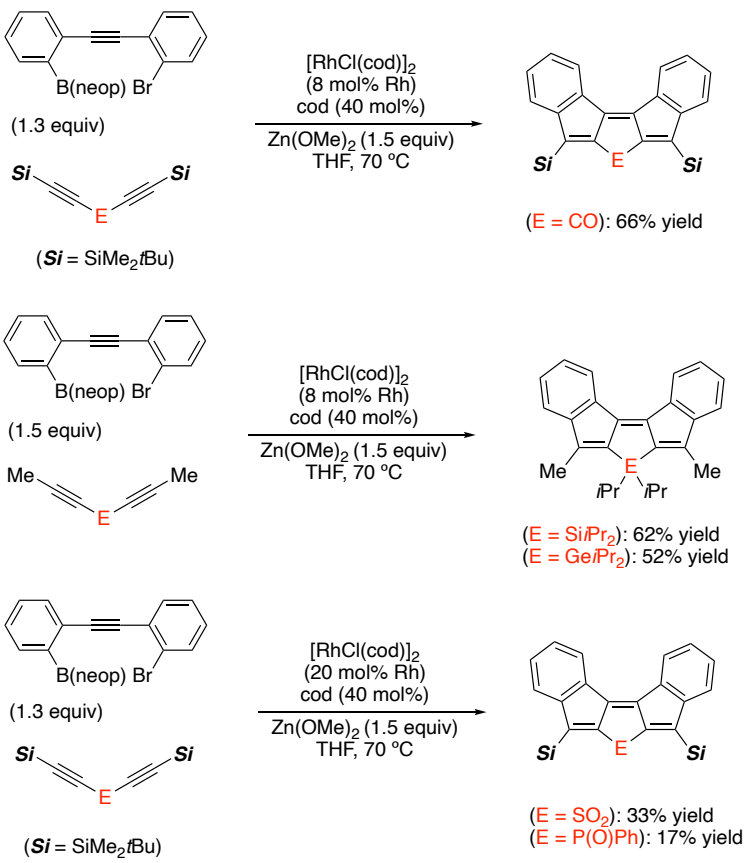

Scheme 45. Synthesis of carbonyl-bridged dibenzofulvalenes and related compounds by the stitching reaction

1.3 Overview of this dissertation

As described above, accessible bridged π-conjugated polymer structures are essentially limited to stable and isolable structures as monomers due to the deficiency of current synthetic methods. It is therefore desirable to devise new polymerization methods to expand the scope of accessible structures in light of their potential utility as optoelectronic materials. On the other hand, rhodium/diene complexes can catalyze well-controlled polymerization of alkyne monomers and they can also catalyze the stitching reaction that allows for the synthesis of bridged π-conjugated compounds from alkyne-containing non-conjugated compounds. In this context, the author considered that the strategy to combine rhodium-catalyzed stitching reaction and rhodium-catalyzed alkyne polymerization can be highly effective to synthesize new bridged π-conjugated polymers having a unit structure which is unstable as a monomer and difficult to synthesize by existing synthetic methods. The development of new polymerization method, rhodium-catalyzed stitching polymerization, to access bridged π-conjugated polymers with novel repeating units is expected to lead to discovery of new functional materials.

As realization of the above-mentioned concept, Chapter 2 describes the development of a rhodium-catalyzed stitching polymerization of non-conjugated 1,5-headiynes containing both terminal and internal alkynes as monomers for the synthesis of ethylene-bridged π-conjugated polymers consisting of a repeating unit that is difficult to prepare as a stable monomer structure. It was found that the polymerization proceeded smoothly with high degree of stitching efficiency (Scheme 46).

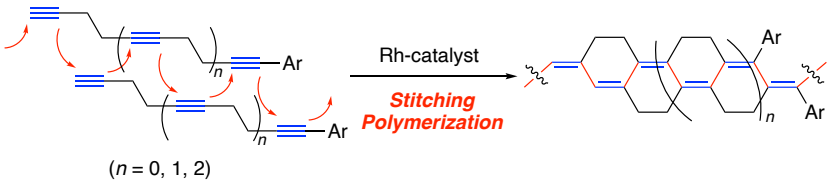

Scheme 46. Rhodium-catalyzed stitching polymerization of 1,5-hexadiynes and related oligoalkynes described in Chapter 2

To expand the scope of this mode of polymerization, Chapter 3 describes a synthesis of silicon-bridged π-conjugated polymers by the rhodium-catalyzed stitching polymerization of alkynylsilylacetylenes, representing the first successful chain-growth polymerization of heteroatom-substituted alkynes under rhodium catalysis. It was found that the diyne structure as monomers was important for the polymerization of silylacetylenes (Scheme 47).

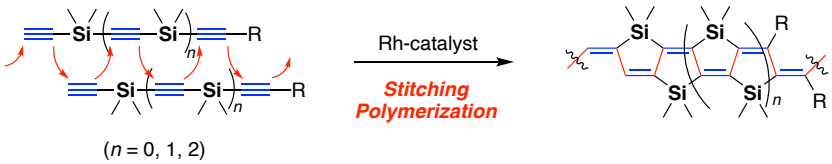

Scheme 47. Rhodium-catalyzed stitching polymerization of alkynylsilylacetylenes described in Chapter 3

1.4 References

[1] For reviews: (a) Lam, J. W. Y.; Tang, B. Z. *Acc. Chem. Res.* **2005**, *38*, 745–754. (b) Liu, J.; Lam, J. W. Y.; Tang, B. Z. *Chem. Rev.* **2009**, *109*, 5799–5867. (c) Masuda, T. *J. Polym. Sci., Part A: Polym. Chem.* **2007**, *45*, 165–180. (d) Aoki, T.; Kaneko, T.; Teraguchi, M. *Polymer* **2006**, *47*, 4867–4892. (e) Mayershofer, M. G.; Nuyken, O. *J. Polym. Sci., Part A: Polym. Chem.* **2005**, *43*, 5723–5747.

[2] For semiconductive materials: (a) Tang, B. Z.; Chen, H. Z.; Xu, R. S.; Lam, J. W. Y.; Cheuk, K. K. L.; Wong, H. N. C.; Wang, M. *Chem. Mater.* **2000**, *12*, 213–221. (b) Kang, E. T.; Ehrlich, P.; Bhatt, A. P.; Anderson, W. A. *Appl. Phys. Lett.* **1982**, *41*, 1136–1138. (c) Zhao, J.; Yang, M.; Shen, Z. *Polym. J.* **1991**, 43, 23–28. (d) Zhao, H.; Yuan, W. Z.; Tang, L.; Sun, J. Z.; Xu, H. P.; Qin, A. J.: Mao, Y.; Jin, J. K.; Tang, B. Z. *Macromolecules* **2008**, *41*, 8566–8574.

[3] For liquid crystallinity: (a) Lam, J. W. Y.; Tang, B. Z. *J. Polym. Sci., Part A: Polym. Chem.* **2003**, *41*, 2607–2629. (b) Kong, X. X.; Tang, B. Z. *Chem. Mater.* **1998**, *10*, 3352–3363. (c) Nagai, K.; Sakajiri, K.; Maeda, K.; Okoshi, K.; Sato, T.; Yashima, E. *Macromolecules* **2006**, *39*, 5371–5380. (d) Kwak, G.; Minakuchi, M.; Sakaguchi, T.; Masuda, T.; Fujiki, M. *Chem. Mater.* **2007**, *19*, 3654–3661.

[4] For gas permeability: (a) Nagai, K.; Masuda, T.; Nakagawa, T.; Freeman, B. D.; Pinnau, Z. *Prog. Polym. Sci.* **2001**, *26*, 721–798. (b) Hu, Y.; Shiotsuki, M.; Sanda, F.; Freeman, B. D.; Masuda, T. *Macromolecules* **2008**, *41*, 8525–8532.

[5] For helix-induced chirality: (a) Yashima, E.; Matsushima, T.; Okamoto, Y. *J. Am. Chem. Soc.* **1997**, *119*, 6345–6359. (b) Yashima, E.; Maeda, K. *Macromolecules* **2008**, *41*, 3–12. (c) Prince, R. B.; Barnes, S. A.; Moore, J. S. *J. Am. Chem. Soc*. **2000**, *122*, 2758–2762. (d) Teraguchi, M.; Suzuki, J.; Kaneko, T.; Aoki, T.; Masuda, T. *Macromolecules* **2003**, *36*, 9694–9697.

[6] For fluorescent materials: (a) Lam, J. W. Y.; Tang, B. Z. *J. Polym. Sci., Part A: Polym. Chem.* **2003**, *41*, 2607–2629. (b) Yuan, W. Z.; Qin, A.; Lam, J. W. Y.; Sun, J. Z.; Dong, Y.; Häussler, M.; Liu, J.; Xu, H. P.; Zheng, Q.; Tang, B. Z. *Macromolecules* **2007**, *40*, 3159–3166. (c) Sun, R.; Zheng, Q.; Zhang, X.; Masuda, T.; Kobayashi, T. *Jpn. J. Appl. Phys.* **1999**, *38*, 2017–2023. (d) Yang, S.-H.; Huang, C.-H.; Chen, C.-H.; Hsu, C.-S. *Macromol. Chem. Phys.* **2009**, *210*, 37–47.

[7] Natta, G.; Mazzanti, G.; Corradini, P.; Accad. A.; Lincei, N.; Classe, R. *Sci. Fis. Mat. Nat.* **1958**, *25*, 3–12. (b) Shirakawa, H.; Louis, E. J.; MacDiarmid, A. G.; Chiang, C. K.; Heeger, A. J. *J. Chem. Soc., Chem. Commun.* **1977**, 578–580. (c) Shirakawa, H. *Angew. Chem., Int. Ed.* **2001**, *40*, 2575–2580. (d) MacDiarmid, A. G. *Angew. Chem., Int. Ed.* **2001**, *40*, 2581–2590. (e) Heeger, A. J. *Angew. Chem., Int. Ed.* **2001**, *40*, 2591–2611.

[8] For Ti complexes: (a) Ito, T.; Shirakawa, H.; Ikeda, S. *J. Polym. Sci., Part A: Polym. Chem.* **1974**, *12*, 11–20. (b) Simionescu, C. I.; Percec, V.; Dumitrescu, S. *J. Polym. Sci. Polym. Chem. Ed.* **1977**, *15*, 2497–2509.

[9] For Fe complexes: Trepka, W. J.; Sonnenfeld, R. J. *J. Polym. Sci., Part A-1: Polym. Chem.* **1970**, *8*, 2721–2724.

[10] For W complexes: (a) Masuda, T.; Thieu, K.-Q.; Sasaki, N.; Higashimura, T. *Macromolecules* **1976**, *9*, 661–664. (b) Wang, J. L.; Menapace, H. L. *J. Org. Chem.* **1968**, *33*, 3794–3796. (c) Maeda, K.; Nozaki, M.; Hashimoto, K.; Shimomura, K.; Hirose, D.; Nishimura, T.; Watanabe, G.; Yashima, E. *J. Am. Chem. Soc.* **2020**, *142*, 7668–7682. (d) Wallace, K. C.; Liu, A. H.; Davis, W. M.; Schrock, R. R. *Organometallics* **1989**, *8*, 644–654. (e) Miyairi, M.; Taniguchi, T.; Nishimura, T.; Maeda, K. *Angew. Chem., Int. Ed.* **2020**, *59*, 14772–14780.

[11] For Mo and W complexes: (a) Xu, K.; Peng, H.; Lam, J. W. Y.; Poon, T. W. H.; Dong, Y.; Xu, H.; Sun, Q.; Cheuk, K. K. L.; Salhi, F.; Lee, P. P. S.; Tang, B. Z. *Macromolecules* **2000**, *33*, 6918–6924. (b) Kunzler, J.; Percec, V. *J. Polym. Sci., Part A: Polym. Chem.* **1990**, *28*, 1043–1057. (c) Kunzler, J.; Percec, V. *J. Polym. Sci., Part A: Polym. Chem*. **1990**, *28*, 1221–1236. (d) Masuda, T.; Sasaki, N.; Higashimura, T. *Macromolecules* **1975**, *8*, 717–721.

[12] For Mo complexes: (a) Masuda, T.; Yoshimura, T.; Fujimori, J.; Higashimura, T. *J. Chem. Soc., Chem. Commun.* **1987**, 1805–1806. (b) Masuda, T.; Mishima, K.; Fujimori, J.; Nishida, M.; Muramatsu, H.; Higashimura, T. *Macromolecules* **1992**, *25*, 1401–1404. (c) Kaneshiro, H.; Masuda, T.; Higashimura, T. *Polym. Bull.* **1995**, *35*, 17–23. (d) Nakano, M.; Masuda, T.; Higashimura, T. *Macromolecules* **1994**, *27*, 1344–1348. (e) Kunzler, J.; Percec, V. *Polym. Bull.* **1992**, *29*, 335–342. (f) Katz, T. J.; Hacker, S. M.; Kendrick, R. D.; Yannoni, C. S. *J. Am. Chem. Soc.* **1985**, *107*, 2182–2183. (g) Schrock, R. R.; Luo, S.; Lee, J. C.; Jr., Zanetti, N. C.; Davis, W. M. *J. Am. Chem. Soc*. **1996**, *118*, 3883–3895.

[13] For Ta complexes: (a) Tsuchihara, K.; Masuda, T.; Higashimura, T. *J. Am. Chem. Soc.* **1991**, *113*, 8548–8549. (b) Tsuchihara, K.; Masuda, T.; Higashimura, T. *Macromolecules* **1992**, *25*, 5816–5820. (c) Sakaguchi, T.; Azuma, S.; Hashimoto, T. *Synth. Met*. **2016**, *212*, 174–179. (d) Sakaguchi, T.; Shimada, H.; Hashimoto, T. *Polym. Chem.* **2020**, *11*, 6471–6478. (e) Wallace, K. C.; Liu, A. H.; Davis, W. M.; Schrock, R. R. *Organometallics* **1989**, *8*, 644–654. (f) Sueyoshi, S.; Taniguchi, T.; Tanaka, S.; Asakawa, H.; Nishimura, T.; Maeda, K. *J. Am. Chem. Soc.* **2021**, *143*, 16136–16146. For Nb and Ta complexes: (g) Cotton, F. A.; Hall, W. T.; Cann, K. J.; Karol, F. J. *Macromolecules* **1981**, *14*, 233–236. (h) Masuda, T.; Takahaski, T.; Niki, A.; Higashimura, T. *J. Polym. Sci., Part A: Polym. Chem.* **1986**, *24*, 809–814.

(i) Niki, A.; Masuda, T.; Higashimura, T. *J. Polym. Sci., Part A: Polym. Chem.* **1987**, *25*, 1553–1562.

[14] For reviews on Rh complexes: (a) Shiotsuki, M.; Sanda, F.; Masuda, T. *Polym. Chem*., **2011**, *2*, 1044–1058. (b) Tan, N. S. L.; Lowe, A. B. *Angew. Chem., Int. Ed*. **2020**, *59*, 5008–5021.

[15] For Pd complexes: (a) Ojwach, S. O.; Guzei, I. A.; Darkwa, J.; Mapolie, S. M. *Polyhedron* **2007**, *26*, 851–861. (b) Li, K.; Mohlala, M. S.; Segapelo, T. V.; Shumbula, P. M.; Guzei, I. A.; Darkwa, J. *Polyhedron* **2008**, *27*, 1017–1023. (c) Li, K.; Wei, G.; Darkwa, J.; Pollack, S. K. *Macromolecules* **2002**, *35*, 4573–4576. (d) Castanon, J. R.; Sano, N.; Shiotsuki, M.; Sanda, F. *ACS Macro Lett.* **2014**, *3*, 51–54. (e) Li, M.; Chen, C. *Polym. Chem*. **2015**, *6*, 7127–7132.

[16] For Ru complexes: (a) Katsumata, T.; Shiotsuki, M.; Sanda, F.; Sauvage, X.; Delaude, L;. Masuda, T. *Macromol. Chem. Phys.* **2009**, *210*, 1891–1902. (b) Csabai, P.; Joó, F.; Trzeciak, A. M.; Ziółkowski, J. J. *J. Organomet. Chem.* **2006**, *691*, 3371–3376.

[17] For Ni complexes: Buchowicz, W.; Wojtczak, W.; Pietrzykowski, A.; Lupa, A.; Jerzykiewicz, L.B.; Makal, A.; Woźniak, K. *Eur. J. Inorg. Chem*. **2010**, *4*, 648–656.

[18] Kern, R. J. *J. Polym. Sci., Part A: Polym. Chem*. **1969**, *7*, 621–623.

[19] Furlani, A.; Napoletano, C.; Russo, V.; Feast, W. *J. Polym. Bull.* **1986**, *16*, 311–317.

[20] Tabata, M.; Yang, W.; Yokota, K. *Polym. J.* **1990**, *22*, 1105–1107.

[21] Kishimoto, Y.; Eckerle, P.; Miyatake, T.; Ikariya, T.; Noyori, R. *J. Am. Chem. Soc.* **1994**, *116*, 12131–12132.

[22] Kishimoto, Y.; Miyatake, T.; Ikariya, T.; Noyori, R. *Macromolecules* **1996**, *29*, 5054–5055.

[23] Kishimoto, Y.; Eckerle, P.; Miyatake, T.; Kainosho, M.; Ono, A.; Ikariya, T.; Noyori, R. *J. Am. Chem. Soc.* **1999**, *121*, 12035–12044.

[24] Jiménez, M. V.; Pérez-Torrente, J. J.; Bartolomé, M. I.; Vispe, E.; Lahoz, F. J.; Oro, L. A. *Macromolecules* **2009**, *42*, 8146–8156. (b) Xue, P.; Sung, H. S. Y.; Williams, I. D.; Jia, G. *J. Organomet. Chem*. **2006**, *691*, 1945–1953.

[25] Ke, Z.; Abe, S.; Ueno, T.; Morokuma, K. *J. Am. Chem. Soc.* **2011**, *133*, 7926–7941.

[26] Misumi, Y.; Masuda, T. *Macromolecules* **1998**, *31*, 7572–7573.

[27] Miyake, M.; Misumi, Y.; Masuda, T. *Macromolecules* **2000**, *33*, 6636–6639.

[28] Saeed, I.; Shiotsuki, M.; Masuda, T. *Macromolecules* **2006**, *39*, 8977–8981.

[29] Taniguchi, T.; Yoshida, T.; Echizen, K.; Takayama, K.; Nishimura, T.; Maeda, K. *Angew. Chem., Int. Ed.* **2020**, *59*, 8670–8680.

[30] Sakamoto, S.; Taniguchi, T.; Sakata, Y.; Akine, S.; Nishimura, T.; Maeda, K. *Angew. Chem., Int. Ed.* **2021**, *60*, 22201–22206.

[31] Echizen, K.; Taniguchi, T.; Nishimura, T.; Maeda, K. *J. Am. Chem. Soc*. **2021**, *143*, 3604–3612.

[32] Vilar, R.; Salcedo, R.; Gavino, R.; Ogawa, T. *Eur. Polym. J.* **1994**, *30*, 1237–1242.

[33] Trhlíková, O.; Zedník, J.; Balcar, H.; Brus, J.; Sedláček, J. *J. Mol. Catal. A: Chem.* **2013**, *378*, 57–66.

[34] Katayama, H.; Yamamura, K.; Miyaki, Y.; Ozawa, F. *Organometallics* **1997**, *16*, 4497–4500.

[35] Furlani, A.; Paolesse, R.; Russo, M. V.; Camus, A.; Marsich, N. *Polymer* **1987**, *28*, 1221–1226.

[36] Kishimoto, Y.; Itou, M.; Miyatake, T.; Ikariya, T.; Noyori, R. *Macromolecules* **1995**, *28*, 6662–6666.

[37] Nomura, R.; Tabei, J.; Masuda, T. *J. Am. Chem. Soc.* **2001**, *123*, 8430–8431.

[38] Suzuki, Y.; Shiotsuki, M.; Sanda, F.; Masuda, T. *Macromolecules*, **2007**, *40,* 1864–1867.

[39] Tabata, M.; Inaba, Y.; Yokota, K.; Nozaki, Y. *J. Macromol. Sci., Pure Appl. Chem*. **1994**, *A31*, 465–475.

[40] Yamada, K.; Nomura, R.; Masuda, T. *Macromolecules* **2000**, *33*, 9179–9181.

[41] Kanki, K.; Masuda, T. *Macromolecules* **2003**, *36,* 1500–1504.

[42] Hanková, V.; Slováková, E.; Zedník, J.; Vohlídal, J.; Sivkova, R.; Balcar, H.; Zukal, A.; Brus, J.; Sedláček, J. *Macromol. Rapid Commun*. **2012**, *33*, 158–163. (b) Slováková, E.; Jesělnik, M.; Žagar, E.; Zedník, J.; Sedláček, J.; Kovacĭc, S. *Macromolecules* **2014**, *47*, 4864–4869.

[43] Zhang, W.; Shiotsuki, M,; Masuda, T. *Polymer* **2006**, *47*, 2956–2961.

[44] Ichikawa, Y.; Nishimura, T.; Hayashi, T. *Organometallics* **2011**, *30*, 2342–2348.

[45] For reviews on bridged π-conjugated polymers: (a) CInar, M. E.; Ozturk, T. *Chem. Rev*. **2015**, *115*, 3036–3140. (b) Zheng, B.; Huo, L. *Sci. China. Chem.* **2021**, *64*, 358–384. (c) Wu, J. S.; Cheng, S. W.; Cheng, Y. J.; Hsu, C. S. *Chem. Soc. Rev.,* **2015**, *44*, 1113–1154. For selected examples of poly(thiophene): (d) Biniek, L.; Schroeder, B. C.; Donaghey, J. E.; Yaacobi-Gross, N.; Ashraf, R. S.; Soon, Y. W.; Nielsen, C. B.; Durrant, J. R.; Anthopoulos, T. D.; McCulloch, I. *Macromolecules* **2013**, *46*, 727–735. (e) Zheng, T.; Lu, L.; Jackson, N. E.; Lou, S. J.; Chen, L. X.; Yu, L. *Macromolecules* **2014**, *47*, 6252–6259. (f) Ma, J.; Liu, Z.; Yao, J.; Wang, Z.; Zhang, G.; Zhang, X.; Zhang, D. *Macromolecules* **2018**, *51*, 6003–6010. (g) Kline, R. J.; McGehee, M. D.; Kadnikova, E. N.; Liu, J.; Fréchet, J. M. J.; Toney, M. F. *Macromolecules* **2005**, *38*, 3312–3319.

[46] For OLED materials: (a) Beaupre, S.; Boudreault, P. L.; Leclerc, M. *Adv. Mater.* **2010**, *22*, E6–E27. (b) Chan, K. L.; McKiernan, M. J.; Towns, C. R.; Holmes, A.

B. *J. Am. Chem. Soc.* **2005***, 127*, 7662–7663. (c) Jiu, Y.; Wang, J.; Yi, J.; Liu, C.-F.; Zhang, X.-W.; Lai W.-Y.; Huang, W. *Polym. Chem*. **2017**, *8*, 851–859. (d) Nishioka, H.; Tsuji, H.; Nakamura, E. *Macromolecules* **2018**, *51*, 2961−2968.

[47] For OFET materials: (a) Takimiya, K.; Shinamura, S.; Osaka, I.; Miyazaki, E. *Adv. Mater.* **2011**, *23*, 4347–4370. (b) Anthony, J. E. *Chem. Rev.* **2006**, *106,* 5028–5048. (c) Facchetti, A. *Chem. Mater.* **2011**, *23*, 733–758. (d) Rieger, R.; Beckmann, D.; Pisula, W.; Kastler, M.; Müllen, K. *Macromolecules* **2010**, *43*, 6264–6267. (e) John, S. V.; Cimrová, V.; Ulbricht, C.; Pokorná, V.; Růzǐcka, A.; Gigueŕe, J. B.; Lambert, A. L.; Morin, J. F.; Iwuoha, E.; Egbe, D. A. M. *Macromolecules* **2017**, *50*, 8357–8371. (f) Tsuji, H.; Nakamura, E. *Acc. Chem. Res.* **2019**, *52*, 2939–2949.

[48] For organic photovoltaics: (a) Liang, Y.; Xu, Z.; Xia, J.; Tsai, S.-T.; Wu, Y.; Li, G.; Ray, C.; Yu, L. *Adv. Mater.* **2010**, *22*, E135–E138. (b) Cao, C.; Xiao, M.; Yang, X.; Zhang, J.; Huang, F.; Cao, Y. *J. Mater. Chem. C* **2018**, *6*, 8020–8027. (c) Bura, T.; Beaupré, S.; Ibraikulov, O. A.; Légaré, M.-A.; Quinn, J.; Lévêque, P.; Heiser, T.; Li, Y.; Leclerc, N.; Leclerc, M. *Macromolecules* **2017**, *50*, 7080–7090. (d) Katsouras, A.; Gasparini, N.; Koulogiannis, C.; Spanos, M.; Ameri, T.; Brabec, C. J.; Chochos, C. L. *Macromol. Rapid Commun.* **2015**, *36*, 1778–1797.

[49] For reviews on cross-coupling reaction: (a) Leone, A. K.; Mueller, E. A.; McNeil, A. J. *J. Am. Chem. Soc*. **2018**, *140*, 15126–15139. For electrochemical synthesis: (b) Martın-Fuentes, C.; Urgel, J. I.; Edalatmanesh, S.; Rodrıguez-Sanchez, E.; Santos, J.; Mutombo, P.; Biswas, K.; Lauwaet, K.; Gallego, J. M.; Miranda, R.; Jelınek, P.; Martín, N.; Écija, D. *Chem. Commun*. **2021**, *57*, 7545–7548.

[50] For reviews on ladder π-conjugated polymer: (a) Teo, Y. C.; Lai, H. W. L.; Xia, Y. *Chem. Eur. J.* **2017**, *23*, 14101–14112. (b) Fukazawa, A.; Yamguchi, S. *Chem. Asian J*. **2009**, *4*, 1386–1400. (c) Scherf, U. *J. Mater. Chem.*, **1999***, 9*, 1853–1864.

(d) Zhu, X.; Tsuji, H.; Navarrete, J. T. L.; Casado, J.; Nakamura, E. *J. Am. Chem. Soc.* **2012**, *134*, 19254–19259. (e) Wu, J.-S.; Cheng, S.-W.; Cheng, Y.-J.; Hsu, C.-S. *Chem. Soc. Rev.* **2015**, *44*, 1113–1154.

[51] Fukuda, M.; Sawada, K.; Yoshino, K. *Jpn. J. Appl. Phys.* **1989**, *28*, L1433–L1435.

[52] Fukuda, M.; Sawada, K.; Yoshino, K. *J. Polym. Sci. Part A: Polym. Chem.* **1993**, *31*, 2465–2471.

[53] Pei, Q.; Yang, Y. *J. Am. Chem. Soc.* **1996**, *118,* 7416–7417.

[54] For poly(2,7-fluorene)s: (a) Ohmori, Y.; Uchida, M.; Muro, K. Yoshino, K. *Jpn. J. Appl. Phys.* **1991**, *30*, L1941–L1943. (b) Janietz, S.; Bradley, D. D. C.; Grell, M.; Giebeler, C.; Ibnbasekaran, M.; Woo, E. P. *Appl. Phys. Lett.* **1998**, *73*, 2453–2455.

[55] Ranger, M.; Leclerc, M. *Chem. Commun.* **1997**, 1597–1598. (b) Ranger, M.; Rondeau, D.; Leclerc, M. *Macromolecules* **1997**, *30,* 7686–7691.

[56] Mikroyannidis, J. A.; Yu, Y.-J.; Lee, S.-H.; Jin. J.-I. *J. Polym.Sci.* **2006**, *44*, 4494–4507.

[57] Kim, D. Y.; Hong, J. M.; Kim, J. K.; Cho, H. N.; Kim, C. Y. *Macromol. Symp.* **1999**, *143*, 221–230.

[58] Mo, Y.; Jiang, X.; Cao, D. *Org. Lett.* **2007**, *9*, 4371–4373.

[59] Yamamoto, T.; Morita, A,; Miyazaki, Y.; Maruyama, T.; Wakayama, H.; Zhou, Z.; Nakamura, Y.; Kanbara, T.; Sasaki, S.; Kubota, L. *Macromolecules* **1992**, *25*, 1214–1223. (b) Saito, N.; Kanbara, T.; Sato, T.; Yamamoto, T. *Polym. Bull*. **1993**, *30*, 285–290.

[60] Kreyenschmidt, M.; Uckert, F.; Müllen, K. *Macromolecules* **1995**, *28*, 4577–4582.

[61] Song, S.; Jin, Y.; Kim, A. H.; Moon, J.; Kim, K.; Kim, J. Y.; Park., S. H.; Lee, K.; Suh, H. *Macromolecules* **2008**, *41*, 7296–7305.

[62] Setayesh, S.; Marsitzky, D.; Müllen, K. *Macromolecules* **2000**, *33*, 2016–2020.

[63] Scherf, U.; Müllen, K. *Die Makromol. Chem. Rapid Commun*. **1991**, *12*, 489–497.

[64] Wu, Y.; Li, J.; Fu, Y.; Bo, Z. *Org. Lett.*, **2004**, *6*, 3485–3487.

[65] Marsitzky, D.; Vestberg, R.; Blainey, P.; Tang, B. T.; Hawker, C. J.; Carter, K. R. *J. Am. Chem. Soc.* **2001**, *123*, 6965–6972. (b) Setayesh, S.; Grimsdale, A. C.; Weil, T.; Enkelmann, V.; Mu¨llen, K.; Meghdadi, F.; List, E. J. W.; Leising, G. *J. Am. Chem. Soc*. **2001**, *123*, 946–953. (c) Gaal, M.; List, E. J. W.; Scherf, U. *Macromolecules* **2003**, *36*, 4236–4237. (d) Shen, W.-J.; Dodda, R.; Wu, C.-C.; Wu, F.-I.; Liu, T.-H.; Chen, H.- H.; Chen, C. H.; Shu, C.-F. *Chem. Mater*. **2004**, *16*, 930–934.

[66] Zotti, G.; Schiavon, G.; Berlin, A.; Fontana, G.; Pagani, G. *Macromolecules* **1994**, *27*, 1938–1942.

[67] Asawapirom, U.; Scherf, U. *Macromol. Rapid Commun*. **2001**, *22,* 746–749.

[68] For poly(cyclopentadithiophene)s: (a) Coppo, P.; Cupertino, D. C.; Yeates, S. G.; Turner, M. L. *J. Mater. Chem.* **2002**, *12*, 2597–2599. (b) Coppo, P.; Cupertino, D. C.; Yeates, S. G.; Turner, M. L. *Macromolecules* **2003**, *36*, 2705–2711. (c) Coppo, P.; Turner, M. *J. Mater. Chem.* **2005**, *15*, 1123–1133. (d) Wu, C.-G.; Lu, M.-I.; Chang, S.-J.; Wei, C.-S. *Ad*v. *Funct. Mater.* **2007**, *17*, 1063–1070.

[69] For OLEDs of silicon-bridged π-conjugated polymers: (a) Beaupre, S.; Boudreault, P. L.; Leclerc, M. *Adv. Mater.* **2010**, *22*, E6–E27. (b) Chan, K. L.; McKiernan, M. J.; Towns, C. R.; Holmes, A. B. *J. Am. Chem. Soc.* **2005***, 127*, 7662–7663. (c) Sanchez, J. C.; DiPasquale, A. G.; Rheingold, A. L.; Trogler, W. C. *Chem. Mater.* **2007**, *19*, 6459–6470.

[70] For OFETs of silicon-bridged π-conjugated polymers: (a) Bassi, M. J.; Benatto, L.; Wouk, L.; Holakoei, S.; Oliveira, C. K.; Rocco, M. L. M.; Roman, L. S. *Phys. Chem. Chem. Phys*. **2020**, *22*, 19923–19931. (b) Usta, H.; Facchetti, A.; Marks, T. J. *J. Am.*

Chem. Soc. **2006**, *128*, 9034–9035. (c) Xiao, H.; Leng, B.; Tian, H. *Polymer* **2005**, *46*, 5707–5713.

[71] For examples of silicon-bridged π-conjugated polymers: (a) Chan, K. L.; McKierman, M. J.; Towns, C. R.; Holmes, A. B. *J. Am. Chem. Soc.* **2005**, *127*, 7662–7663. (b) Lu, G.; Usta, Y.; Guzei, I. A.; West, R. *Silicon Chem.* **2002**, *1*, 57–60. (c) Wang, E.; Li, C.; Peng, J.; Cao, Y. *J. Polym. Sci. A Polym. Chem.* **2007**, *45*, 4941–4949. (d) Chan, K. L.; Watkins, S. E.; Mak, C. S. K.; McKiernan, M. J.; Towns, C. R.; Pascu, S. I.; Holmes, A. B. *Chem. Commun.* **2005**, *46*, 5766–5768. (e) Mo, Y.; Tian, R.; Shi, W.; Cao, Y. *Chem. Commun*. **2005**, *39*, 4925–4926. (f) Zhang, X.; Jiang, C.; Mo, Y.; Xu, Y.; Shi, H.; Cao, Y. *Appl. Phys. Lett.* **2006**, *88*, 051116/1–051116/3. (g) Xu, C.; Yamada, H.; Wakamiya, A.; Yamaguchi, S.; Tamao, K. *Macromolecules* **2004**, *37*, 8978–8983. (h) Ohshita, J.; Kumura, K.; Lee, K.-H.; Kunai, A.; Kwak, Y.-W.; Son, E.-C.; Kunugi, Y. *J. Polym. Sci. A Polym. Chem*. **2007**, *45*, 4588–4596. (i) Liao, L.; Dai, L.; Smith, A.; Durstock, M.; Lu, J.; Ding, J.; Tao, Y. *Macromolecules* **2007**, *40*, 9406–9412. (J) Ohshita, J.; Hamamoto, D.; Kimura, K.; Kunai, A. *J. Organometal. Chem*. **2005**, *690*, 3027–3032. (k) Xiao, H.; Leng, B.; Tian, H. *Polymer* **2005**, *46*, 5707–5713.

[72] For a review on cyclopolymerization of 1,6-heptadiynes: (a) Choi, A. K.; Gal, Y. S.; Jin, S. H.; Kim, H. K. *Chem. Rev.* **2000**, *100*, 1645–1682. For selected examples: (b) Lee, H.-J.; Choi, S.-K.; Gal, Y.-S. *J. Macromol. Sci. Pure Appl. Chem.* **1995**, *A32*, 1863–1874. (c) Gal, Y.-S.; Lee, H.-J.; Choi, S.-K. *Macromol. Rep.* **1996**, *A33*, 57–63.

[73] Still, J. K.; Frey, D. A. *J. Am. Chem. Soc.* **1961**, *83*, 1697–1701.

[74] Fox, H. H.; Wolf, M. O.; O'Dell, R.; Lin, B. L.; Schrock, R. R.; Wrighton, M. S. *J. Am. Chem. So*c. **1994**, *116*, 2827–2843. (b) Kang, E. H.; Kang, C.; Yang, S.; Oks, E.; Choi, T. L. *Macromolecules* **2016**, *49*, 6240–6250.

[75] Jung, K.; Kang, E. H.; Sohn, J. H.; Choi, T. L. *J. Am. Chem. Soc.* **2016**, *138*, 11227–11233.

[76] Tang, B. Z.; Law, C. C. W.; Lam, J. W. Y.; Dong, Y.; Tong, H. *Macromolecules* ***2005***, *38*, 660–662.

[77] For OLEDs of ladder π-conjugated polymers: (a) Scherf, U. *J. Mater. Chem*. **1999**, *9*, 1853–1864. (b) Piok, T.; Gamerith, S.; Gadermaier, C.; Plank, H.; Wenzl, F. P.; Patil, S.; Montenegro, R.; Kietzke, T.; Neher, D.; Scherf, U.; Landfester, K.; List, E. J. W. *Adv. Mater*. **2003**, *15*, 800–804.

[78] For OFETs of ladder π-conjugated polymers: (a) Durban, M. M.; Kazarinoff, P. D.; Segawa, Y.; Luscombe, C. K. *Macromolecules* **2011**, *44* , 4721–4728. (b) Babel, A.; Jenekhe, S. A. *Adv. Mater*. **2002**, *14* , 371–374. (c) Babel, A.; Jenekhe, S. A. *J. Am. Chem. Soc*. **2003**, *125*, 13656–13657.

[79] Goldfinger, M. B.; Swager, T. M. *J. Am. Chem. Soc.* **1994**, *116*, 7895–7896.

[80] Yang, W.; Lucotti, A.; Tommasini, M.; Chalifoux, W. A. *J. Am. Chem. Soc*. **2016**, *138*, 9137–9144.

[81] (a) Yang, X. Y.; Dou, X.; Rouhanipour, A.; Zhi, L. J.; Rader, H. J.; Müllen, K. *J. Am. Chem. Soc.* **2008**, *130*, 4216–4217.

[82] For examples of synthesis of ladder π-conjugated polymers by the Scholl reaction: (a) Huang, W.; Zhang, H.; Ma, J.; Chen, M.; Zhu, H.; Wang, W. *J. Mater. Chem. C* **2015**, *3*, 6200–6208. (b) Narita, A.; Wang, X. Y.; Feng, X.; Müllen, K. *Chem. Soc. Rev.* **2015**, *44*, 6616–6643. (c) Takagi, K.; Yamada, Y. *Polymer* **2019**, *179*,

121607–121613. (d) Dössel, L.; Gherghel, L.; Fengand, X.; Müllen, K. *Angew. Chem., Int. Ed*. **2011**, *50*, 2540–2543.

[83] Shintani, R.; Iino, R.; Nozaki, K. *J. Am. Chem. Soc*. **2016**, *138*, 3635–3638.

[84] Shintani, R.; Kishikawa, S.; Nakamura, K.; Tsuda, T.; Nozaki, K. *Chem. Commun.* **2019**, *55*, 1072–1075.

Chapter 2

Rhodium-Catalyzed Stitching Polymerization of 1,5-Hexadiynes and Related Oligoalkynes

2.1 Introduction

Bridged π-conjugated compounds are intensively investigated as useful structural motifs for functional organic materials due to their optoelectronic properties derived from the extended π-systems with rigid planar structures.[1] They also often appear in (a part of) repeating units of π-conjugated (co)polymers,[2,3] which are typically synthesized by condensation (co)polymerization of preformed bridged π-conjugated monomers. Although this synthetic process is a powerful and reliable approach, applicable repeating units are inherently limited to stable and isolable structures as monomers.

Recently, our group developed a rhodium/diene-catalyzed stitching reaction as a new strategy for the intermolecular synthesis of polycyclic bridged π-conjugated compounds through multiple carbon–carbon bond formations via successive insertion of alkynes.[4] This method allows for the construction of a rigid planar structure and extension of π-conjugation at the same time in a single catalytic process. Based on this attractive feature of the stitching reaction, the author imagined that polymers having a bridged π-conjugated repeating unit could be readily synthesized from easily accessible non-conjugated oligoalkynes without the necessity of preparation of corresponding π-conjugated monomers beforehand, and this would be particularly advantageous when the repeating unit is difficult to prepare as a stable monomer. In this Chapter, the author disclose the new polymerization strategy, rhodium-catalyzed stitching polymerization, for the synthesis of π-conjugated polymers with bridged repeating units by employing 1,5-

hexadiynes and their extended triynes and a tetrayne as monomers which possess both terminal and internal alkyne moieties.[5–8]

2.2 Results and Discussion

2.2.1 Reaction development and structural elucidation

A schematic representation of the proposed rhodium-catalyzed stitching polymerization pathway of 1-aryl-1,5-hexadiyne as a model monomer is illustrated in Scheme 1.[9] A catalytic amount of organorhodium(I) complex undergoes insertion of a terminal alkyne of the monomer to give alkenylrhodium(I) intermediate **A**.[10] Successive insertion of a terminal alkyne of another monomer would lead to dienylrhodium(I) species **B**. This then undergoes intramolecular insertion of an internal alkyne of the initially incorporated monomer in a six-*exo-dig* fashion to form a six-membered ring with concomitant generation of trienylrhodium(I) species **C**. Subsequent six-membered ring-forming intramolecular insertion of an internal alkyne of the secondly incorporated monomer gives tetraenylrhodium(I) species **D** possessing a conjugated bicyclic structure. Repeating this four-step sequence would eventually lead to π-conjugated polymer **E**.

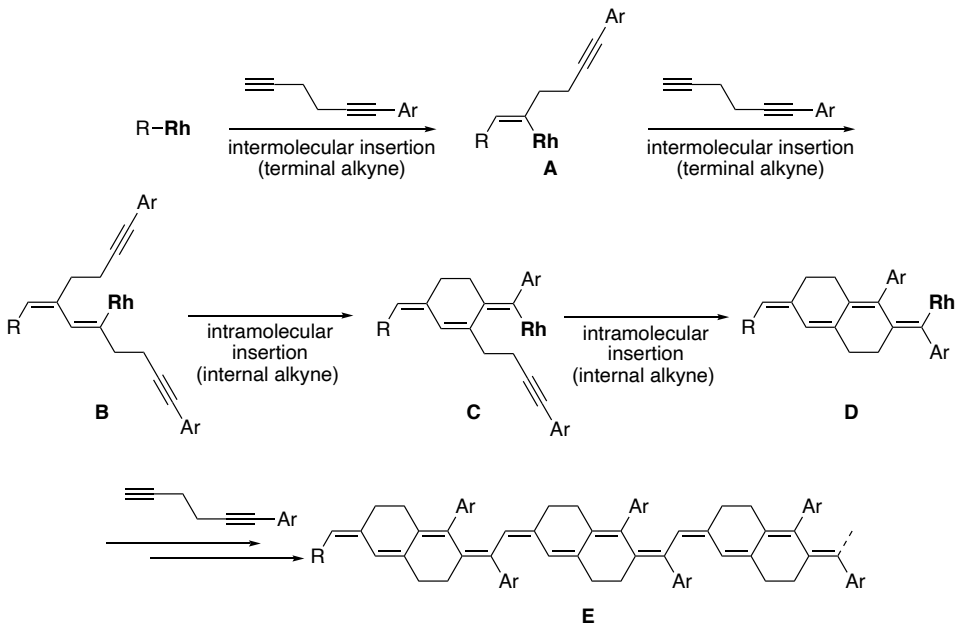

Scheme 1. Schematic representation of rhodium-catalyzed stitching polymerization of 1-aryl-1,5-hexadiyne

As a starting point, the author employed 1-(4-methylphenyl)-1,5-hexadiyne as the monomer and found that the polymerization proceeded smoothly in the presence of $[Rh(OH)(cod)]_2$ (3 mol% Rh) in THF at 60 ºC to give 81% yield of **poly-1a** after reprecipitation (Table 1, entry 1). The number-averaged molecular weight (M_n) was calculated to be 5400 g mol^{-1} with M_w/M_n of 1.8 using size-exclusion chromatography against a polystyrene standard. In comparison, the presence of a phosphine ligand such as PPh_3 or binap significantly lowered the polymerization efficiency (entries 2 and 3).

Table 1. Rhodium-catalyzed polymerization of **1a**

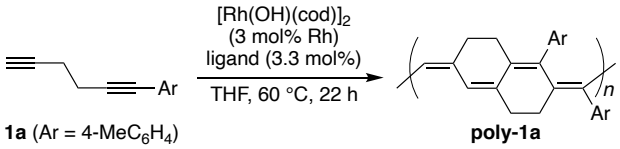

entry	ligand	yield (%)	M_n (g/mol)[a]	M_w/M_n[a]
1	none	81	5400	1.8
2	PPh_3	42	6000	2.2
3	Binap	23	5900	2.4

[a] Determined using size-exclusion chromatography against a polystyrene standard.

The structural information of **poly-1a** was mainly obtained by ^{13}C NMR analysis. Figure 1 shows ^{13}C NMR spectra of (a) monomer **1a** and (b) **poly-1a** prepared in Table 1, entry 1. According to these spectra, **poly-1a** showed essentially no residual peaks in the sp-carbon region, indicating that both terminal and internal alkynes of monomer **1a** were successfully incorporated into the main chain as alkenyl sp^2-carbons. The chemical shifts of methylene carbons were also significantly downfield-shifted, which corresponds to the change of propargylic carbons to allylic carbons.

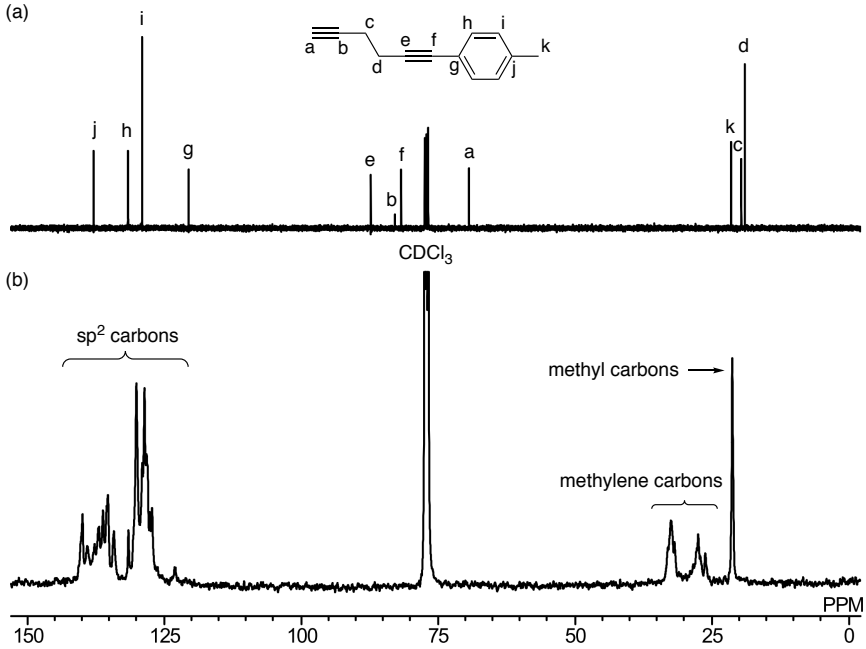

Figure 1. ^{13}C NMR spectra of (a) monomer **1a** and (b) **poly-1a** obtained in Table 1, entry 1 (101 MHz in $CDCl_3$ at 30 ºC)

To gain more insights into the structure of **poly-1a**, monomer **1a-^{13}C** possessing a ^{13}C-labeled carbon at one of the internal alkyne carbons was prepared, and conducted the present polymerization reaction to give **poly-(1a-^{13}C)** in 83% yield with M_n of 6400 g mol^{-1} and M_w/M_n of 1.9 (eq. 1). As indicated by the quantitative ^{13}C NMR spectrum in Figure 2, although some labeled internal alkyne peak remained at 90 ppm, more than 95% of the labeled carbon was shifted to sp^2-carbon region as two sets of peaks (140 ppm and 134 ppm) with almost equal intensity, which supports the proposed stitched structure of **poly-1a**.

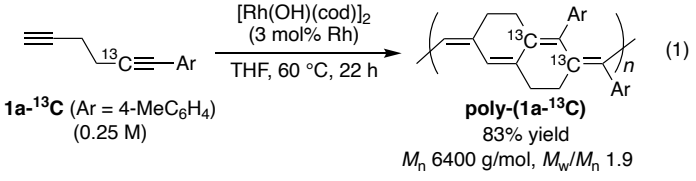

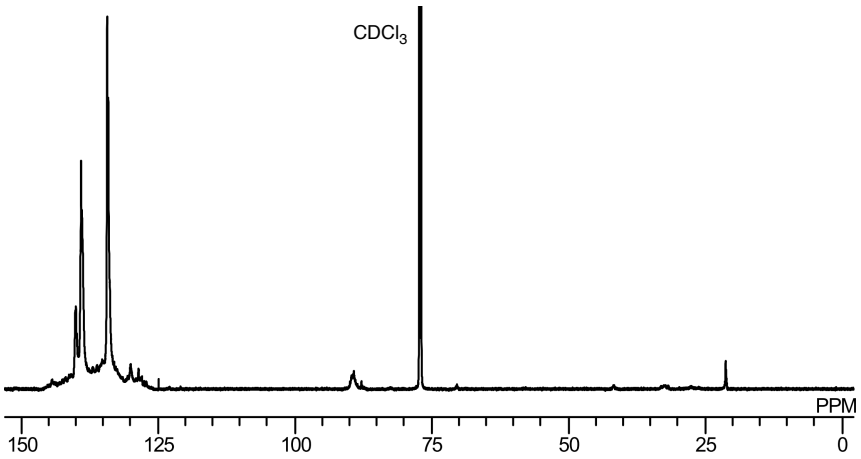

Figure 2. Inverse gated ^{1}H decoupling ^{13}C NMR spectrum of **poly-(1a-^{13}C)** obtained in eq. 1 (176 MHz in $CDCl_3$ at 25 ºC)

In addition, the author verified its structure by comparing the observed ^{13}C NMR chemical shifts with the calculated ones for the middle unit of model trimer **tri-1a** due to the lack of reference compounds in small molecules for experimental comparison. The selected values of the middle section of **tri-1a** in transoid-transoid conformer are shown in Figure 3-(a). Based on these data, observed signals for sp^3-carbon region of **poly-1a** are consistent with the proposed structure, and two sets of peaks in **poly-(1a-^{13}C)** at 140 ppm and 134 ppm with almost equal intensity can also be reasonably explained. Moreover, considering the existence of transoid/cisoid conformers at the bolded carbon–carbon single bonds (Figure 3-(a)–(d)), the red carbon signal was calculated to appear at 137.7–136.4 ppm and the blue carbon signal was calculated to appear at 132.6–132.2 ppm depending on the conformation. Accordingly, the observed ^{13}C-labeled carbon chemical shifts at 140–139 and 134 ppm could be reasonably assigned (Figure 4). These results indicate that the main chain structure of polymers prepared in the present catalytic conditions is consistent with the proposed structure.

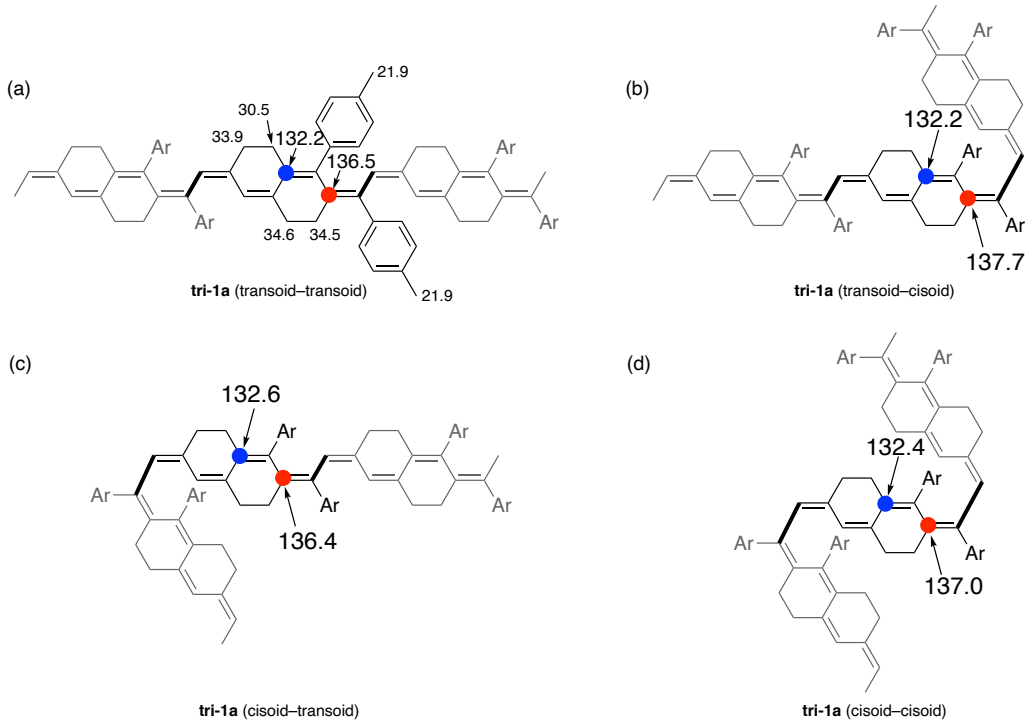

Figure 3. Selected ^{13}C NMR chemicals shifts (ppm) for the corresponding carbons of **tri-1a** in (b) transoid–transoid, (c) transoid–cisoid, (d) cisoid–transoid, (e) cisoid–cisoid conformers (Ar = 4-MeC_6H_4) by DFT calculation at the B3LYP/6-31G(d) level of theory

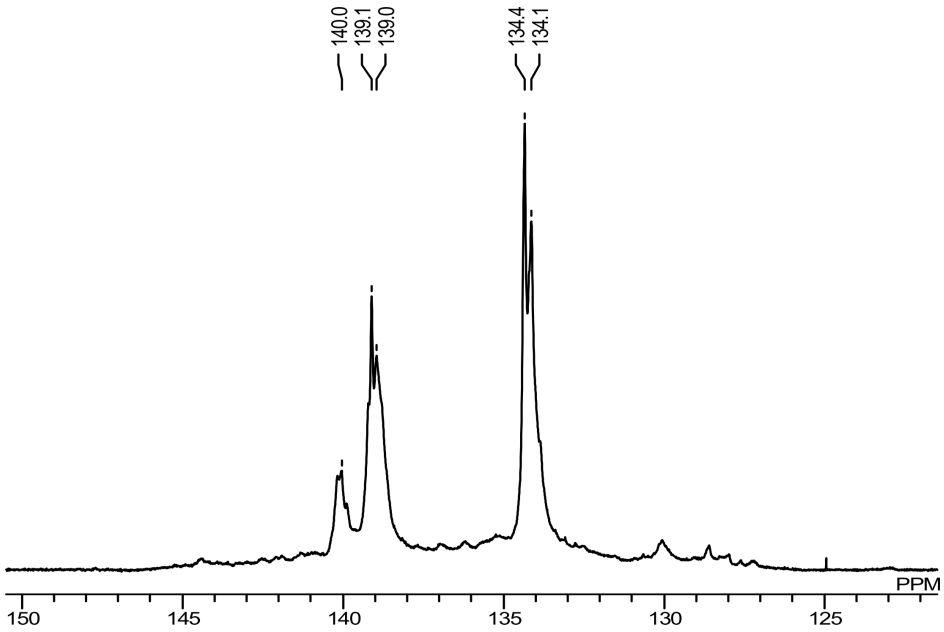

Figure 4. 150–122 ppm region of inverse gated ^{1}H decoupling ^{13}C NMR spectrum of **poly-(1a-^{13}C)** in $CDCl_3$

2.2.2 Reaction scope for the polymerization of diyne monomers and their derivatives

The present stitching polymerization could also be applied to other 1-aryl-1,5-hexadiynes. For example, monomers having an electron-donating group (**1b**) or an electron-withdrawing group (**1c** and **1d**) at the 4-position of the aryl group gave the corresponding stitched polymers **poly-1b**, **poly-1c**, and **poly-1d** in 71–80% yield with M_n of 3000–9700 g mol^{-1} (eq. 2). Polymerization of monomers **1e** and **1f** having 3,5-dialkylphenyl group also proceeded smoothly to give corresponding **poly-1e** and **poly-1f** in 71–90% yield with somewhat higher molecular weight (M_n 15600–21000 g mol^{-1}). The ^{13}C NMR spectra of these polymers suggest that the main chain structures are the same as that of **poly-1a** with essentially no residual peaks in the sp-carbon region.

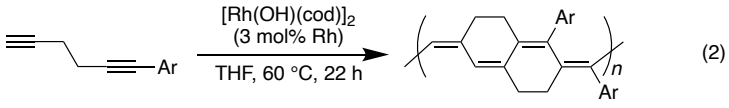

(2)

1b: Ar = 4-$MeOC_6H_4$
1c: Ar = 4-$MeO_2CC_6H_4$[a]
1d: Ar = 4-$CF_3C_6H_4$[a]
1e: Ar = 3,5-$Me_2C_6H_3$
1f: Ar = 3,5-*t*-$Bu_2C_6H_3$
(0.25 M)

poly-1b: 80% yield, M_n 5200 g/mol, M_w/M_n 2.2
poly-1c: 72% yield, M_n 3000 g/mol, M_w/M_n 1.9
poly-1d: 71% yield, M_n 9700 g/mol, M_w/M_n 1.4
poly-1e: 71% yield, M_n 21000 g/mol, M_w/M_n 1.8
poly-1f: 90% yield, M_n 15600 g/mol, M_w/M_n 1.6

[a] 6 mol% of rhodium catalyst was used in the presence of 30 mol% of cod.

In addition, the author also examined the polymerization of triynes **2** for the synthesis of polymers possessing a longer bridged π-conjugated repeating unit. As shown in eq. 3, polymerization of **2a** took place efficiently to give **poly-2a** in 70% yield with M_n of 7100 g mol^{-1} and M_w/M_n of 2.2. According to the quantitative ^{13}C NMR spectrum of this polymer (Figure 5), some residual peaks were observed in the sp-carbon region and peaks observed at 20 and 19 ppm could be assigned as propargylic carbons. Based on the area ratio of sp^2, sp, and sp^3 carbon peaks, however, incorporation efficiency of internal

alkynes into the main chain was estimated to be as high as 93%. This indicates that the desired stitching polymerization of triyne **2a** did proceed successfully for the most part with some minor defects. Similarly, **poly-2b** was obtained in 68% yield with M_n of 11200 g mol^{-1} and M_w/M_n of 1.8, and its incorporation efficiency of internal alkynes into the main chain was estimated to be 86%.

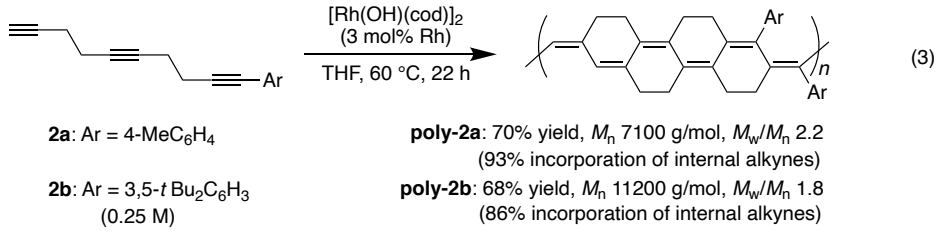

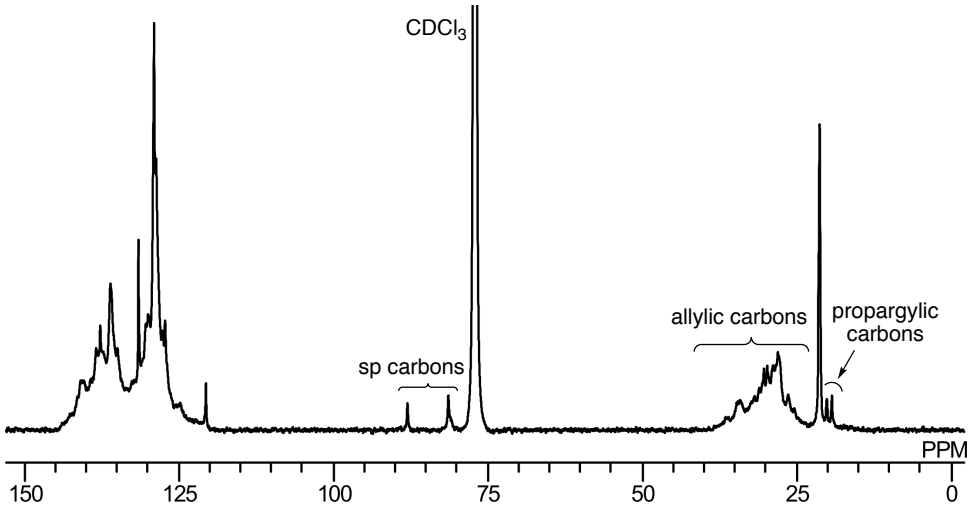

Figure 5. Inverse gated ^{1}H decoupling ^{13}C NMR spectrum of **poly-2a** obtained in eq. 3 (176 MHz in $CDCl_3$ at 25 °C)

Furthermore, it was found that even tetrayne **3** could be employed for the present stitching polymerization, although the incorporation efficiency of internal alkynes became somewhat lower. Thus, **poly-3** was obtained in 69% yield with M_n of 5000 g mol^{-1} and M_w/M_n of 2.0 (eq. 4), and ca. 82% of internal alkynes were stitched into the main chain according to the same analysis as that for **poly-2**.

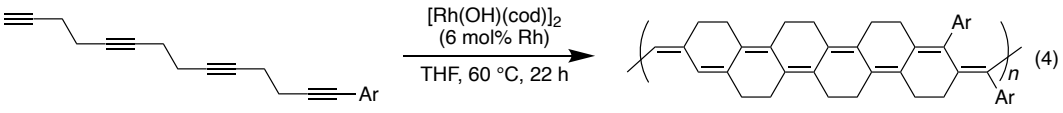

(4)

3: Ar = 4-MeC_6H_4
(0.25 M)

poly-3: 69% yield, M_n 5000 g/mol, M_w/M_n 2.0
(82% incorporation of internal alkynes)

2.2.3 Optical properties of the obtained polymers

These polymers can also be regarded as *cis*-polyacetylenes with rigid repeating units, and the author examined their optical properties using UV-vis spectrophotometry. As shown in Figure 6 and Table 2, **poly-1a** derived from diyne **1a** possessing 4-MeC_6H_4 group showed absorption maximum at 434 nm and its absorption edge reached up to ca. 615 nm. **Poly-1** possessing relatively electron-rich aryl groups (**poly-1a** (4-MeC_6H_4), **poly-1b** (4-MeOC_6H_4), and **poly-1e** (3,5-$Me_2C_6H_3$)) displayed similar absorption profiles with one another, whereas **poly-1** with electron-deficient aryl groups (**poly-1c** (4-$MeO_2CC_6H_4$) and **poly-1d** (4-$CF_3C_6H_4$)) showed bathochromic shifts in their absorption edge. It is worth noting that **poly-1f** possessing 3,5-*t*$Bu_2C_6H_3$ groups showed more significant bathochromic shift in its absorption spectrum. This observation is consistent with the reported trend for polyarylacetylenes and could be attributed to more effective conjugation in the main chain due to the restricted conformations of the bulky 3,5-*t*$Bu_2C_6H_3$ groups.[11]

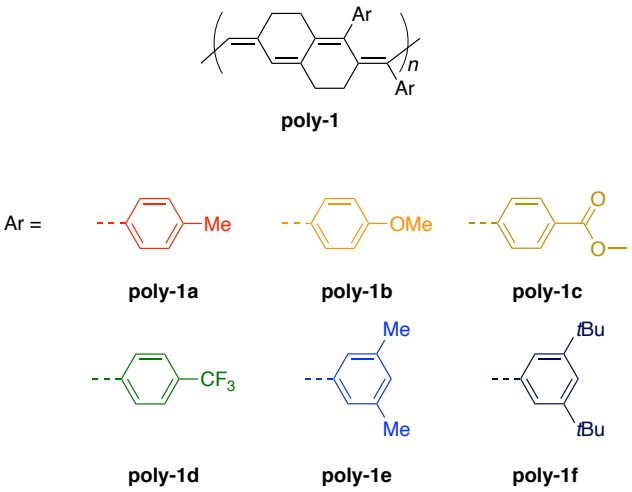

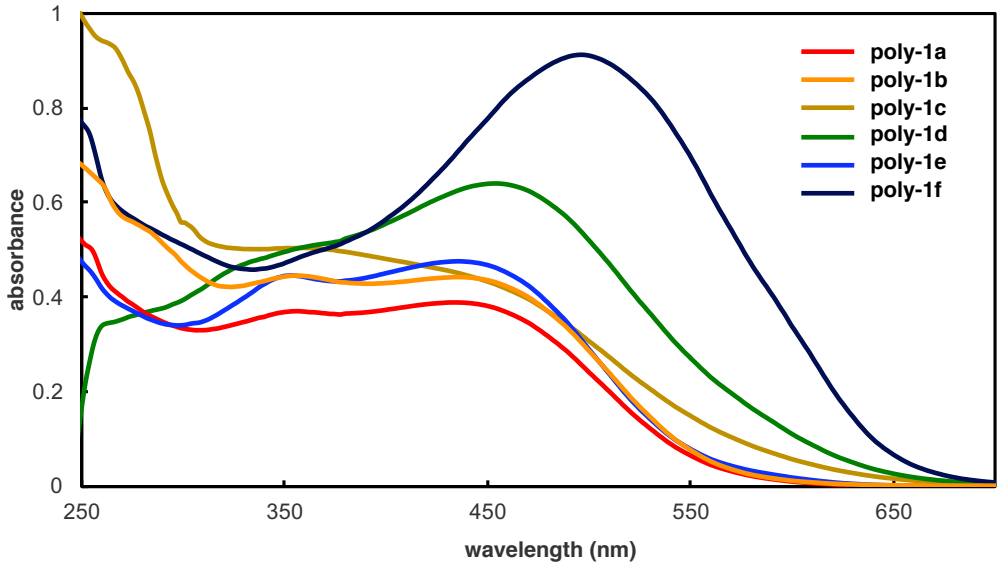

Figure 6. UV-vis spectra of **poly-1a** (red line; at 1.6 x 10^{-2} g/L), **poly-1b** (orange line; at 1.6 x 10^{-2} g/L), **poly-1c** (yellow line; at 1.4 x 10^{-2} g/L), **poly-1d** (green line; at 2.4 x 10^{-2} g/L), and **poly-1e** (blue line; at 1.6 x 10^{-2} g/L), **poly-1f** (deep blue line; at 3.0 x 10^{-2} g/L) in THF at 25 ºC

Table 2. UV-vis absorption of **poly-1**

polymer	λ_{max}/nm (absorbance/a.u.)	λ_{edge}/nm
poly-1a	356 (0.37), 434 (0.39)	ca. 615
poly-1b	355 (0.44), 435 (0.44)	ca. 615
poly-1c	359 (0.50)	ca. 685
poly-1d	454 (0.70)	ca. 700
poly-1e	353 (0.45), 436 (0.68)	ca. 630
poly-1f	496 (0.91)	ca. 705

As shown in Figure 7, it was found that absorption edge showed bathochromic shift by extending the bridged π-conjugation unit as demonstrated with **poly-1a** (λ_{edge} = ca. 615 nm), **poly-2a** (λ_{edge} = ca. 630 nm), and **poly-3** (λ_{edge} = ca. 660 nm). In comparison, *cis*-

poly-4-methylphenylacetylene (M_n = 30000 g mol^{-1}, M_w/M_n = 1.3), a related π-conjugated polymer possessing no bridged π-conjugation units, showed absorption maximum at 329 nm with absorption edge of ca. 520 nm. These results strongly suggest that polymers obtained in the present stitching polymerization show effective extension of π-conjugation by introduction of rigid bridged structures during the polymerization reaction.

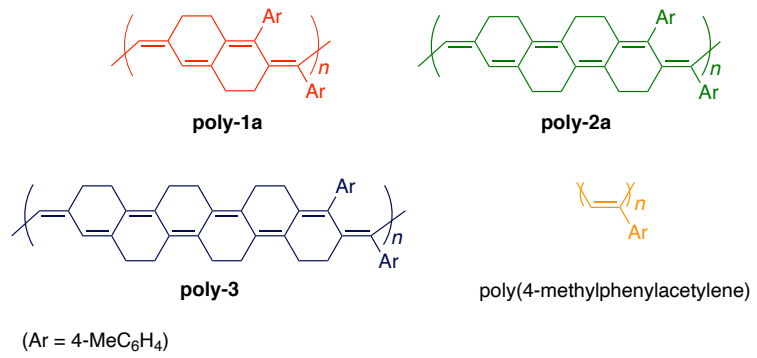

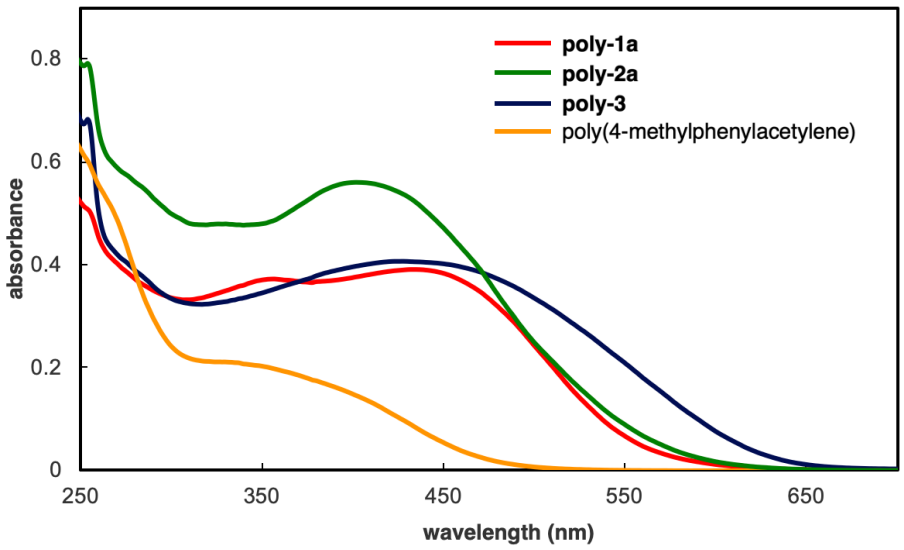

Figure 7. UV-vis spectra of **poly-1a** (red line; at 1.6 x 10^{-2} g/L), **poly-2a** (green line; at 2.1 x 10^{-2} g/L), **poly-3** (deep blue line; at 1.3 x 10^{-2} g/L), and poly(4-methylphenylacetylene) (orange line; at 1.2 x 10^{-2} g/L) in THF at 25 ºC

2.2.4 Post-derivatization of the obtained polymers

The author explored post-derivatization of the obtained polymers. For example, **poly-1f** was found to be readily oxidized by treatment with DDQ to give poly(2,6-naphthylene vinylene) **poly-1f-ox** in 94% yield (eq. 5), which showed hypsochromic shift in the UV-vis absorption spectrum (λ_{max} = 355 nm whereas λ_{max} = 496 nm for **poly-1f**) and was found emissive (λ_{max} = 483 nm whereas non-emissive for **poly-1f**) (Figure 8).[12,13] The same oxidation protocol was also applied to **poly-2b** derived from triyne **2b** to give poorly soluble polymer **poly-2b-ox**, which is presumably the corresponding poly(2,8-chrysenylene vinylene) based on its UV-vis absorption and emission spectra (eq. 6 and Figure 9. These results demonstrate the potential utility of **poly-1–3** as promising precursors for poly(arylene vinylene)s possessing an extended polyaromatic hydrocarbon repeating unit.[14]

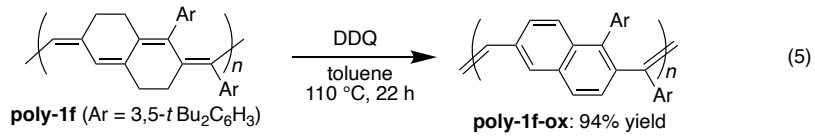

poly-1f (Ar = 3,5-*t* $Bu_2C_6H_3$) **poly-1f-ox**: 94% yield (5)

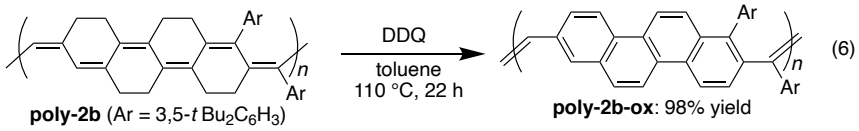

poly-2b (Ar = 3,5-*t* $Bu_2C_6H_3$) **poly-2b-ox**: 98% yield (6)

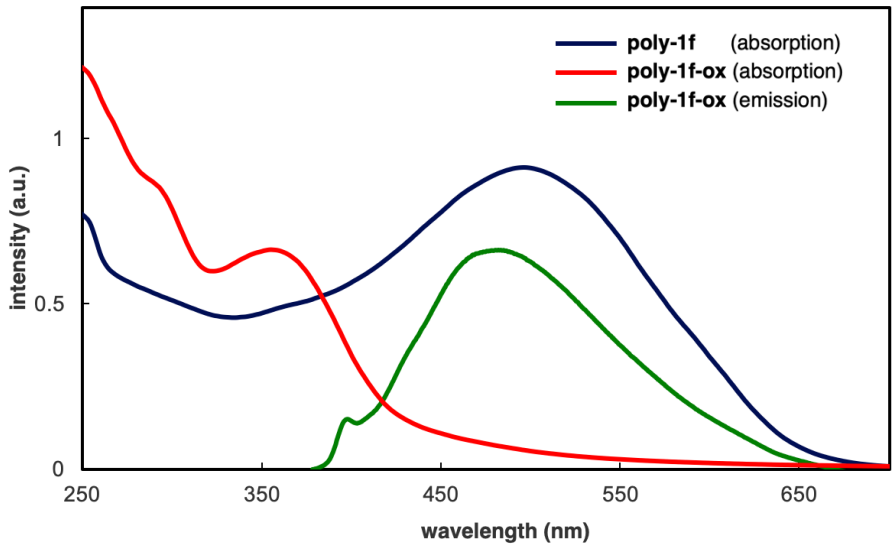

Figure 8. UV-vis spectra of **poly-1f** (deep blue line; at 3.0 x 10^{-2} g/L) and **poly-1f-ox** (red line; at 2.7 x 10^{-2} g/L), and fluorescence spectrum of **poly-1f-ox** (green line; at 5.1 x 10^{-3} g/L; excited at 355 nm) in THF at 25 ºC

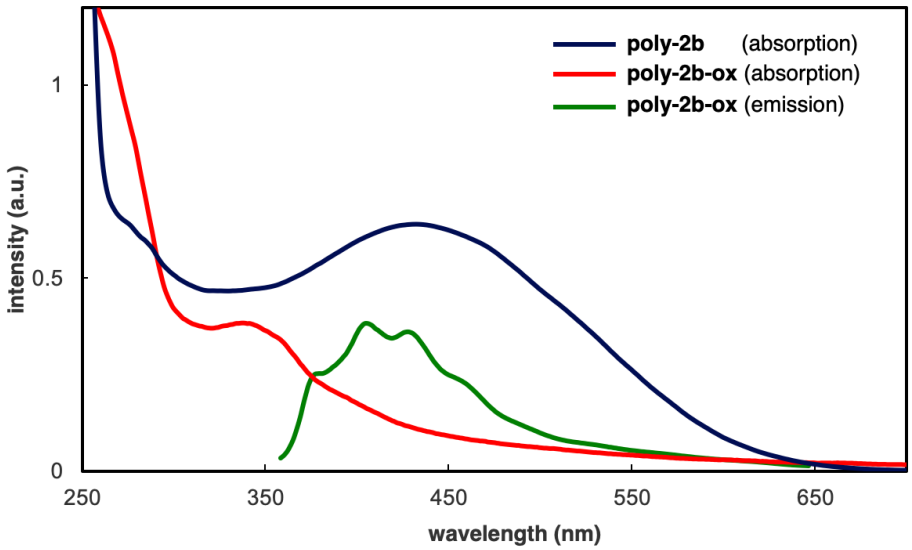

Figure 9. UV-vis spectra of **poly-2b** (deep blue line; at 3.1 x 10^{-2} g/L) and **poly-2b-ox** (red line; soluble part), and fluorescence spectrum of **poly-2b-ox** (green line; soluble part; excited at 338 nm) in THF at 25 ºC

2.3 Conclusion

The author developed a new mode of polymerization, rhodium-catalyzed stitching polymerization, for the synthesis of π-conjugated polymers with bridged repeating units by employing 1,5-hexadiynes containing both terminal and internal alkyne moieties as monomers. The polymerization proceeded smoothly with high degree of stitching efficiency under mild conditions, and 1,5,9-decatriyne and 1,5,9,13-tetradecatetrayne monomers could also be employed. Because the use of preformed bridged π-conjugated monomers is not required, this method could be particularly beneficial for the synthesis of polymers consisting of a repeating unit that is difficult to prepare as a stable monomer.

2.4 Experimental Section

General

All air- and moisture-sensitive manipulations were carried out with standard Schlenk techniques under nitrogen. NMR spectra were recorded on JEOL JNM-ECS400, Agilent Unity-Inova500, or BRUKER AVANCE Ⅲ 700 spectrometers. Size-exclusion chromatography analyses were performed with JASCO-GPC900 columns using THF as an eluent and the molecular weights were calibrated against standard polystyrene samples. Mass spectra were recorded on JEOL JMS700 spectrometer. Thermogravimetric analyses were performed with SII Exstar TG/DTA6200 under nitrogen atmosphere. UV-vis spectra were recorded on HITACHI U-2900 spectrophotometer. Fluorescence spectra were recorded on HORIBA FLmax-3 Spectrofluorometer.

Et_3N (Wako Chemicals) was distilled over KOH under vacuum. MeOH (Wako Chemicals) was distilled over Mg turnings under nitrogen. EtOH (Kishida Chemical) was dried over K_2CO_3 and degassed by purging nitrogen. CH_2Cl_2 (Nacalai Tesque) was distilled over CaH_2 under nitrogen. THF (Kanto Chemical; dehydrated) and CH_3CN (Wako Chemicals; dehydrated) were degassed by purging nitrogen. 1,5-Hexadiyne (TCI), 4-iodotoluene (TCI), 4-iodoanisole (TCI), methyl 4-iodobenzoate (TCI), 4-bromobenzotrifluoride (Aldrich), 1-iodo-3,5-dimethylbenzene (Wako Chemicals), 1-bromo-3,5-di-*tert*-butylbenzene (Kanto Chemical), 4-methylphenylacetylene (TCI), 4-methylbenzaldehyde (Wako Chemicals), iodomethane-^{13}C (ISOTEC), tetrabromomethane (TCI), paraformaldehyde (Wako Chemicals), 1-(trimethylsilyl)-1-propyne (TCI), hexamethylphosphoric triamide (TCI), PPh_3 (Wako Chemicals), *n*BuLi (Kanto Chemical; 1.55–1.57 M solution in hexane), *t*BuOK (Nacalai Tesque), tetra-*n*-butylammonium fluoride (Wako Chemicals; trihydrate), K_2CO_3 (Wako chemicals), Br_2 (Nacalai Tesque), and CuI (Kanto Chemical) were used as received.

$[Rh(OH)(cod)]_2$,[15] $Pd(PPh_3)_4$,[16] 1,1-diethoxy-3-iodopropane,[17] and dimethyl (1-diazo-2-oxopropyl)phosphonate[18] were synthesized following the literature procedures.

Representative Procedures:

1-(1,5-Hexadiynyl)-4-methylbenzene (1a)

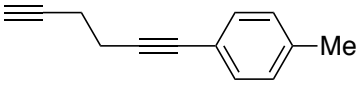

Et_3N (2.68 mL, 19.2 mmol), 1,5-hexadiyne (1.21 g, 15.5 mmol) and THF (6.0 mL) were successively added to a mixture of $Pd(PPh_3)_4$ (22.3 mg, 0.193 mmol), 4-iodotoluene (1.68 g, 7.71 mmol), and CuI (73.6 mg, 0.386 mmol) in THF (5.0 mL) at room temperature, and the resulting mixture was stirred for 7.5 h at room temperature. The precipitates were removed by passing through a pad of silica gel with Et_2O and the solvent was removed under vacuum. The residue was chromatographed on silica gel with hexane to afford compound **1a** as a pale yellow oil (565 mg, 3.36 mmol; 44% yield).

^1H NMR ($CDCl_3$): δ 7.29 (d, $^3J_{HH}$ = 8.3 Hz, 2H), 7.09 (d, $^3J_{HH}$ = 7.8 Hz, 2H), 2.69-2.59 (m, 2H), 2.55-2.45 (m, 2H), 2.33 (s, 3H), 2.04 (t, $^4J_{HH}$ = 2.5 Hz, 1H). ^{13}C NMR ($CDCl_3$): δ 137.9, 131.6, 129.1, 120.6, 87.3, 82.9, 81.8, 69.4, 21.5, 19.7, 19.0. HRMS (EI) calcd for $C_{13}H_{12}$ (M^+) 168.0934, found 168.0935

1-(1,5-Hexadiynyl-2-^{13}C)-4-methylbenzene (1a-^{13}C)

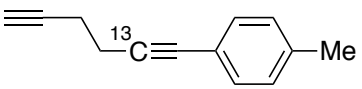

Iodomethane-^{13}C (4.45 g, 31.1 mmol; 99% ^{13}C) was added slowly over 10 min to a solution of PPh_3 (9.23 g, 35.2 mmol) in THF (55 mL) at room temperature and the mixture was refluxed for 1 h. After cooled to room temperature, the precipitates were collected by filtration, washed with THF, and dried under vacuum to afford (methyl-

^{13}C)triphenylphosphonium iodide (CAS 81826-67-7) as a white solid (12.1 g, 29.8 mmol; 96% yield).

^{1}H NMR ($CDCl_3$): δ 7.84-7.79 (m, 3H), 7.79-7.74 (m, 6H), 7.70 (td, $^3J_{HH}$ = 7.7 Hz and $^4J_{PH}$ = 3.7 Hz, 6H), 3.26 (dd, $^1J_{CH}$ = 135 Hz and $^2J_{PH}$ = 13.1 Hz, 3H).

*t*BuOK (4.88 g, 43.5 mmol) was added to a solution of (methyl-^{13}C)triphenylphosphonium iodide (12.1 g, 29.8 mmol) in THF (73 mL) at 0 ºC, and the mixture was stirred for 1 h at room temperature. After cooled to 0 ºC, 4-methylbenzaldehyde (3.58 g, 29.8 mmol) was added slowly over 10 min to it and the resulting mixture was stirred for 14 h at room temperature. The reaction was quenched with saturated NH_4Claq and this was extracted with Et_2O. The organic layer was washed with saturated NaClaq, dried over $MgSO_4$, filtered, and concentrated under vacuum. The residue was chromatographed on silica gel with pentane to afford 1-methyl-4-(vinyl-2-^{13}C)benzene as a colorless oil (4.65 g, 25.1 mmol; 84% yield, 64 wt% in pentane).

^{1}H NMR ($CDCl_3$): δ 7.31 (d, $^3J_{HH}$ = 8.2 Hz, 2H), 7.13 (d, $^3J_{HH}$ = 7.8 Hz, 2H), 6.69 (dd, $^3J_{HH}$ = 17.8 and 11.0 Hz, 1H), 5.69 (dd, $^1J_{CH}$ = 154 Hz and $^3J_{HH}$ = 17.9 Hz, 1H), 5.18 (dd, $^1J_{CH}$ = 160 Hz and $^3J_{HH}$ = 10.6 Hz, 1H), 2.34 (s, 3H). ^{13}C NMR ($CDCl_3$): δ 137.8, 136.9 (d, $^1J_{CC}$ = 70.0 Hz), 135.0, 129.4, 126.3 (d, $^3J_{CC}$ = 4.8 Hz), 112.9, 21.3.

Br_2 (4.50 g, 28.1 mmol) was added slowly over 15 min to a solution of 1-methyl-4-(vinyl-2-^{13}C)benzene (4.65 g, 25.1 mmol; 64 wt% in pentane)) in CH_2Cl_2 (10 mL) at 0 ºC and the mixture was stirred for 30 min at 0 ºC and for 4 h at room temperature. The reaction mixture was quenched with $Na_2S_2O_3$aq, and this was extracted with Et_2O. The organic layer was washed with saturated NaClaq, dried over $MgSO_4$, filtered, and concentrated under vacuum to afford 1-(1,2-dibromoethyl-2-^{13}C)-4-methylbenzene as an orange solid (5.50 g, 19.7 mmol; 79% yield).

^{1}H NMR ($CDCl_3$): δ 7.30 (d, $^{3}J_{HH}$ = 8.2 Hz, 2H), 7.19 (d, $^{3}J_{HH}$ = 7.8 Hz, 2H), 5.19-5.10 (m, 1H), 4.07 (ddd, $^{1}J_{CH}$ = 158 Hz, $^{2}J_{HH}$ = 10.1 Hz, and $^{3}J_{HH}$ = 5.0 Hz, 1H), 4.02 (dt, $^{1}J_{CH}$ = 155 Hz, J_{HH} = 10.3 Hz, 1H), 2.36 (s, 3H). ^{13}C NMR ($CDCl_3$): δ 139.4, 135.8, 129.7, 127.7, 51.2 (d, $^{1}J_{CC}$ = 39.3 Hz), 35.2, 21.4.

*t*BuOK (5.65 g, 50.4 mmol) was added to a solution of 1-(1,2-dibromoethyl-2-^{13}C)-4-methylbenzene (5.50 g, 19.7 mmol) in THF (100 mL) and the mixture was stirred for 16 h at room temperature. The reaction was quenched with H_2O and this was extracted with Et_2O. The organic layer was washed with saturated NaClaq, dried over $MgSO_4$, filtered, and concentrated under vacuum. The residue was chromatographed on silica gel with pentane to afford 1-(ethynyl-2-^{13}C)-4-methylbenzene as a colorless oil (2.30 g, 15.8 mmol; 80% yield, 80 wt% in pentane).

^{1}H NMR ($CDCl_3$): δ 7.40 (d, $^{3}J_{HH}$ = 8.2 Hz, 2H), 7.14 (d, $^{3}J_{HH}$ = 8.7 Hz, 2H), 3.03 (d, $^{1}J_{CH}$ = 251 Hz, 1H), 2.37 (s, 3H). ^{13}C NMR ($CDCl_3$): δ 139.1, 132.2 (d, $^{3}J_{CC}$ = 1.9 Hz), 129.2, 119.2 (d, $^{2}J_{CC}$ = 13.4 Hz), 84.1 (d, $^{1}J_{CC}$ = 176 Hz), 76.6, 21.6.

*n*BuLi (12.2 mL, 18.9 mmol; 1.55 M solution in hexane) was added slowly over 20 min to a solution of 1-(ethynyl-2-^{13}C)-4-methylbenzene (2.30 g, 15.8 mmol; 80 wt% in pentane) in THF (25 mL) at –78 ºC and the mixture was stirred for 40 min. Paraformaldehyde (664 mg, 22.1 mmol) was then added to it, and the resulting mixture was stirred for 13 h at room temperature. The reaction was quenched with saturated NH_4Claq and this was extracted with Et_2O. The organic layer was dried over $MgSO_4$, filtered, and concentrated under vacuum. The residue was chromatographed on silica gel with hexane/EtOAc = 49/1 to afford 3-(4-methylphenyl)-2-propynol-2-^{13}C as a yellow oil (1.58 g, 10.7 mmol; 68% yield).

^{1}H NMR ($CDCl_3$): δ 7.33 (d, $^{3}J_{HH}$ = 8.0 Hz, 2H), 7.12 (d, $^{3}J_{HH}$ = 8.0 Hz, 2H), 4.49 (dd, $^{2}J_{CH}$ = 7.3 Hz and $^{3}J_{HH}$ = 6.3 Hz, 2H), 2.35 (s, 3H), 1.64 (td, $^{3}J_{HH}$ = 6.1 Hz and $^{3}J_{CH}$ = 2.9

Hz, 1H). ^{13}C NMR ($CDCl_3$): δ 138.7, 131.7 (d, $^3J_{CC}$ = 2.9 Hz), 129.2, 119.6 (d, $^2J_{CC}$ = 12.5 Hz), 86.7, 85.1 (d, $^1J_{CC}$ = 219 Hz), 51.6 (d, $^1J_{CC}$ = 73.8 Hz), 21.5.

PPh_3 (3.38 g ,12.9 mmol) was added to a solution of 3-(4-methylphenyl)-2-propynol-2-^{13}C (1.58 g, 10.7 mmol) and tetrabromomethane (4.28 g, 12.9 mmol) in CH_2Cl_2 (36 mL) at 0 ºC and the reaction mixture was stirred for 3 h at 0 ºC. The solvent was removed under vacuum and the residue was chromatographed on silica gel with hexane to afford 1-(3-bromopropyn-1-yl-2-^{13}C)-4-methylbenzene as a yellow oil (1.90 g, 9.04 mmol; 85% yield).

^{1}H NMR ($CDCl_3$): δ 7.34 (d, $^3J_{HH}$ = 7.8 Hz, 2H), 7.12 (d, $^3J_{HH}$ = 7.8 Hz, 2H), 4.17 (d, $^2J_{CH}$ = 7.8 Hz, 2H), 2.35 (s, 3H). ^{13}C NMR ($CDCl_3$): δ 139.2, 131.9 (d, $^3J_{CC}$ = 1.9 Hz), 129.2, 119.2 (d, $^2J_{CC}$ = 13.4 Hz), 87.3 (d, $^1J_{CC}$ = 176 Hz), 83.7, 21.6, 15.7 (d, $^1J_{CC}$ = 81.5 Hz).

*n*BuLi (8.71 mL, 13.5 mmol; 1.55 M solution in hexane) was added slowly over 30 min to a solution of 1-(trimethylsilyl)-1-propyne (2.02 mL, 13.5 mmol) in THF (23 mL) at –78 ºC and the reaction mixture was stirred for 1 h at –78 ºC. A solution of 1-(3-bromopropyn-1-yl-2-^{13}C)-4-methylbenzene (1.90 g, 9.04 mmol) in THF (8.0 mL) was then added slowly over 45 min to it and the mixture was stirred for 1 h at –78 ºC and for 1 h at room temperature. The reaction was quenched with H_2O and this was extracted with Et_2O. The organic layer was washed with saturated NaClaq, dried over $MgSO_4$, filtered, and concentrated under vacuum. The residue was chromatographed on silica gel with hexane to afford (6-(4-methylphenyl)-1,5-hexadiyn-1-yl-5-^{13}C)trimethylsilane as a yellow oil (1.04 g). This oil was dissolved in THF (5.0 mL) and a solution of tetra-*n*-butylammonium fluoride (2.05 g, 6.51 mmol; trihydrate) in THF (10 mL) was added to it at 0 ºC. The reaction mixture was stirred for 1.5 h at 0 ºC, and it was quenched with H_2O. After extraction with Et_2O, the organic layer was washed with saturated NaClaq, dried

over $MgSO_4$, filtered, and concentrated under vacuum. The residue was chromatographed on silica gel with hexane to afford compound **1a-^{13}C** as a yellow oil (617 mg, 3.64 mmol; 40% yield).

^{1}H NMR ($CDCl_3$): δ 7.30 (d, $^3J_{HH}$ = 8.0 Hz, 2H), 7.09 (d, $^3J_{HH}$ = 8.0 Hz, 2H), 2.68-2.61 (m, 2H), 2.53-2.47 (m, 2H), 2.33 (s, 3H), 2.04 (td, $^4J_{HH}$ = 2.7 Hz and $^5J_{CH}$ = 0.7 Hz, 1H). ^{13}C NMR ($CDCl_3$): δ 137.9, 131.6 (d, $^3J_{CC}$ = 2.9 Hz), 129.1, 120.6 (d, $^2J_{CC}$ = 13.4 Hz), 87.3, 82.9 (d, $^3J_{CC}$ = 5.7 Hz), 81.6 (d, $^1J_{CC}$ = 179 Hz), 69.4, 21.5, 19.7 (d, $^1J_{CC}$ = 69.1 Hz), 19.0 (d, $^2J_{CC}$ = 3.8 Hz). HRMS (EI) calcd for $C_{12}{}^{13}CH_{12}$ (M^+) 169.0967, found 169.0974.

1-(1,5,9-Decatriynyl)-4-methylbenzene (2a)

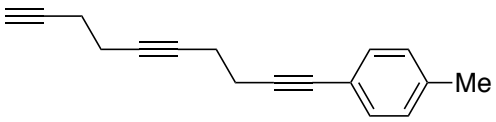

*n*BuLi (7.04 mL, 10.9 mmol; 1.55 M solution in hexane) was added slowly over 15 min to a solution of compound **1a** (1.76 g, 10.4 mmol) in THF (20 mL) at –78 ºC. The reaction mixture was warmed to –50 ºC and hexamethylphosphoric triamide (1.86 g, 10.4 mmol) was added to it. A solution of 1,1-diethoxy-3-iodopropane (2.70 g, 10.4 mmol) in THF (10 mL) was then added slowly over 5 min, and the reaction mixture was stirred for 13 h while gradually raising the temperature to room temperature. The reaction was quenched with saturated NH_4Claq and this was extracted with Et_2O. The organic layer was washed with saturated NaClaq, dried over K_2CO_3, filtered, and concentrated under vacuum. The residue was chromatographed on silica gel with hexane/EtOAc = 49/1 to afford 1-(9,9-diethoxy-1,5-nonadiynyl)-4-methylbenzene as a yellow oil (2.17 g, 9.85 mmol; 70% yield).

^{1}H NMR ($CDCl_3$): δ 7.29 (d, $^{3}J_{HH}$ = 7.8 Hz, 2H), 7.08 (d, $^{3}J_{HH}$ = 8.0 Hz, 2H), 4.62 (t, $^{3}J_{HH}$ = 5.6 Hz, 1H), 3.63 (dq, $^{2}J_{HH}$ = 9.2 Hz and $^{3}J_{HH}$ = 7.0 Hz, 2H), 3.49 (dq, $^{2}J_{HH}$ = 9.5 Hz and $^{3}J_{HH}$ = 7.0 Hz, 2H), 2.58 (t, $^{3}J_{HH}$ = 7.3 Hz, 2H), 2.44 (t, $^{3}J_{HH}$ = 7.1 Hz, 2H), 2.33 (s, 3H), 2.25 (t, $^{3}J_{HH}$ = 6.9 Hz, 2H), 1.79 (td, $^{3}J_{HH}$ = 7.1 and 5.8 Hz, 2H), 1.19 (t, $^{3}J_{HH}$ = 7.1 Hz, 6H). ^{13}C NMR ($CDCl_3$): δ 137.8, 131.6, 129.0, 120.8, 102.0, 88.0, 81.5, 80.6, 79.0, 61.6, 33.1, 21.5, 20.2, 19.3, 15.5, 14.5.

2 M HClaq (10.2 mL) was added slowly over 5 min to a solution of 1-(9,9-diethoxy-1,5-nonadiynyl)-4-methylbenzene (2.02 g, 6.77 mmol) in THF (35 mL) and H_2O (7.5 mL), and the mixture was stirred for 4 h at room temperature. This was poured slowly into saturated $NaHCO_3$aq and extracted with Et_2O. The organic layer was washed with saturated NaClaq, dried over $MgSO_4$, filtered, and concentrated under vacuum. The residue was chromatographed on silica gel with hexane/EtOAc = 19/1 to afford 9-(4-methylphenyl)-4,8-nonadiynal as a yellow oil (1.07 g, 4.77 mmol; 71% yield).

^{1}H NMR ($CDCl_3$): δ 9.80 (t, $^{3}J_{HH}$ = 1.4 Hz, 1H), 7.29 (d, $^{3}J_{HH}$ = 7.8 Hz, 2H), 7.09 (d, $^{3}J_{HH}$ = 7.8 Hz, 2H), 2.66-2.60 (m, 2H), 2.60-2.54 (m, 2H), 2.54-2.47 (m, 2H), 2.47-2.40 (m, 2H), 2.33 (s, 3H). ^{13}C NMR ($CDCl_3$): δ 201.0, 137.9, 131.6, 129.1, 120.7, 87.8, 81.6, 80.0, 79.2, 43.0, 21.5, 20.1, 19.3, 12.3.

Dimethyl (1-diazo-2-oxopropyl)phosphonate (1.37 g, 7.13 mmol) was added to a mixture of 9-(4-methylphenyl)-4,8-nonadiynal (1.07 g, 4.77 mmol) and K_2CO_3 (1.65 g, 11.9 mmol) in MeOH (60 mL), and this was stirred for 2 h at room temperature. The precipitates were filtered off by passing through a pad of silica gel with hexane and the solvent was removed under vacuum. The residue was chromatographed on silica gel with hexane to afford compound **2a** as a white solid (765 mg, 3.47 mmol; 73% yield).

^{1}H NMR ($CDCl_3$): δ 7.29 (d, $^{3}J_{HH}$ = 8.2 Hz, 2H), 7.09 (d, $^{3}J_{HH}$ = 7.8 Hz, 2H), 2.63-2.55 (m, 2H), 2.50-2.43 (m, 2H), 2.43-2.36 (m, 4H), 2.33 (s, 3H), 1.99 (t, $^{4}J_{HH}$ = 2.5 Hz,

1H). ^{13}C NMR ($CDCl_3$): δ 137.8, 131.6, 129.1, 120.7, 87.9, 83.1, 81.5, 79.9, 79.4, 69.2, 21.5, 20.1, 19.3, 19.1, 19.0. HRMS (EI) calcd for $C_{17}H_{16}$ (M^+) 220.1247, found 220.1247.

Analytical Data for Other Monomers:

1-(1,5-Hexadiynyl)-4-methoxybenzene (1b)

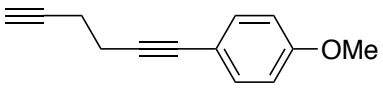

^{1}H NMR ($CDCl_3$): δ 7.34 (d, $^3J_{HH}$ = 8.7 Hz, 2H), 6.81 (d, $^3J_{HH}$ = 8.7 Hz, 2H), 3.80 (s, 3H), 2.63 (t, $^3J_{HH}$ = 7.3 Hz, 2H), 2.49 (td, $^3J_{HH}$ = 7.6 Hz and $^4J_{HH}$ = 2.3 Hz, 2H), 2.04 (t, $^4J_{HH}$ = 2.3 Hz, 1H). ^{13}C NMR ($CDCl_3$): δ 159.4, 133.1, 115.8, 114.0, 86.5, 83.0, 81.5, 69.4, 55.4, 19.7, 19.1. HRMS (EI) calcd for $C_{13}H_{12}O$ (M^+) 184.0883, found 184.0885.

Methyl 4-(1,5-hexadiynyl)benzoate (1c)

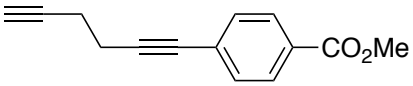

^{1}H NMR ($CDCl_3$): δ 7.96 (d, $^3J_{HH}$ = 8.2 Hz, 2H), 7.46 (d, $^3J_{HH}$ = 8.2 Hz, 2H), 3.91 (s, 3H), 2.68 (t, $^3J_{HH}$ = 7.3 Hz, 2H), 2.51 (td, $^3J_{HH}$ = 7.3 Hz and $^4J_{HH}$ = 2.3 Hz, 2H), 2.06 (t, $^4J_{HH}$ = 2.5 Hz, 1H). ^{13}C NMR ($CDCl_3$): δ 166.7, 131.7, 129.5, 129.3, 128.4, 91.4, 82.6, 81.2, 69.6, 52.3, 19.7, 18.8. HRMS (EI) calcd for $C_{14}H_{12}O_2$ (M^+) 212.0832, found 212.0832.

1-(1,5-Hexadiynyl)-4-(trifluoromethyl)benzene (1d)

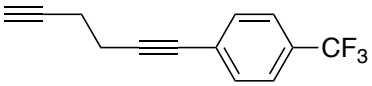

^{1}H NMR ($CDCl_3$): δ 7.53 (d, $^3J_{HH}$ = 8.3 Hz, 2H), 7.49 (d, $^3J_{HH}$ = 8.0 Hz, 2H), 2.66 (t, $^3J_{HH}$ = 7.2 Hz, 2H), 2.57-2.43 (m, 2H), 2.05 (s, 1H). ^{13}C NMR ($CDCl_3$): δ 132.0, 129.8

(q, $^{2}J_{CF}$ = 32.6Hz), 127.6, 125.3 (q, $^{3}J_{CF}$ = 3.8 Hz), 124.1 (q, $^{1}J_{CF}$ = 272 Hz), 90.9, 82.5, 80.6, 69.6, 19.6, 18.8. HRMS (EI) calcd for $C_{13}H_9F_3$ (M^+) 222.0651, found 222.0655.

1-(1,5-Hexadiynyl)-3,5-dimethylbenzene (1e)

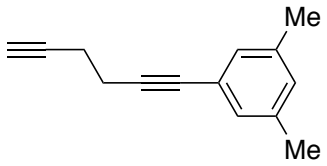

^{1}H NMR ($CDCl_3$): δ 7.04 (s, 2H), 6.92 (s, 1H), 2.68-2.60 (m, 2H), 2.52-2.45 (m, 2H), 2.27 (s, 6H), 2.05 (t, $^{4}J_{HH}$ = 2.5 Hz, 1H). ^{13}C NMR ($CDCl_3$): δ 137.8, 129.8, 129.4, 123.3, 87.3, 82.9, 82.0, 69.4, 21.2, 19.6, 19.0. HRMS (EI) calcd for $C_{14}H_{14}$ (M^+) 182.1090, found 182.1092.

1-(1,5-Hexadiynyl)-3,5-di-*tert*-butylbenzene (1f)

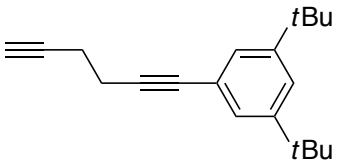

^{1}H NMR ($CDCl_3$): δ 7.36 (t, $^{4}J_{HH}$ = 1.6 Hz, 1H), 7.28 (d, $^{4}J_{HH}$ = 1.4 Hz, 2H), 2.71-2.64 (m, 2H), 2.56-2.49 (m, 2H), 2.06 (s, 1H), 1.32 (s, 18H). ^{13}C NMR ($CDCl_3$): δ 150.8, 126.0, 122.6, 122.4, 86.7, 83.0, 82.7, 69.4, 34.9, 31.5, 19.7, 19.1. HRMS (EI) calcd for $C_{20}H_{26}$ (M^+) 266.2029, found 266.2030.

1-(1,5,9-Decatriynyl)- 3,5-di-*tert*-butylbenzene (2b)

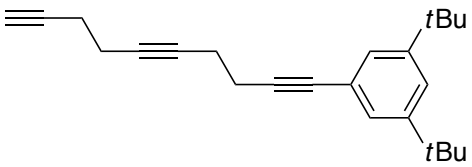

^{1}H NMR ($CDCl_3$): δ 7.35 (s, 1H), 7.26 (s, 2H), 2.62 (d, $^3J_{HH}$ = 7.4 Hz, 2H), 2.52-2.47 (m, 2H), 2.46-2.37 (m, 4H), 2.00 (s, 1H), 1.31 (s. 18H). ^{13}C NMR ($CDCl_3$): δ 150.8, 126.0, 122.7, 122.3, 87.3, 83.1, 82.5, 80.0, 79.5, 69.2, 34.9, 31.5, 20.1, 19.4, 19.2, 19.1. HRMS (EI) calcd for $C_{24}H_{30}$ (M^+) 318.2342, found 318.2346.

1-Methyl-4-(1,5,9,13- tetradecatetraynyl)benzene (3)

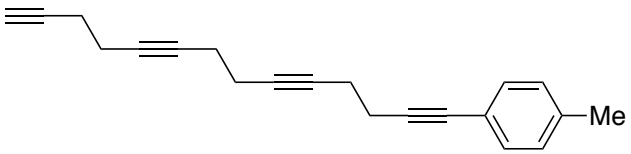

^{1}H NMR ($CDCl_3$): δ 7.29 (d, $^3J_{HH}$ = 7.8 Hz, 2H), 7.09 (d, $^3J_{HH}$ = 8.2 Hz, 2H), 2.65-2.55 (m, 2H), 2.45 (t, $^3J_{HH}$ = 7.6 Hz, 2H), 2.43-2.33 (m, 8H), 2.33 (s, 3H), 2.00 (t, $^4J_{HH}$ = 2.1 Hz, 1H). ^{13}C NMR ($CDCl_3$): δ 137.8, 131.6, 129.1, 120.7, 87.9, 83.1, 81.5, 80.1, 79.9, 79.7, 79.3, 69.2, 21.5, 20.2, 19.5, 19.4, 19.2, 19.0. HRMS (EI) calcd for $C_{21}H_{19}$ ($[M–H]^+$) 271.1481, found 271.1487.

General procedure for Table 1, entry 1 and equations 1–4.

Monomer **1**, **2**, or **3** (0.500 mmol) and THF (0.5 mL) were added to a solution of $[Rh(OH)(cod)]_2$ (3.4 mg, 15 μmol Rh) in THF (1.5 mL), and the mixture was stirred for 22 h at 60 ºC. After cooled to room temperature, this was added dropwise into stirring MeOH (50 mL) with the aid of CH_2Cl_2 (5.0 mL), and the precipitates that formed were collected by filtration with MeOH. The resulting solid was dissolved in CH_2Cl_2 (5.0 mL) and this was added dropwise into stirring pentane (50 mL) with the aid of CH_2Cl_2 (5.0 mL). The precipitates that formed were collected by filtration with pentane and dried under vacuum to afford **poly-1**, **poly-2**, or **poly-3**.

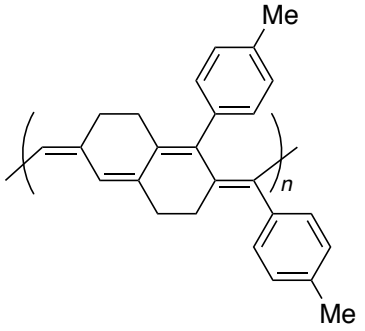

Table 1, Entry 1 (poly-1a). Red solid. 81% yield. T_d = 326 ºC (5% weight loss).

^{1}H NMR spectrum (400 MHz in $CDCl_3$)

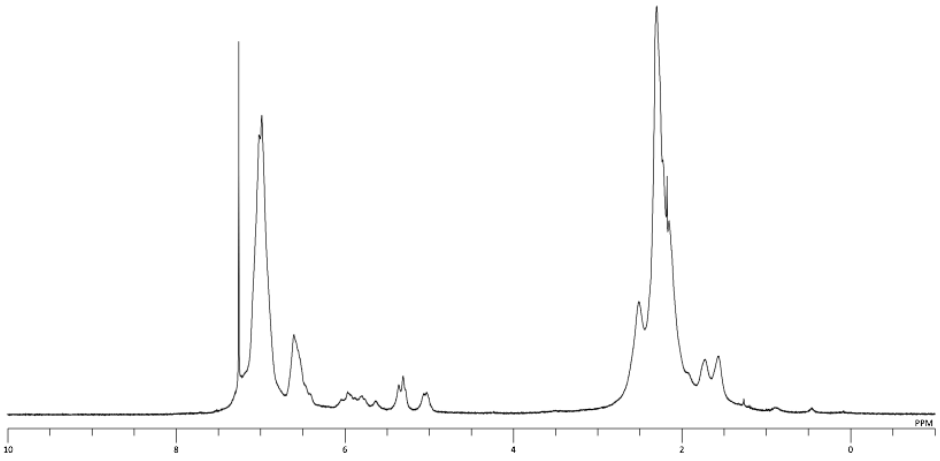

^{13}C NMR (101 MHz in $CDCl_3$)

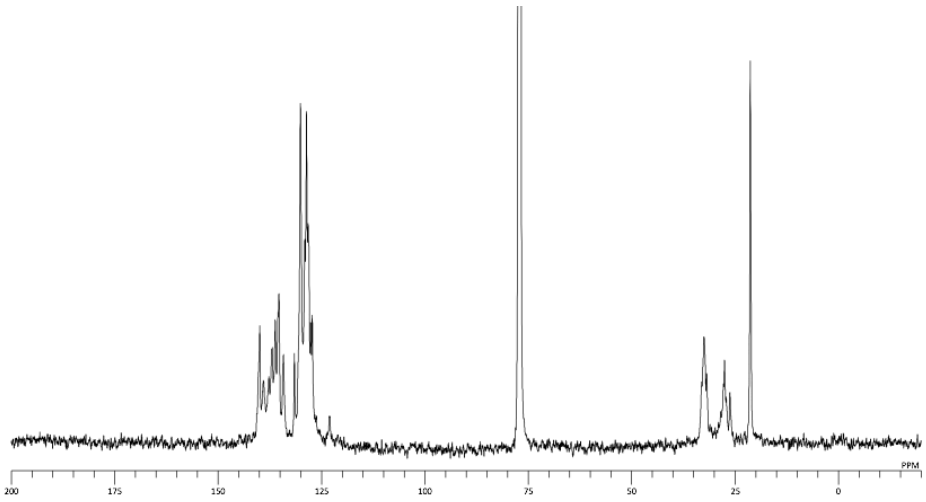

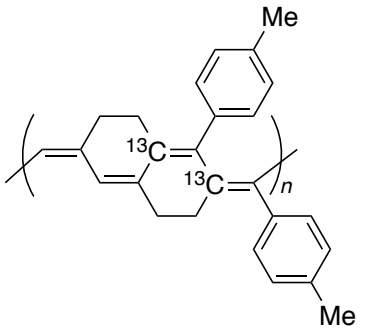

Equation 1 (poly-(1a-^{13}C)). Red solid. 83% yield. Incorporation efficiency of internal alkynes was estimated by the area ratio of labeled sp^2 carbon peaks and labeled sp carbon peaks of the quantitative ^{13}C NMR spectrum.

^{1}H NMR (400 MHz in $CDCl_3$)

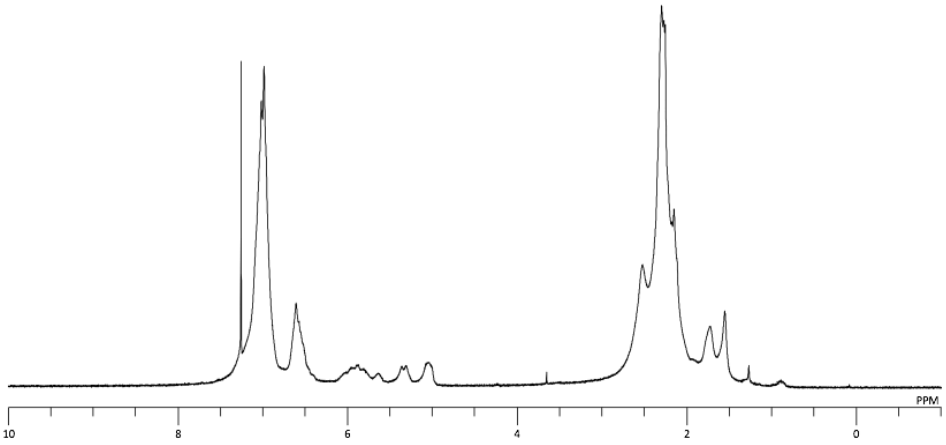

Inverse gated ^{1}H decoupling ^{13}C NMR (176 MHz in $CDCl_3$)

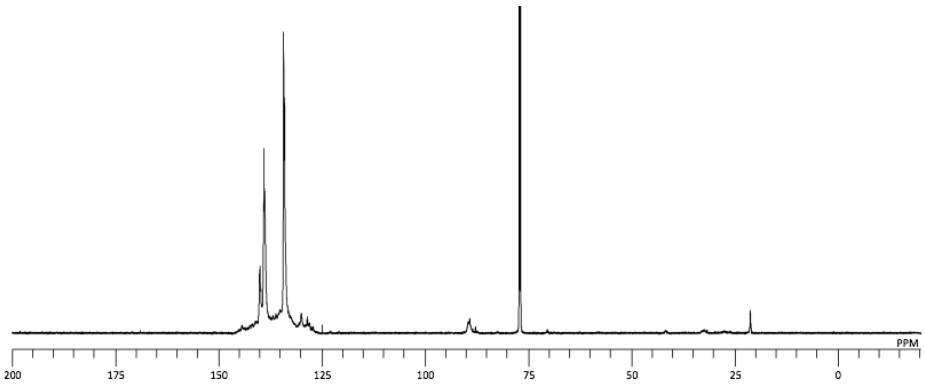

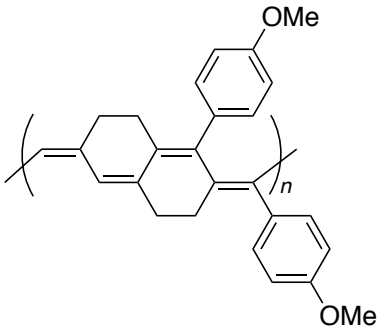

Equation 2, Ar = 4-MeOC$_6$H$_4$ (poly-1b). Red solid. 80% yield. T_d = 321 ºC (5% weight loss).

^{1}H NMR (498 MHz in $CDCl_3$)

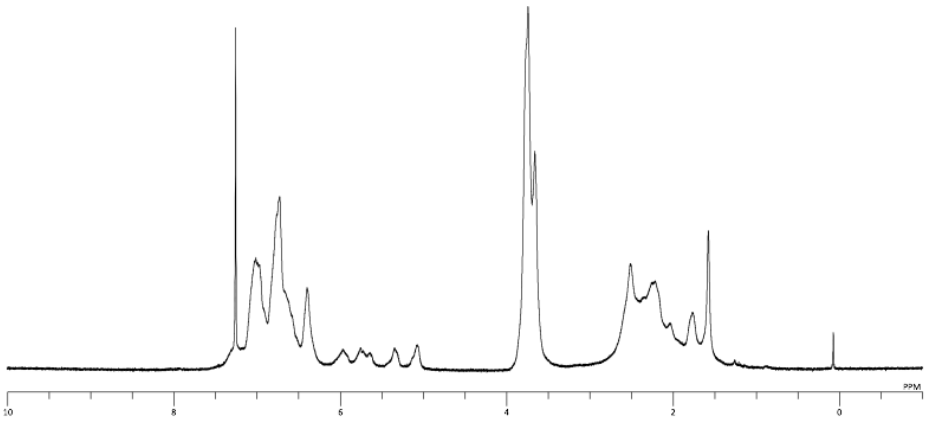

^{13}C NMR (101 MHz in $CDCl_3$)

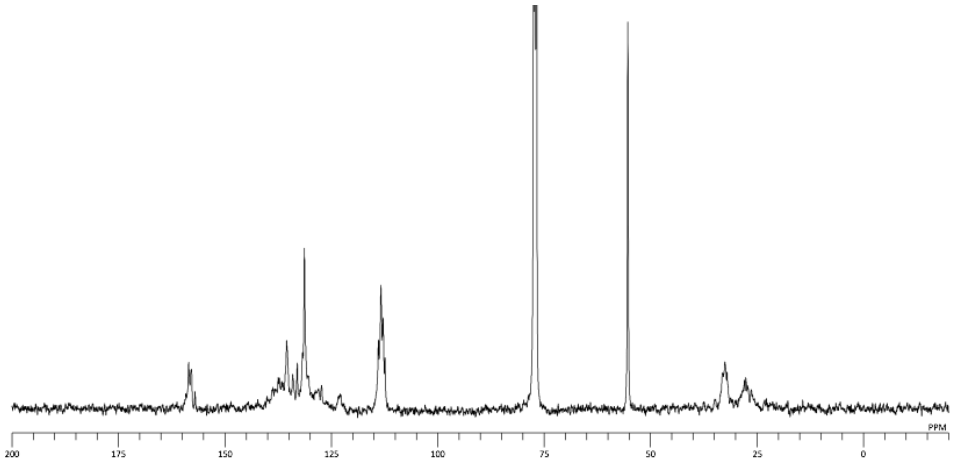

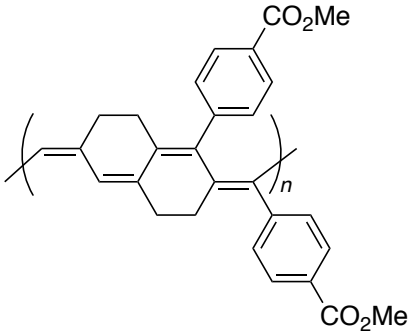

Equation 2, Ar = 4-$MeO_2CC_6H_4$ (poly-1c). The polymerization was carried out in the presence of $[Rh(OH)(cod)]_2$ (6 mol% Rh) and 1,5-cyclooctadiene (30 mol%). Dark red solid. 72% yield. T_d = 324 ºC (5% weight loss).

^{1}H NMR (400 MHz in $CDCl_3$)

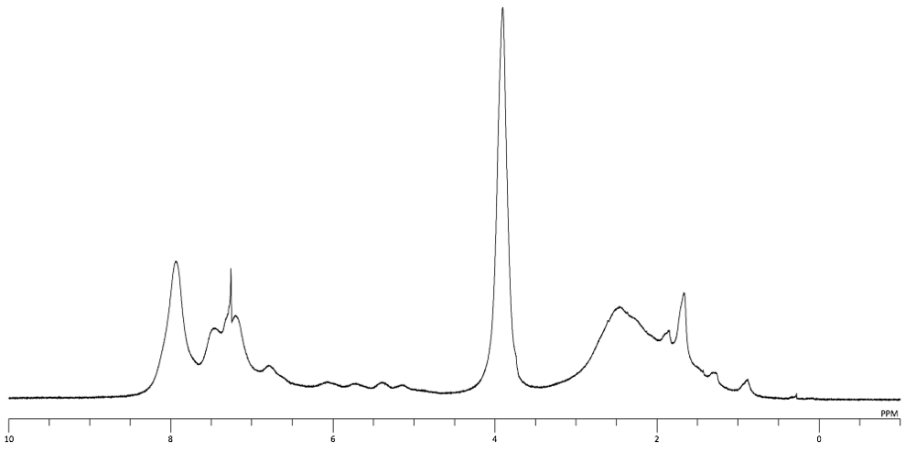

^{13}C NMR (101 MHz in $CDCl_3$)

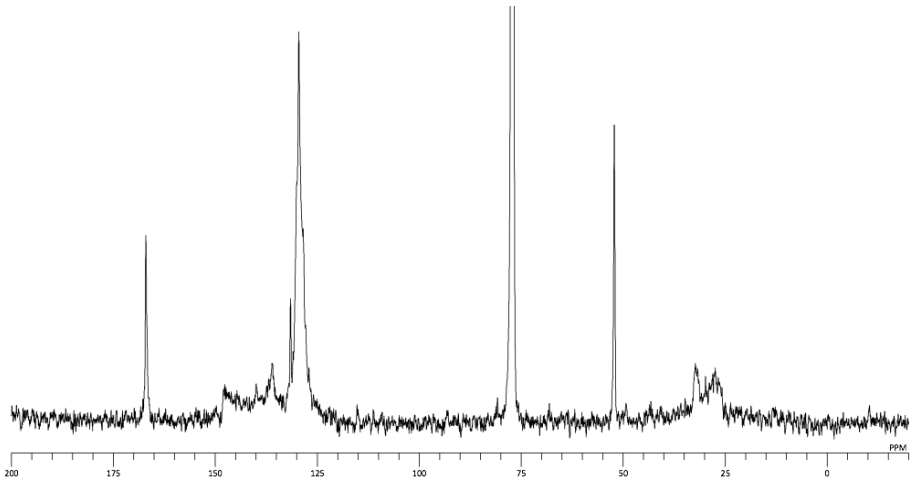

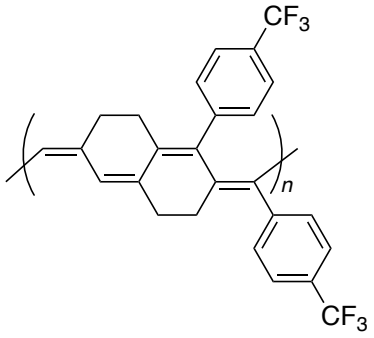

Equation 2, (poly-1d). The polymerization was carried out in the presence of $[Rh(OH)(cod)]_2$ (6 mol% Rh) and 1,5-cyclooctadiene (30 mol%). Red-black solid. 71% yield. T_d = 307 ºC (5% weight loss).

^{1}H NMR (400 MHz in $CDCl_3$)

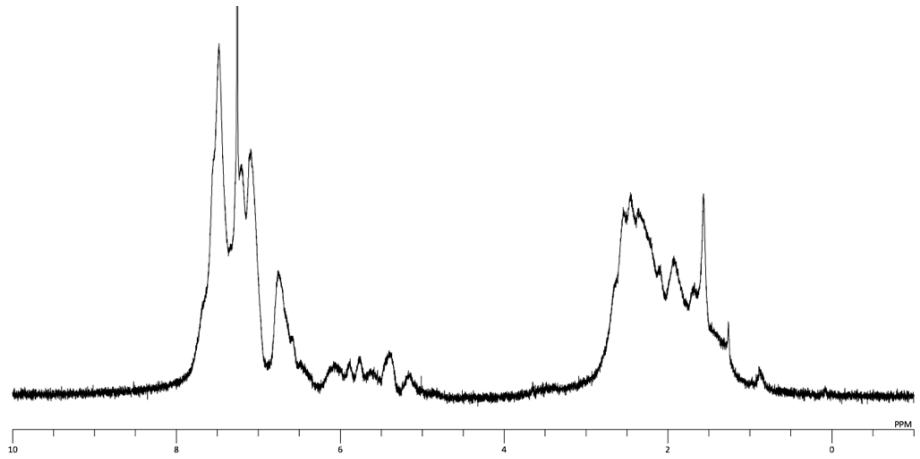

^{13}C NMR (101 MHz in $CDCl_3$)

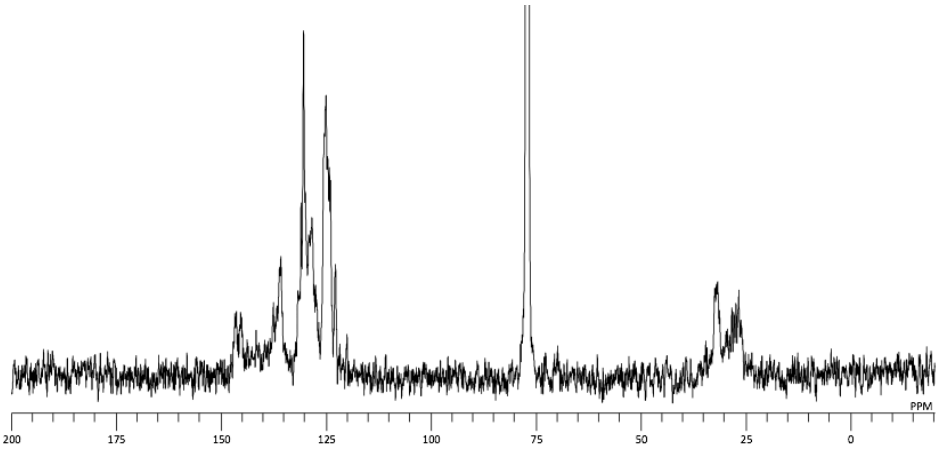

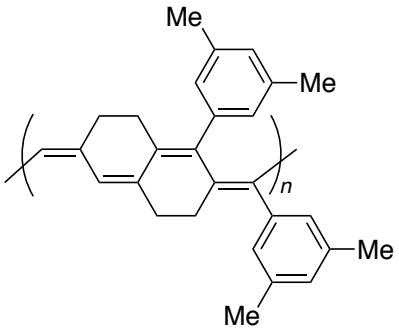

Equation 2, Ar = 3,5-$Me_2C_6H_3$ (poly-1e). Red solid. 71% yield. T_d = 335 ºC (5% weight loss).

^{1}H NMR (400 MHz in $CDCl_3$)

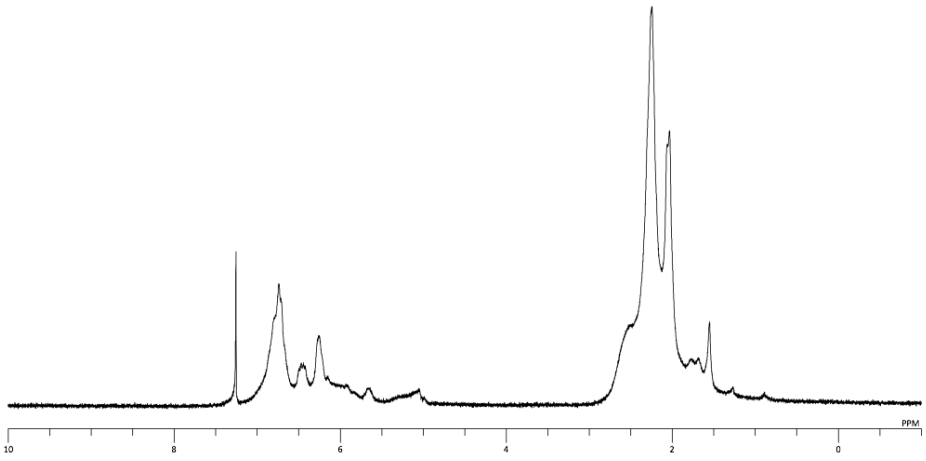

^{13}C NMR (101 MHz in $CDCl_3$)

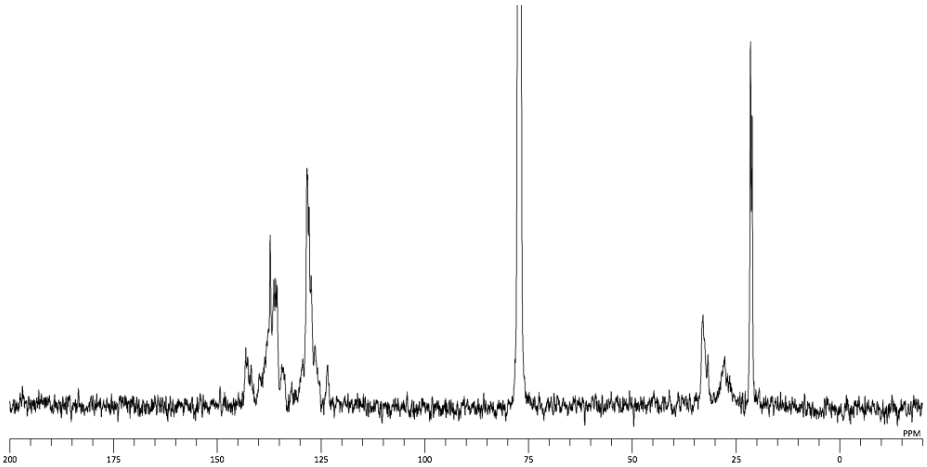

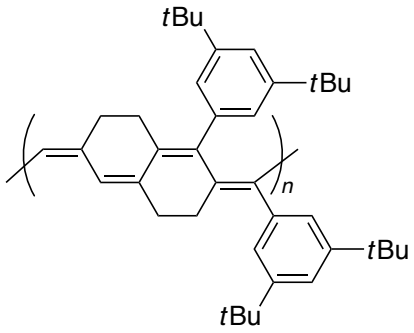

Equation 2, Ar = 3,5-*t*Bu$_2$C$_6$H$_3$ (poly-1f). Purple solid. 90% yield. T_d = 330 ºC (5% weight loss).

^{1}H NMR (400 MHz in $CDCl_3$)

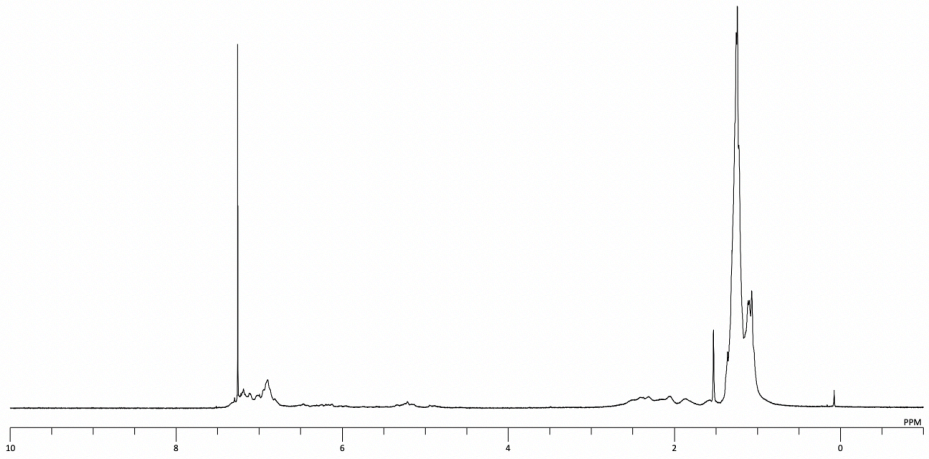

^{13}C NMR (101 MHz in $CDCl_3$)

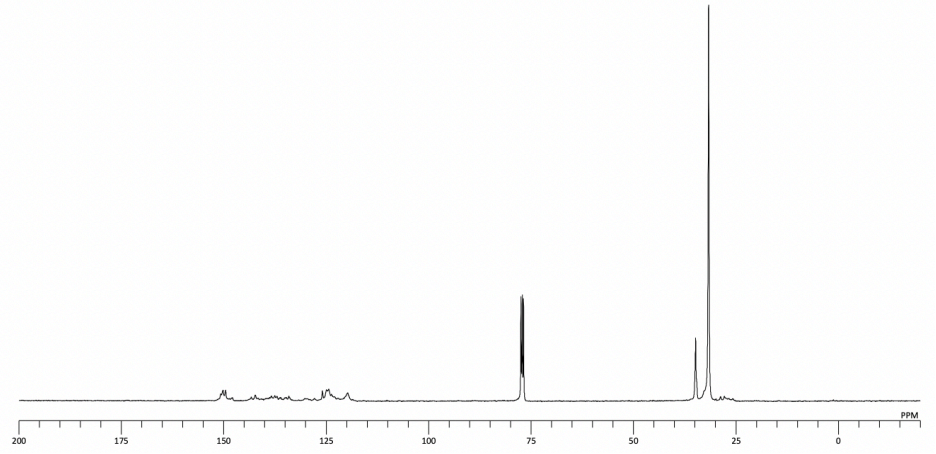

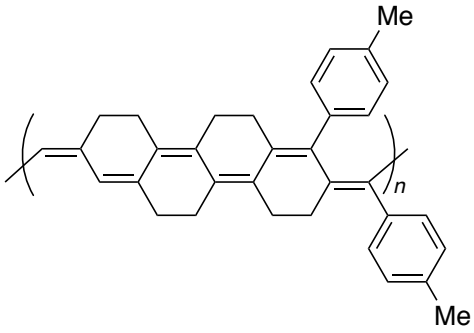

Equation 3 (poly-2a). Red solid. 70% yield. Incorporation efficiency of internal alkynes was estimated by the area ratio of sp^2 carbon peaks, sp carbon peaks, and sp^3 carbon peaks of the quantitative ^{13}C NMR spectrum. T_d = 356 ºC (5% weight loss).

^1H NMR (400 MHz in $CDCl_3$)

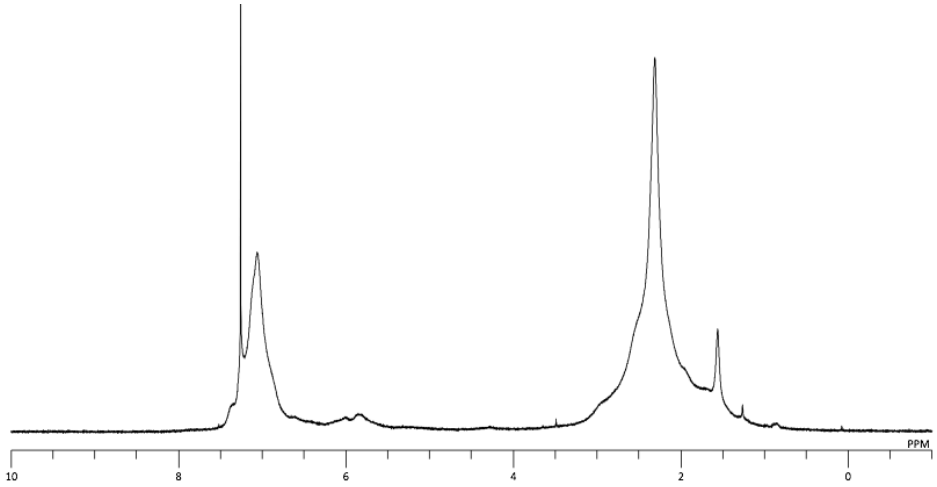

Inverse gated ^1H decoupling ^{13}C NMR (176 MHz in $CDCl_3$)

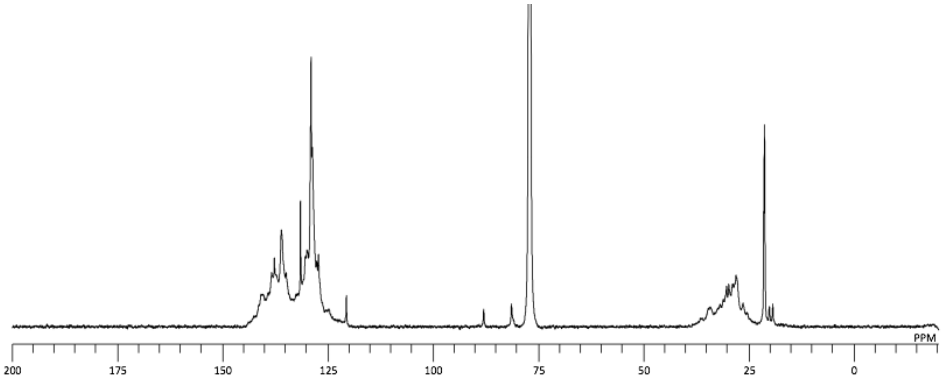

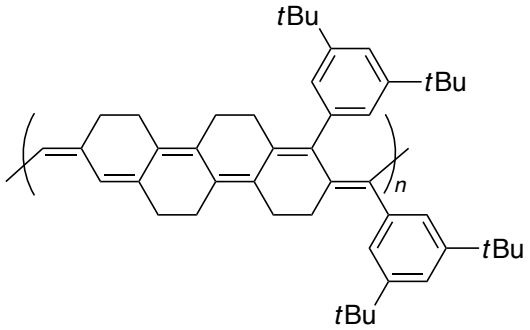

Equation 3 (poly-2b). Red solid. 68% yield. Incorporation efficiency of internal alkynes was estimated by the area ratio of sp^2 carbon peaks, sp carbon peaks, and sp^3 carbon peaks of the quantitative ^{13}C NMR spectrum. T_d = 341 ºC (5% weight loss).

^1H NMR (400 MHz in $CDCl_3$)

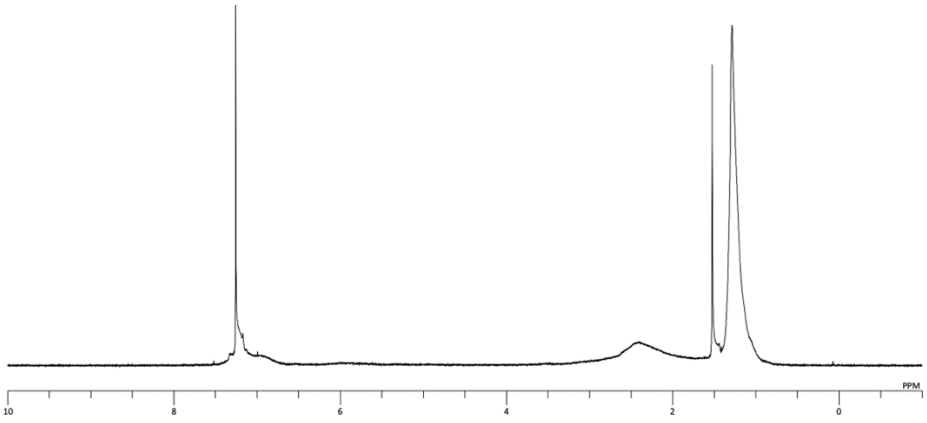

Inverse gated ^1H decoupling ^{13}C NMR (176 MHz in $CDCl_3$)

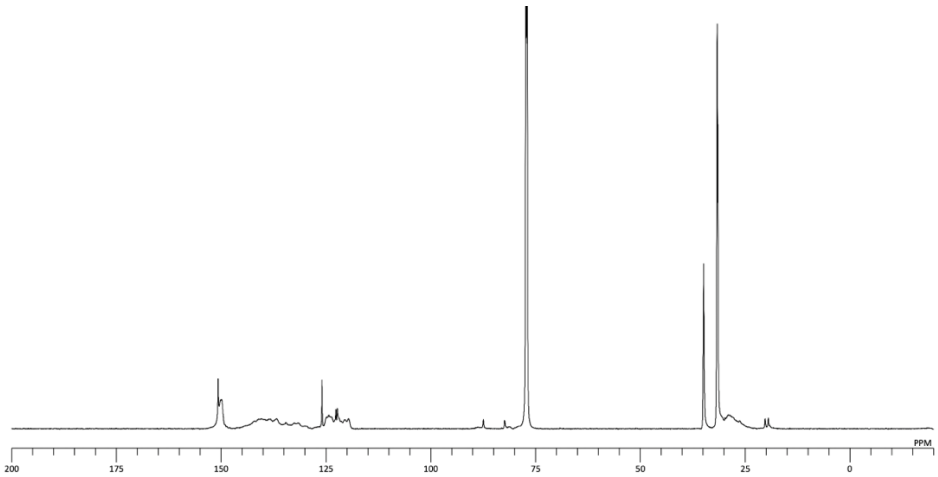

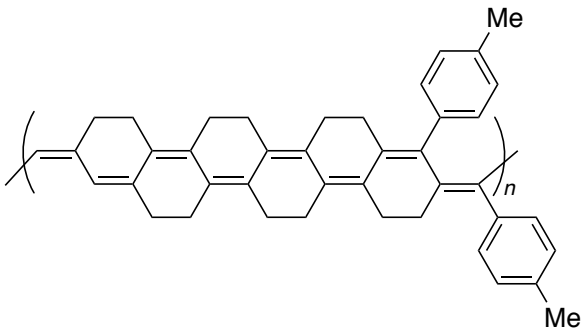

Equation 4 (poly-3). The polymerization was carried out in the presence of $[Rh(OH)(cod)]_2$ (6 mol% Rh). Red-black solid. 69% yield. Incorporation efficiency of internal alkynes was estimated by the area ratio of sp^2 carbon peaks, sp carbon peaks, and sp^3 carbon peaks of the quantitative ^{13}C NMR spectrum. T_d = 373 ºC (5% weight loss).

^1H NMR (400 MHz in $CDCl_3$)

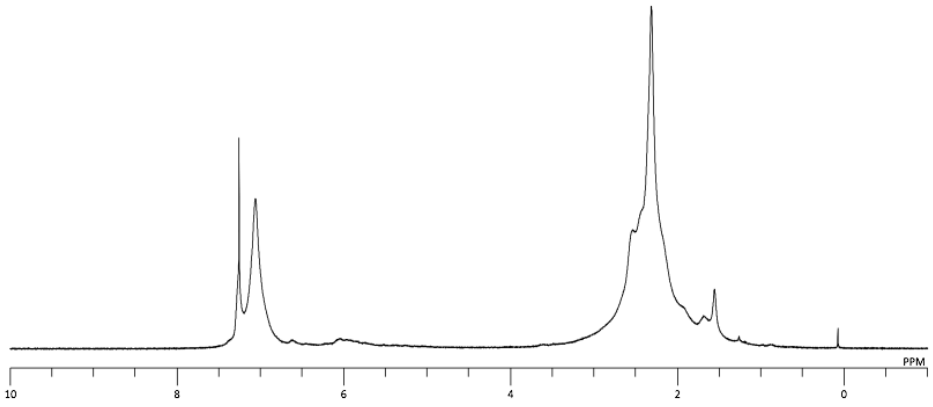

Inverse gated ^1H decoupling ^{13}C NMR (176 MHz in $CDCl_3$)

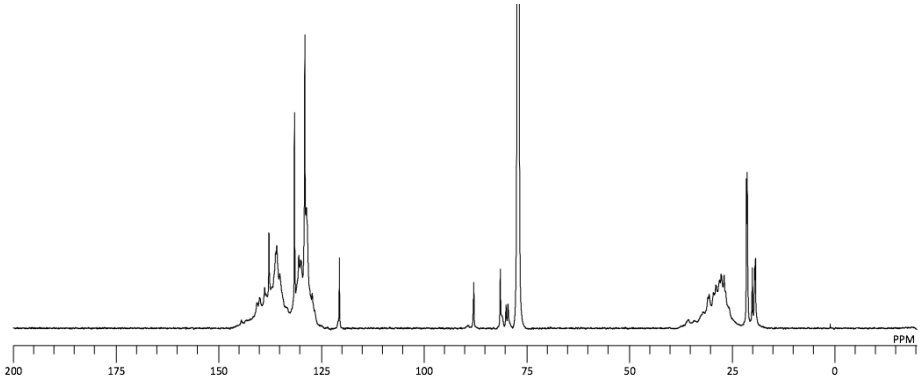

Procedure for poly-4-methylphenylacetylene

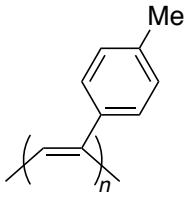

4-Methylphenylacetylene (116 mg, 1.00 mmol) and THF (1.0 mL) were added to a solution of $[Rh(OH)(cod)]_2$ (22.8 mg, 0.100 mmol Rh) and PPh_3 (26.2 mg, 99.9 μmol) in THF (3.0 mL), and the mixture was stirred for 22 h at 60 ºC. After cooled to room temperature, this was added dropwise into stirring MeOH (50 mL) with the aid of CH_2Cl_2 (5.0 mL), and the precipitates that formed were collected by filtration with MeOH. The resulting solid was dissolved in CH_2Cl_2 (5.0 mL) and this was added dropwise into stirring pentane (50 mL) with the aid of CH_2Cl_2 (5.0 mL). The precipitates that formed were collected by filtration with pentane and dried under vacuum to afford poly-4-methylphenylacetylene as an orange solid (49.5 mg; 43% yield, M_n 30000, M_w/M_n 1.3). T_d = 274 ºC (5% weight loss).

^1H NMR (400 MHz in $CDCl_3$)

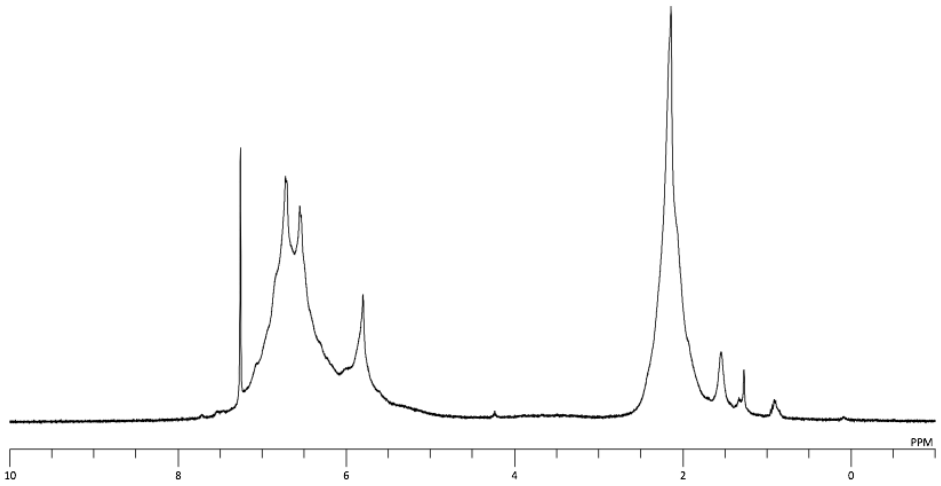

^{13}C NMR (101 MHz in $CDCl_3$)

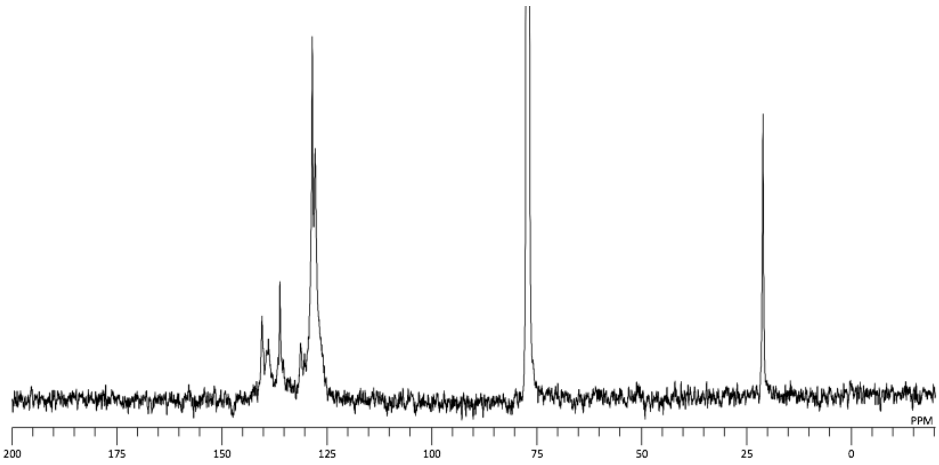

Procedure for Equation 5.

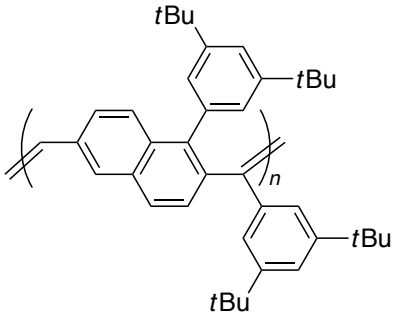

2,3-Dichloro-5,6-dicyano-*p*-benzoquinone (136 mg, 0.599 mmol) was added to a solution of **poly-1f** (79.8 mg) in toluene (6.0 mL), and the mixture was stirred for 22 h at 110 ºC. After cooled to room temperature, this was added dropwise into stirring MeOH (50 mL) with the aid of CH_2Cl_2 (5.0 mL), and the precipitates that formed were collected by filtration with MeOH. The resulting solid was dissolved in CH_2Cl_2 (5.0 mL) and this was added dropwise into stirring pentane (50 mL) with the aid of CH_2Cl_2 (5.0 mL). The precipitates that formed were collected by filtration with pentane and dried under vacuum to afford **poly-1f-ox** as a brown solid (73.7 mg; 94% yield). The molecular weight could not be accurately determined due to the limited solubility in THF. T_d = 271 ºC (5% weight loss).

^{1}H NMR (498 MHz in $CDCl_3$)

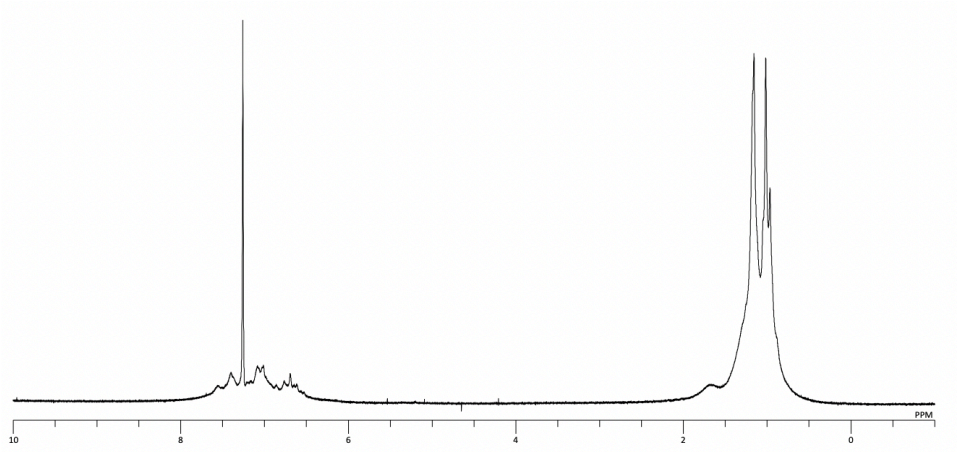

^{13}C NMR (101 MHz in $CDCl_3$)

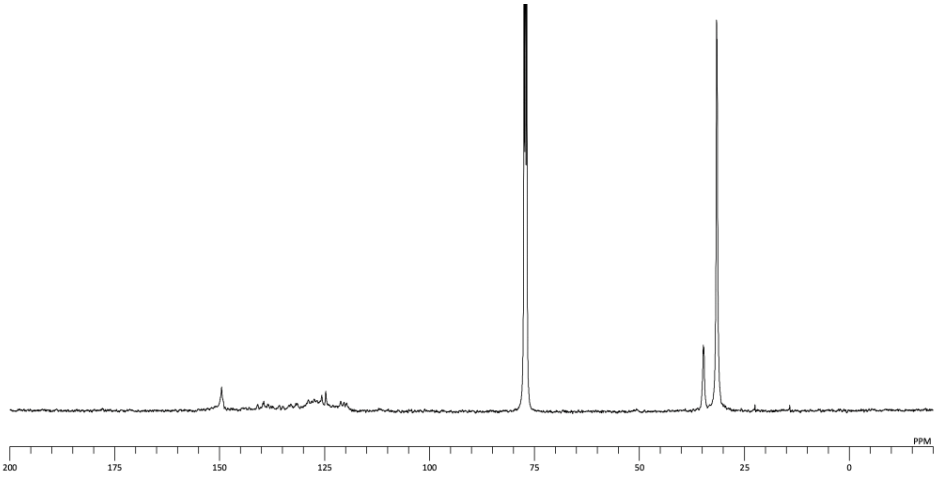

Procedure for Equation 6.

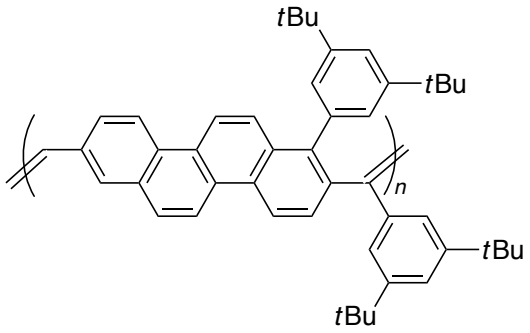

2,3-Dichloro-5,6-dicyano-*p*-benzoquinone (272 mg, 1.20 mmol) was added to a solution of **poly-2b** (95.5 mg) in toluene (6.0 mL), and the mixture was stirred for 22 h

at 110 ºC. After cooled to room temperature, this was added dropwise into stirring CH_2Cl_2 (50 mL) with the aid of CH_2Cl_2 (5.0 mL), and the precipitates that formed were collected by filtration with CH_2Cl_2 and dried under vacuum to afford **poly-2b-ox** as a black solid (92.6 mg; 98% yield). ^{1}H and ^{13}C NMR spectra and the molecular weight were not obtained due to the poor solubility of this polymer. T_d = 264 ºC (5% weight loss).

2.5 References

[1] For reviews: (a) Cinar, M. E.; Ozturk, T. *Chem. Rev.* **2015**, *115*, 3036–3140. (b) Takimiya, K.; Shinamura, S.; Osaka, I.; Miyazaki, E. *Adv. Mater.* **2011**, *23*, 4347–4370. (c) Fukazawa, A.; Yamaguchi, S. *Chem. Asian J.* **2009**, *4*, 1386–1400. (d) Anthony, J. E. *Chem. Rev.* **2006**, *106*, 5028–5048.

[2] For reviews: (a) Teo, Y. C.; Lai, H. W. H.; Xia, Y. *Chem. Eur. J.* **2017**, *23*, 14101–14112. (b) Wu, J.-S.; Cheng, S.-W.; Cheng, Y.-J.; Hsu, C.-S. *Chem. Soc. Rev.* **2015**, *44*, 1113–1154. (c) Facchetti, A. *Chem. Mater.* **2011**, *23*, 733–758. (d) Scherf, U. *J. Mater. Chem.* **1999**, *9*, 1853–1864. (e) Scherf, U.; Müllen, K. The Synthesis of Ladder Polymers, in *Adv. Polym. Sci.* (Eds.: A. Abe, et al.), Springer, Berlin, **1995**, Vol. 123, pp. 1-40. See also: (f) Scherf, U.; Müllen, K. *Makomol. Chem. Rapid Commun.* **1991**, *12*, 489–497.

[3] For selected recent examples: (a) Nishioka, H.; Tsuji, H.; Nakamura, E. *Macromolecules* **2018**, *51*, 2961–2968. (b) Huang, W.; Zhang, H.; Ma, J.; Chen, M.; Zhu, H.; Wang, W. *J. Mater. Chem. C* **2015**, *3*, 6200–6208. (c) Zheng, T.; Lu, L.; Jackson, N. E.; Lou, S. J.; Chen, L. X.; Yu, L. *Macromolecules* **2014**, *47*, 6252–6259. (d) Biniek, L.; Schroeder, B. C.; Donaghey, J. E.; Yaacobi-Gross, N.; Ashraf, R. S.; Soon, Y. W.; Nielsen, C. B.; Durrant, J. R.; Anthopoulos, T. D.; McCulloch, I. *Macromolecules* **2013**, *46*, 727–735. (e) Rieger, R.; Beckmann, D.; Pisula, W.; Kastler, M.; Müllen, K. *Macromolecules* **2010**, *43*, 6264–6267.

[4] Shintani, R.; Iino, R.; Nozaki, K. *J. Am. Chem. Soc*. **2016**, *138*, 3635–3638. (b) Shintani, R.; Misawa, N.; Tsuda, T.; Iino, R.; Fujii, M.; Yamashita, K.; Nozaki, K. *J. Am. Chem. Soc*. **2017**, *139*, 3861–3867. (c) Shintani, R.; Kishikawa, S.; Nakamura, K.; Tsuda, T.; Nozaki, K. *Chem. Commun.* **2019**, *55*, 1072–1075.

[5] For reviews on rhodium-catalyzed polymerization of terminal alkynes: (a) Shiotsuki, M.; Sanda, F.; Masuda, T. *Poly. Chem.* **2011**, *2*, 1044–1058. (b) Aoki, T.; Kaneko, T.; Teraguchi, M. *Polymer* **2006**, *47*, 4867–4892. See also: (c) Masuda, T. *J. Polym. Sci., Part A: Polym. Chem.* **2007**, *45*, 165–180.

[6] For selected early examples of rhodium-catalyzed polymerization of terminal alkynes: (a) Tabata, M.; Yang, W.; Yokota, K. *Polym. J.* **1990**, *22*, 1105–1107. (b) Yang, W.; Tabata, M.; Kobayashi, S.; Yokota, K.; Shimizu, A. *Polym. J.* **1991**, *23*, 1135–1138. (c) Aoki, T.; Kokai, M.; Shinohara, K.; Oikawa, E. *Chem. Lett.* **1993**, 2009–2012. (d) Tabata, M.; Yang, W.; Yokota, K. *J. Polym. Sci., Part A: Polym. Chem.* **1994**, *32*, 1113–1120. (e) Kishimoto, Y.; Eckerle, P.; Miyatake, T.; Ikariya, T.; Noyori, R. *J. Am. Chem. Soc.* **1994**, *116*, 12131–12132. (f) Tabata, M.; Yokota, K.; Namioka, M. *Macromol. Chem. Phys.* **1995**, *196*, 2969–2977. (g) Aramata, K.; Kajiwara, A.; Kamachi, M. *Macromolecules* **1995**, *28*, 4774–4776. (h) Kishimoto, Y.; Itou, M.; Miyatake, T.; Ikariya, T.; Noyori, R. *Macromolecules* **1995**, *28*, 6662–6666.

[7] For examples of polymerization of internal alkynes catalyzed by other transition metals: (a) Thanedar, S.; Farona, M. F. *Polym. Bull.* **1982**, *8*, 429–435. (b) Hayano, S.; Masuda, T. *Macromol. Chem. Phys.* **2000**, *201*, 233–238. (c) Kubo, H.; Hayano, S.; Masuda, T. *J. Poym. Sci., Part A: Poym. Chem.* **2000**, *38*, 2697–2701. (d) Dong, Y.; Lam, J. W. Y.; Peng, H.; Cheuk, K. K. L.; Kwok, H. S.; Tang, B. Z. *Macromolecules* **2004**, *37*, 6408–6417. (e) Lam, J. W. Y.; Dong, Y.; Cheuk, K. K. L.; Law, C. C. W.; Lai, L. M.; Tang, B. Z. *Macromolecules* **2004**, *37*, 6695–6704. (f) Castanon, J. R.; Sano, N.; Shiotsuki, M.; Sanda, F. *ACS Macro Lett.* **2014**, *3*, 51–54. (g) Wised, K.; Nomura, K. *Organometallics* **2016**, *35*, 2773–2777. See also: (h) Yang, H.; Jin, Y.; Du, Y.; Zhang, W. *J. Mater. Chem. A* **2014**, *2*, 5986–5993.

[8] Cyclopolymerization of diynes have been reported. For a review: (a) Czekelius, C. *Indian J. Chem.* **2009**, *48B*, 1704–1708. For examples: (b) Cataldo, F. *Polym. Int.* **1993**, *30*, 375–379. (c) Zhang, W.; Shiotsuki, M.; Masuda, T. *Polymer* **2006**, *47*, 2956–2961. (d) Ichikawa, Y.; Nishimura, T.; Hayashi, T. *Organometallics* **2011**, *30*, 2342–2348. See also: (e) Okada, S.; Hayamizu, K.; Matsuda, H.; Masaki, A.; Nakanishi, H. *Bull. Chem. Soc. Jpn.* **1991**, *64*, 857–863. (f) Nishiura, M.; Hou, Z. *J. Mol. Catal. A: Chem.* **2004**, *213*, 101–106. (g) Sugiyama, Y.; Okamoto, S. *J. Polym. Sci., Part A: Polym. Chem.* **2016**, *54*, 345–351.

[9] For mechanistic studies on the rhodium-catalyzed polymerization of phenylacetylenes: (a) Kishimoto, Y.; Eckerle, P.; Miyatake, T.;. Kainosho, M; Ono, A.; Ikariya, T.; Noyori, R. *J. Am. Chem. Soc.* **1999**, *121*, 12035–12044. (b) Ke, Z.; Abe, S.; Ueno, T.; Morokuma, K. *J. Am. Chem. Soc.* **2011**, *133*, 7926–7941. (c) Angoy, M.; Jiménez, M. V.; Modrego, F. J.; Oro, L. A.; Passarelli, V.; Pérez-Torrente, J. J. *Organometallics* **2018**, *37*, 2778–2794.

[10] The initiation group R in Scheme 1 could be either 6-aryl-1,5-hexadiyn-1-yl or H. See Ref. [9] for proposed initiation mechanisms.

[11] Nishide, H.; Yoshioka, N.; Inagaki, K.; Kaku, T.; Tsuchida, E. *Macromolecules* **1992**, *25*, 569–575. (b) Miura, Y.; Matsumoto, M.; Ushitani, Y.; Teki, Y.; Takui, T.; Itoh, K. *Macromolecules* **1993**, *26*, 6673–6675.

[12] Lynch, P. J.; O'Neill, L.; Bradley, D.; Byrne, H. J.; McNamara, M. *Macromolecules* **2007**, *40*, 7895–7901. (b) O'Neill, L.; Lynch, P. J.; McGoldrick, N.; Byrne, H. J.; McNamara, M. *J. Luminescence* **2012**, *132*, 2217–2223. For substituent effects of poly(arylene vinylene)s on the UV-vis absorption, see: (c) Young, C. A.; Saowsupa, S.; Hammack, A.; Tangonan, A. A.; Anuragudom, P.; Jia, H.; Jamison, A. C.;

Panichphant, S.; Gnade, B. E.; Lee, T. R. *J. Appl. Polym. Sci.* **2014**, *131*, 41162/1–41162/12.

[13] Although it is difficult to quantify the degree of oxidation precisely, based on the changes of ^{1}H and ^{13}C NMR spectra of **poly-1f** and **poly-1f-ox** as well as UV-vis absorption spectra in Figure 8 upon DDQ oxidation, it can be concluded that the oxidation proceeded successfully.

[14] For reviews: (a) Denton, F. R.; III, Lahti, P. M. *Plastics Engineering* **1998**, *49*, 61–102. (b) Haque, T.; Nomura, K. *Catalysts* **2015**, *5*, 500–517.

[15] Uson, R.; Oro, L.A.; Cabeza, J. A. *Inorg. Synth*. **1985**, *23*, 126–130.

[16] Coulson, D. R.; Satek, L. C.; Grim, S. O. *Inorg. Synth.* **1972**, *13*, 121–124.

[17] Whitby, R.; Stec, J.; Blind, R.; Dixon, S.; Leesnitzer, L.; Orband-Miller, L.; Williams, S.; Willson, T.; Xu, R.; Zuercher, W.; Cai, F.; Ingraham, H. *J. Med. Chem*. **2011**, *54*, 2266–2281.

[18] Quesada, E.; Raw, S.; Reid M.; Roman, E.; Taylor, R. *Tetrahedron*, **2006**, *62*, 6673–6680.

Chapter 3

Rhodium-Catalyzed Stitching Polymerization of Alkynylsilylacetylenes

3.1 Introduction

Rhodium-catalyzed polymerization of terminal alkynes such as phenylacetylene is one of the well explored chain polymerizations to give π-conjugated polymers (Scheme 1-(a)).[1] In addition to the development of highly effective catalyst systems[2] as well as the detailed studies on the polymerization mechanism,[3] applications toward functional materials possessing various properties such as helix-induced chirality,[4] fluorescent characteristics,[5] liquid crystallinity,[6] and gas permeability,[7] have also been actively investigated through introduction of appropriately functionalized substituents to the monomers. However, only carbon-substituted alkynes have been employed as monomers to date, and the reported polymerization patterns were either simple coordination–insertion of monoynes or cyclopolymerization of diynes[8] until recently, which significantly limited the accessible structures of the main chain repeating unit.

On the other hand, polymers possessing a silicon-bridged π-conjugated repeating unit have been widely explored as potentially useful organic optoelectronic materials such as solar cells and light-emitting devices, particularly due to their electronic effects based on the σ*–π* conjugation in addition to their structural rigidity.[9] These polymers are usually synthesized by polycondensation of the corresponding silicon-bridged π-conjugated monomers, but this method is inherently restricted to the synthesis of polymers consisting of repeating units that can be prepared as stable monomers beforehand, which narrows the applicable structures of silicon-bridged π-conjugated repeating units. As described in Chapter 2, the author developed a new type of rhodium-catalyzed alkyne polymerization

named “stitching polymerization” as a complementary approach toward polymers with a bridged π-conjugated repeating unit, which allowed for the construction of bridged repeating units and the chain growth at the same time in a single polymerization sequence, and he successfully synthesized polymers possessing an ethylene-bridged π-conjugated repeating unit by employing 1,5-hexadiynes and related oligoalkynes as non-conjugated monomers (Scheme 1-(b)).[10] In this Chapter, to expand the scope of accessible silicon-bridged unit structures of functional π-conjugated polymers, the author describe the development of a rhodium-catalyzed stitching polymerization of alkynylsilylacetylenes and related oligoalkynes (Scheme 1-(c)), representing the first successful chain-growth polymerization of heteroatom-substituted alkynes under rhodium catalysis.[11,12] The author also investigated post-derivatization and physical properties of the resulting polymers.

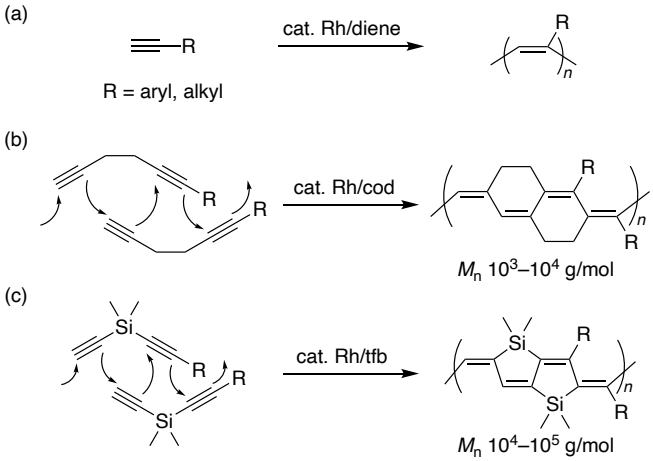

Scheme 1. Schematic representation of (a) conventional rhodium-catalyzed alkyne polymerization (b) rhodium-catalyzed stitching polymerization of 1,5-hexadiynes (Chapter 2) (c) rhodium-catalyzed stitching polymerization of alkynylsilylacetylenes (this Chapter)

3.2 Results and Discussion

3.2.1 Reaction development and structural consideration

In an initial investigation, the author employed dihexyl(phenylethynyl)silylacetylene (**1a**) as the monomer and conducted the polymerization under the previously developed conditions in Chapter 2 using $[Rh(OH)(cod)]_2$ (3 mol% Rh) in THF at 60 ºC (Table 1, entry 1).[10] As a result, stitched polymer **poly-1a** was successfully obtained in 89% yield after reprecipitation, and the number-averaged molecular weight (M_n) was calculated to be 9000 with M_w/M_n of 2.0 using size-exclusion chromatography against a polystyrene standard. In comparison, polymerization of simple trimethylsilylacetylene did not proceed under the same conditions,[2c] indicating that the diyne structure is important to promote the rhodium-catalyzed polymerization of silylacetylenes. The use of $[Rh(cod)\{(\eta^6\text{-}C_6H_5)BPh_3\}]$ instead of $[Rh(OH)(cod)]_2$ gave similar results for the polymerization of **1a** (entry 2).[2c] The author subsequently found that the degree of polymerization (DP) became higher by conducting the reaction using $[Rh(OH)(cod)]_2$ at lower temperatures (entries 3 and 4), achieving M_n = 45000 (M_w/M_n = 1.6) in 95% yield at –10 ºC. In contrast, $[Rh(cod)\{(\eta^6\text{-}C_6H_5)BPh_3\}]$ did not promote the polymerization at –10 ºC, but $[Rh(OH)(cod)]_2$ could be replaced by more readily accessible $[RhCl(cod)]_2$ with Et_3N without affecting the polymerization efficiency (entry 5). Finally, we could obtain **poly-1a** with a much higher molecular weight of M_n = 84000 (average DP = 260, M_w/M_n = 2.1) by using the catalyst system composed of $[RhCl(tfb)]_2$ and Et_3N while keeping the high catalytic activity (96% yield; entry 6).[2h,i,m] The superiority of tfb ligand could be explained by its high π-acidity, which stabilizes an electron-rich rhodium(I) species and facilitates the coordination of monomer **1a** to the rhodium center toward polymerization.[2i] To further confirm the importance of diyne monomers for the polymerization of silylacetylenes, the author attempted polymerization of related

silylacetylenes having alkyl (**2a**), alkenyl (**2b**), or aryl (**2c**) group on the silicon atom under the conditions in entry 6, and found that no polymerization took place with these monomers.[13]

Table 1. Rhodium-catalyzed stitching polymerization of **1a**

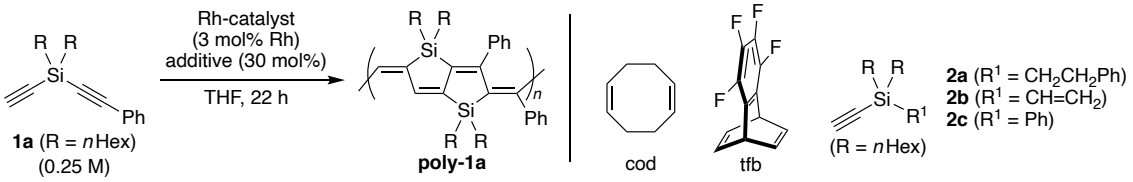

entry	Rh-catalyst	additive	temp (ºC)	yield (%)	M_n (g/mol)[a]	M_w/M_n[a]
1	$[Rh(OH)(cod)]_2$	none	60	89	9000	2.0
2	$[Rh(cod)\{(\eta^6\text{-}C_6H_5)BPh_3\}]$	none	60	98	9400	1.8
3	$[Rh(OH)(cod)]_2$,	none	20	93	18000	2.0
4	$[Rh(OH)(cod)]_2$	none	–10	95	45000	1.6
5	$[RhCl(cod)]_2$	Et_3N	–10	98	45000	1.6
6	$[RhCl(tfb)]_2$	Et_3N	–10	96	84000	2.1

[a] Determined using size-exclusion chromatography against a polystyrene standard.

The author examined the polymerization of other alkynylsilylacetylenes (Table 2). For example, monomers having a substituted phenyl group (**1b**), an alkyl group (**1c**), or an electron-withdrawing group (**1d**) on one of the alkynes gave the corresponding stitched polymers **poly-1b**, **poly-1c**, or **poly-1d** in 82–92% yield with M_n = 39000–46000 (entries 2–4). Polymerization of monomer **1e** having two unsubstituted ethynyl groups also proceeded smoothly by conducting the reaction at 20 ºC to give the corresponding **poly-1e** in 95% yield with M_n = 23000. The ^{13}C NMR spectra of these polymers suggested that both alkynes on the silicon atom of monomers **1** were successfully incorporated into the

main chain with essentially no residual peaks in the sp-carbon region, indicating the high stitching efficiency. It was also confirmed that the present polymerization conditions worked well for the stitching polymerization of 1,5-hexadiyne **3** as well, giving **poly-3** in 98% yield with M_n = 17000 (eq 1), which is significantly higher than that obtained under the conditions described in Chapter 2 (M_n = 8500).[10]

Table 2. Rhodium-catalyzed stitching polymerization of **1**

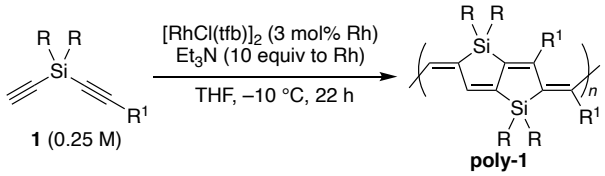

entry	monomer (R^1, R)	yield (%)	M_n (g/mol)[a]	M_w/M_n[a]
1	**1a** (Ph, *n*Hex)	96	84000	2.1
2	**1b** (4-($MeOCH_2CH_2O$)C_6H_4, Et)	88	46000	2.0
3[b]	**1c** (*n*Pr, *n*Hex)	92	46000	1.8
4[b]	**1d** ($CONMe_2$, *n*Hex)	82	39000	2.0
5[b,c]	**1e** (H, 2-ethylhexyl)	95	23000	2.4

[a] Determined using size-exclusion chromatography against a polystyrene standard. [b] 6 mol% of Rh was used. [c] The reaction was conducted at 20 ºC.

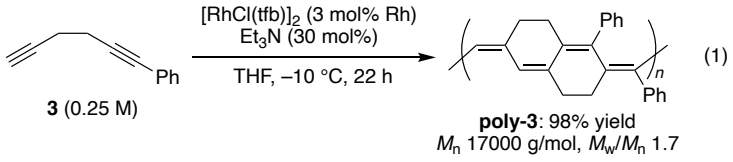

(1)

The structures of polymer repeating units were analyzed by using the ^1H and ^{13}C NMR data of **poly-1e** coupled with the DFT calculations of model trimer **tri-1e** in Table 3. For the ^1H NMR spectrum shown in Figure 1, two broad singlets at 7.34 ppm and 6.82 ppm

were assigned as alkenyl protons **H**^{c} and **H**^{a} on the main chain, respectively, and the alkyl protons were also consistent with the 2-ethylhexyl signals as indicated by black, blue, and red marks. For the ^{13}C NMR spectrum shown in Figure 2, sp^{2}-carbon signals at 158, 146, 139, and 129 ppm were assigned as alkenyl carbons **d**, **b**, **c**, and **a**, respectively, and the alkyl carbons were also consistent with the 2-ethylhexyl signals. In overall, the polymer repeating units can be concluded as drawn through the expected stitching polymerization.

Table 3. Calculated ^{1}H and ^{13}C NMR chemical shifts of compound **tri-1e** (in ppm, calculated at the B3LYP/6-31G(d) level of theory)

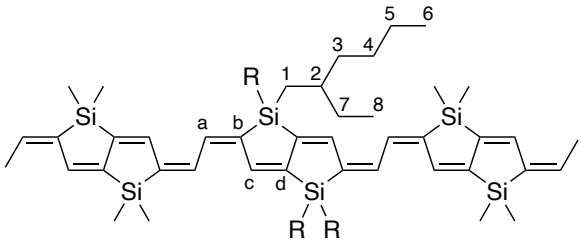

tri-1e (R = 2-ethylhexyl)

	a	**b**	**c**	**d**	**1**	**2**	**3**	**4**	**5**	**6**	**7**	**8**
^{1}H	6.92	—	7.22	—	0.90	1.67	1.45	1.50	1.33	0.95	1.43	1.01
^{13}C	123.9	139.5	133.6	152.7	23.2	37.8	38.0	32.7	26.2	16.4	35.0	14.7

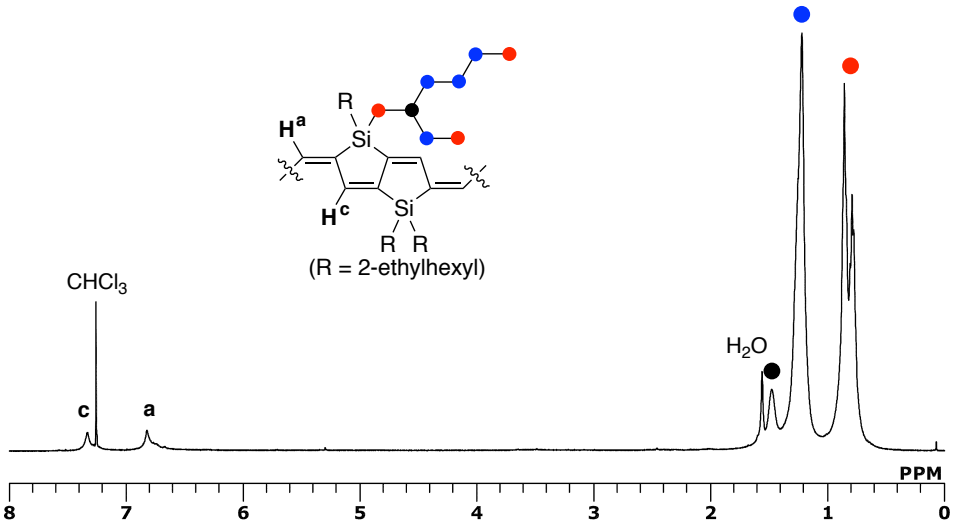

Figure 1. ^{1}H NMR signal assignment for **poly-1e**

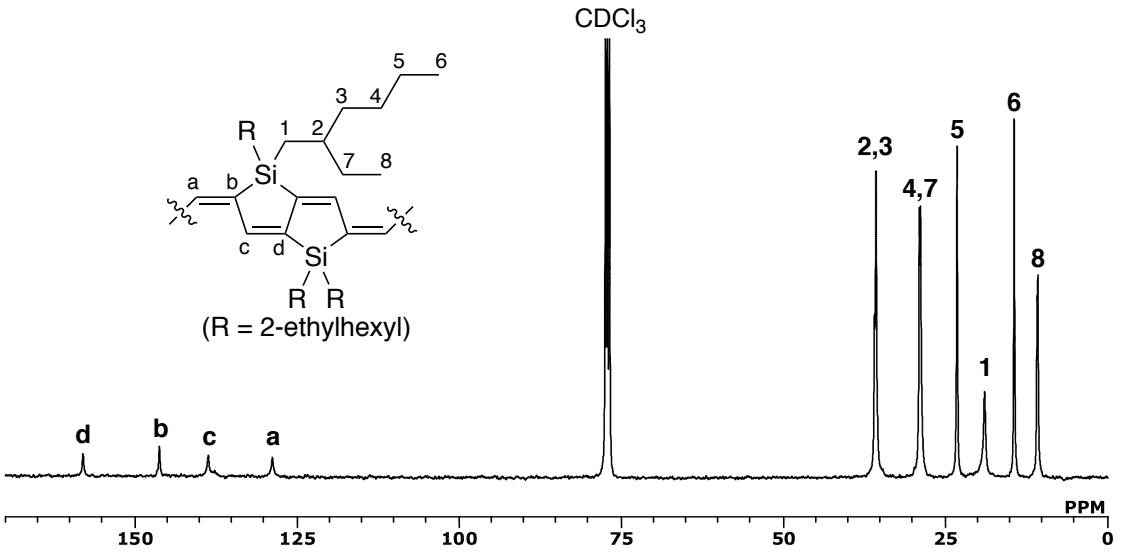

Figure 2. ^{13}C NMR signal assignment for **poly-1e**

The present stitching polymerization can also be applied to triyne **4a** connected by two silicon atoms for the synthesis of a polymer possessing a longer silicon-bridged π-conjugated repeating unit. As shown in Table 4, entry 1, the polymerization took place efficiently by using the same $[RhCl(tfb)]_2/Et_3N$ catalyst system to give **poly-4a** in 78% yield with M_n = 72000 (M_w/M_n = 1.9). According to the quantitative ^{13}C NMR spectrum of this polymer, essentially no residual peaks were observed in the sp-carbon region, indicating that the stitching efficiency is near perfect, which favorably compares with the system described in Chapter 2 for the stitching polymerization of ethylene-linked triynes.[10] The superiority of tfb over cod as the ligand for rhodium was more pronounced in the polymerization of triyne **4a**. Thus, as shown in entry 2, the use of $[RhCl(cod)]_2$ in place of $[RhCl(tfb)]_2$ led to a much lower yield (37% yield) with a lower molecular weight (M_n = 7600). The polymerization of triyne **4b** having a substituted phenyl group at the terminal also proceeded efficiently in the presence of $[RhCl(tfb)]_2$ to give **poly-4b** in 93% yield with M_n = 107000 (average DP = 210, M_w/M_n = 1.9; entry 3). On the other hand,

diyne **1f** having two silicon atoms, one as a linker and the other at the terminal as trimethylsilyl group, was found to be unreactive toward the present polymerization.

Table 4. Rhodium-catalyzed stitching polymerization of **4**

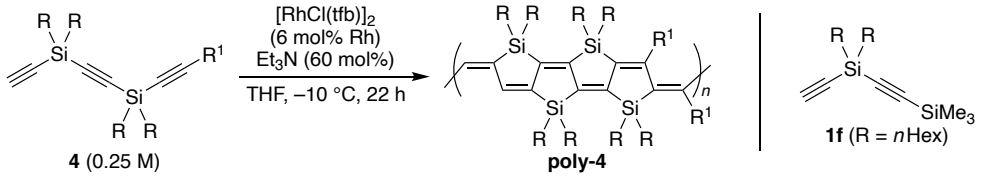

entry	monomer (R^1, R)	yield (%)	M_n (g/mol)[a]	M_w/M_n[a]
1	**4a** (Ph, *n*Hex)	78	72000	1.9
2[b]	**4a**	37	7600	1.5
3	**4b** (4-($MeOCH_2CH_2O$)C_6H_4, *n*Bu)	93	107000	1.9

[a] Determined using size-exclusion chromatography against a polystyrene standard. [b] $[RhCl(cod)]_2$ was used instead of $[RhCl(tfb)]_2$.

Furthermore, it was found that tetrayne **5** connected by three silicon atoms was also applicable to the stitching polymerization (Table 5). Although polymerization of **5a** having two *n*-hexyl groups on all the silicon atoms showed some decrease in the stitching efficiency (entry 1), replacement of the central di(*n*-hexyl)silylene by diphenylsilylene (**5b**) realized highly efficient stitching polymerization to give **poly-5b** having a repeating unit composed of a conjugated hexadecaoctaene bridged by six silicon atoms in 89% yield with M_n = 24000 (M_w/M_n = 1.7; entry 2).

Table 5. Rhodium-catalyzed stitching polymerization of **5**

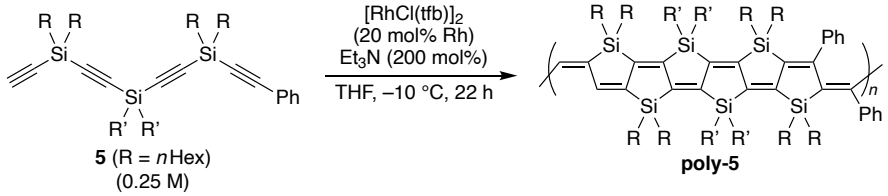

entry	monomer (R')	yield (%)	M_n (g/mol)[a]	M_w/M_n[a]	stitching efficiency (%)
1	**5a** (*n*Hex)	79	11000	1.9	83
2	**5b** (Ph)	89	24000	1.7	97

[a] Determined using size-exclusion chromatography against a polystyrene standard. [b] Incorporation efficiency of internal alkynes determined by quantitative ^{13}C NMR

3.2.2 Mechanistic consideration

A simplified possible reaction pathway for the present stitching polymerization of alkynylsilylacetylenes **1** is illustrated in Scheme 2.[3,10] Thus, the reaction of a chlororhodium complex (Cl–**Rh**; **Rh** = Rh(tfb)) with the terminal alkyne of **1** in the presence of Et_3N gives active alkynylrhodium species R–**Rh**. This initiates the polymerization by successively incorporating monomers **1** in a stitching manner to give alkenylrhodium species **D** via **A**, **B**, and **C**.[14] The polymer chain grows by repeating the stitching reaction with incoming monomers **1** to give intermediate **E**. Protonation of the rhodium-bound chain-end by the terminal alkyne of **1** releases **poly-1** with regeneration of R–**Rh** (chain transfer).[15] To gain some insights into the present polymerization mechanism, the author prepared deuterium-labeled monomer **1a-*d*** and compared the polymerization efficiency with non-deuterated monomer **1a** (Table 6). As a result, **poly-1a-*d*** was obtained in 90% yield with a higher molecular weight (M_n = 115000; entry 2) compared with **poly-1a** (M_n = 84000; entry 1), indicating that the chain propagation (alkyne insertion) is sufficiently fast and the rate of a C(sp)–H bond cleaving step (either initiation or chain transfer) would determine the overall polymerization outcome. To elucidate which of these two elemental steps (initiation or chain transfer) is the key factor, the polymerization was conducted in the presence of (1,2,2-triphenylvinyl)lithium to accelerate the initiation step (entries 3 and 4).[2f–h] Under these conditions, the degree of polymerization became somewhat lower compared to entries 1 and 2, but essentially no difference in the molecular weight was observed between **poly-1a** and **poly-1a-*d***, suggesting that the chain transfer does not seem to affect the overall process of the present polymerization. These results indicate that the initiation step to form R–**Rh** from R–H and Cl–**Rh** is most likely the rate-determining step under the standard polymerization conditions ($[RhCl(tfb)]_2/Et_3N$ system). This can also explain the increase of molecular

weights by lowering the polymerization temperature (Table 1), which would decrease the initiation efficiency (the amount of active rhodium species) even with the same catalyst loading, leading to a longer chain propagation on each rhodium species. The initiation efficiency is typically 0.1–0.2 under the optimized conditions for monomers **1**, **4**, and **5**.

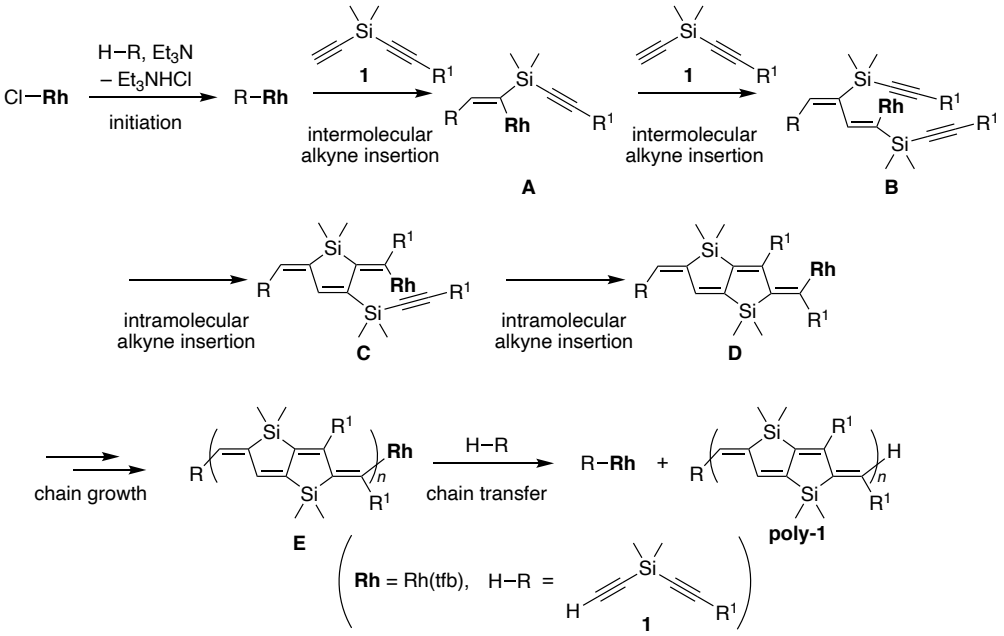

Scheme 2. A proposed reaction pathway of rhodium-catalyzed stitching polymerization of alkynylsilylacetylenes **1**

Table 6. Comparison of **1a** and **1a-*d*** in the rhodium-catalyzed stitching polymerization

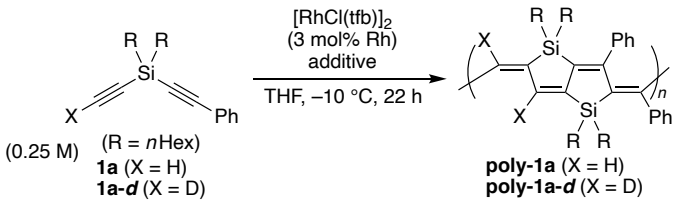

entry	monomer	additive	yield (%)	M_n (g/mol)[a]	M_w/M_n[a]
1	**1a**	Et_3N (30 mol%)	96	84000	2.1
2	**1a-*d***	Et_3N (30 mol%)	90	115000	1.7
3	**1a**	$Ph_2C{=}C(Ph)Li$ (4.5 mol%)	82	67000	1.9
4	**1a-*d***	$Ph_2C{=}C(Ph)Li$ (4.5 mol%)	90	69000	1.9

[a] Determined using size-exclusion chromatography against a polystyrene standard.

With regard to the relationship between monomer substituents and applicability to the rhodium-catalyzed polymerization, it was shown that simple silylacetylenes such as trimethylsilylacetylene and compounds **2a–2c** did not undergo polymerization unlike alkynylsilylacetylenes **1a–1e** in Table 2. In addition, although triynes **4a** and **4b** having two silicon atoms polymerized efficiently, no polymerization took place with diyne **1f** having trimethylsilyl group at the terminal (Table 4). These results suggest that the successful chain growth, *i.e.*, intermolecular insertion of an alkyne to alkenylrhodium species **D**, requires $R^1 \neq SiR_3$ (R = alkyl, alkenyl, or aryl) in Scheme 2, although the author does not have a conclusive explanation for its origin at this stage.[16]

3.2.3 Functionalization and Post-derivatization.

Alkynylsilylacetylene monomers employed so far had simple alkyl substituents such as *n*-hexyl group on the silicon atoms to primarily focus on the reaction development itself. However, the author imagined that solubility (affinity to different types of solvents) of the polymers could be controlled by introducing appropriate functional groups at these positions without perturbing the polymer main chains. To this end, the author obtained **poly-1g** derived from monomer **1g** possessing amino groups (eq 2)[17] and **poly-1h** derived from monomer **1h** with polyfluoroalkyl groups (eq 3).[18] While **poly-1e** having 2-ethylhexyl groups is soluble in typical organic solvents such as hexane and CH_2Cl_2 (1.0 g/L) and insoluble in aqueous phase, **poly-1g** was found to be soluble in diluted aqueous hydrochloric acid (1.0 g/L in 0.05 M HClaq) over hexane (Figure 3-(a)). On the other hand, **poly-1h** is soluble in fluorous solvents such as perfluorohexane (4.0 g/L) favorably over CH_2Cl_2 (Figure 3-(b)).

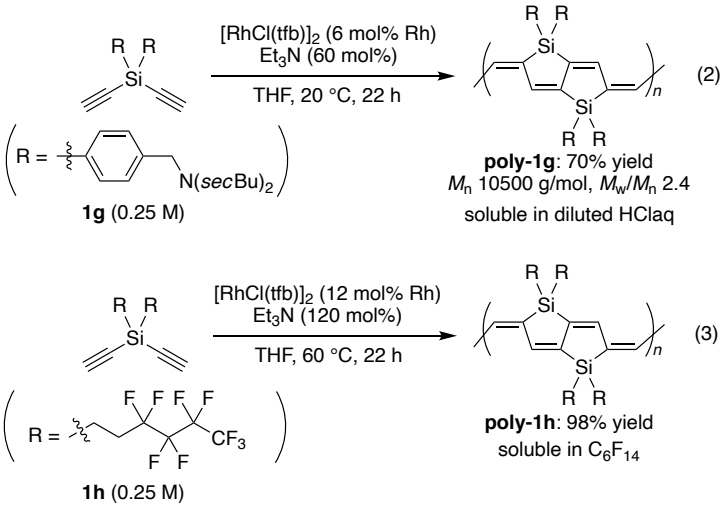

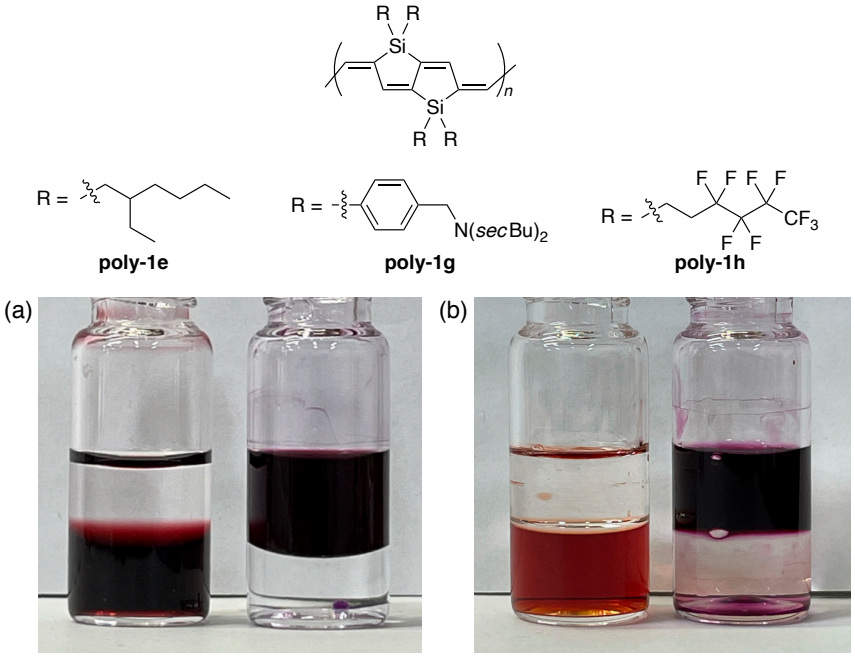

Figure 3. Photographs of solutions: (a) left **poly-1g** in 0.05 M HClaq (bottom phase) with hexane (top phase); right **poly-1e** in hexane (top phase) with 0.05 M HClaq (bottom phase). (b) left **poly-1h** in perfluorohexane (bottom phase, d = 1.67) with CH_2Cl_2 (top phase, d = 1.33); right **poly-1e** in CH_2Cl_2 (top phase) with perfluorohexane (bottom phase).

The polymers obtained by the present stitching polymerization are of interest themselves as a new type of π-conjugated polymers possessing a silicon-bridged π-conjugated repeating unit, but they can also be used as precursors of sequence-controlled functionalized polyacetylenes that are difficult to prepare using existing methods. For example, protodesilylation of **poly-1b** proceeded smoothly by treating it with nBu$_4$NF•3H$_2$O to give **poly-6b** in 84% yield, which can be regarded as a periodic copolymer of acetylene and arylacetylene in an AABB fashion (eq 4). Similarly, triyne-derived **poly-4b** was converted to protodesilylated **poly-7b**, an AAAABB periodic copolymer of acetylene and arylacetylene, in 95% yield (eq 5).

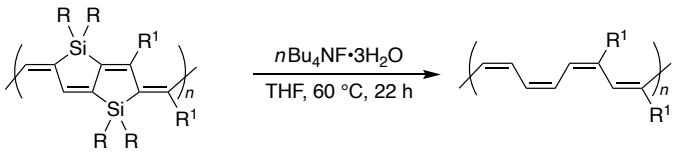

(4)

poly-1b (R = Et, R^1 = 4-MeO$(CH_2)_2OC_6H_4$)
M_w 92000 g/mol (MALS)

poly-6b (R^1 = 4-MeO$(CH_2)_2OC_6H_4$)
84% yield (95% desilylated)
M_w 31000 g/mol (MALS)

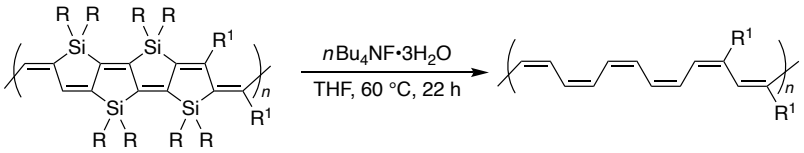

(5)

poly-4b (R = *n*Bu, R^1 = 4-MeO$(CH_2)_2OC_6H_4$)
M_w 190000 g/mol (MALS)

poly-7b (R^1 = 4-MeO$(CH_2)_2OC_6H_4$)
95% yield (94% desilylated)
M_w 60000 g/mol (MALS)

3.2.4 Physical properties

The author examined their optical properties using UV-vis spectrophotometry. **Poly-1a** possessing phenyl group showed absorption maximum at 549 nm, and **poly-1d** with amide group as an electron withdrawing group and **poly-1e** without substituent displayed relatively similar absorption profiles with one another, whereas **poly-1c** with an alkyl group as an electron-donating group showed hypsochromic shift (Figure 4, Table 7). As shown in Figure 5, it is worth noting that the UV-vis spectrum of **poly-1a** is in stark contrast to that of polyphenylacetylene (M_n = 24000, M_w/M_n = 1.8), a related π-conjugated polymer possessing no ladder-type π-conjugation units, which showed absorption maximum at 335 nm with absorption edge of ca. 520 nm (Figure 5). It was also confirmed that the absorption band of silicon-bridged **poly-1a** is significantly red-shifted compared with the corresponding ethylene-bridged **poly-3** (λ_{max} = 417 nm and λ_{edge} = ca. 610 nm). These results demonstrate that polymers obtained in the stitching polymerization of diynes show substantial extension of π-conjugation by introduction of rigid bridged structures in the repeating unit, and the effective conjugation length can be controlled by the type of bridging groups. On the other hand, absorption spectra of diyne-derived **poly-1a**, triyne-derived **poly-4a**, and tetrayne-derived **poly-5b** are not significantly different with one another (Figure 6), which suggests that the effective conjugation lengths are more or less the same in this series of polymers.

Regarding the protodesilylated polymers, the UV-vis absorption spectrum of **poly-7b** is shown in Figure 7, along with those of its precursor **poly-4b** and the related polyarylacetylene [aryl = 4-(2-methoxyethoxy)phenyl; M_n = 44000, M_w/M_n = 2.2]. Because the main chain no longer possesses bridged structures in **poly-7b**, the absorption spectrum became similar to that of simple polyarylacetylene. However, presumably due to the existence of unsubstituted polyene units, the effective conjugation length of **poly-**

7b is much longer and its absorption edge reached ca. 680 nm (vs. λ_{edge} = ca. 540 nm for polyarylacetylene).

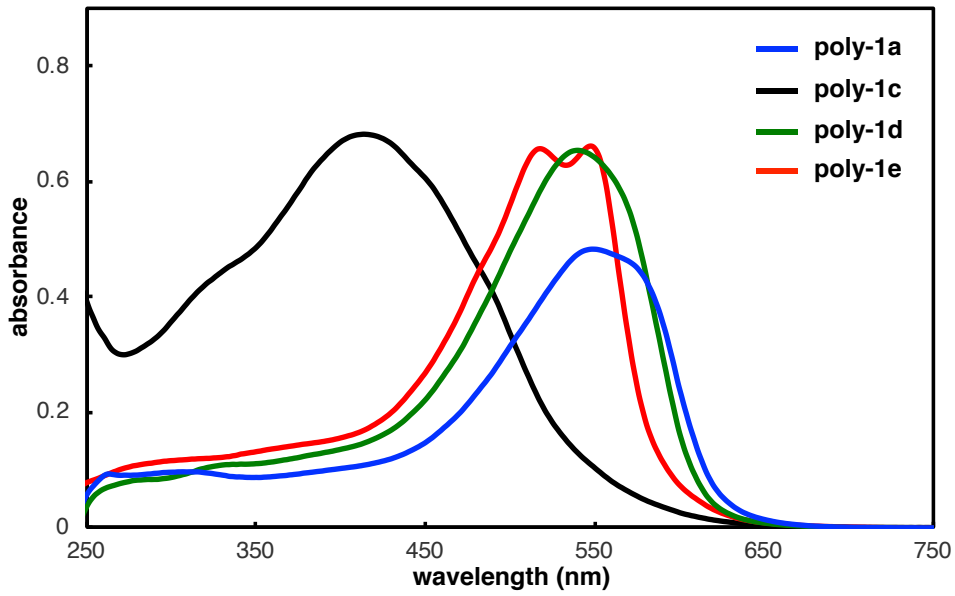

Figure 4. UV-vis spectra of **poly-1a** (blue line; at 1.6 x 10^{-2} g/L), **poly-1c** (black line; at 2.9 x 10^{-2} g/L), and **poly-1d** (green line; at 1.2 x 10^{-2} g/L), and **poly-1e** (red line; at 1.3 x 10^{-2} g/L) in THF at 25 ºC

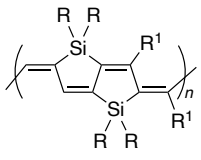

poly-1

Table 7. UV-vis absorption of **poly-1**

polymer	(R, R^1)	λ_{max}/nm (absorbance/a.u.)	λ_{edge}/nm
poly-1a	(*n*Hex, Ph)	549 (0.47)	ca. 691
poly-1c	(*n*Hex, *n*Pr)	540 (0.66)	ca. 701
poly-1d	(*n*Hex, $CONMe_2$)	548 (0.66), 518 (0.66)	ca. 713
poly-1e	(2-ethylhexyl, H)	414 (0.68)	ca. 668

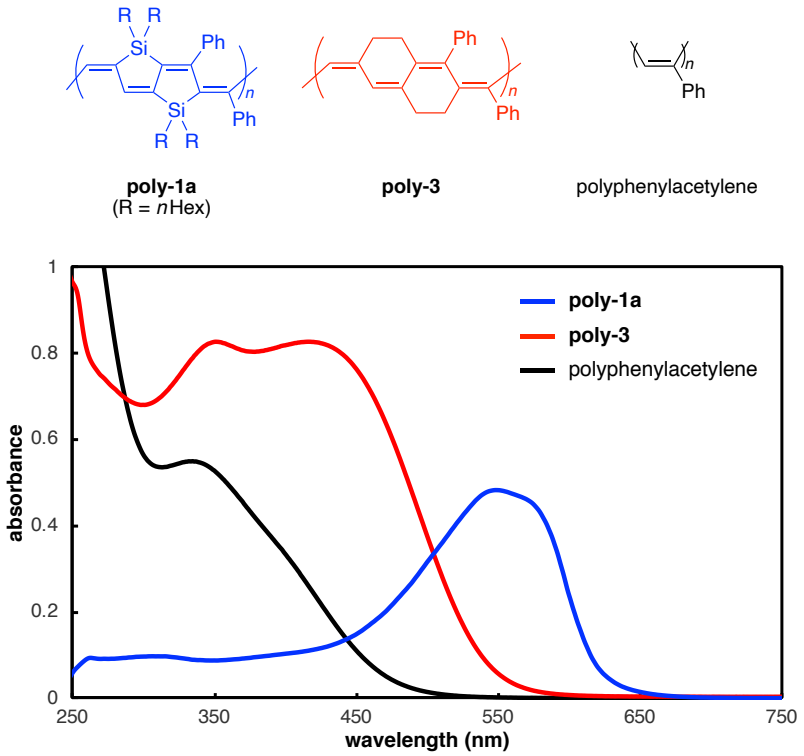

Figure 5. UV-vis spectra of **poly-1a** (blue line; at 1.6 x 10^{-2} g/L), **poly-3** (red line; at 2.1 x 10^{-2} g/L), and polyphenylacetylene (black line; at 2.4 x 10^{-2} g/L) in THF at 25 ºC

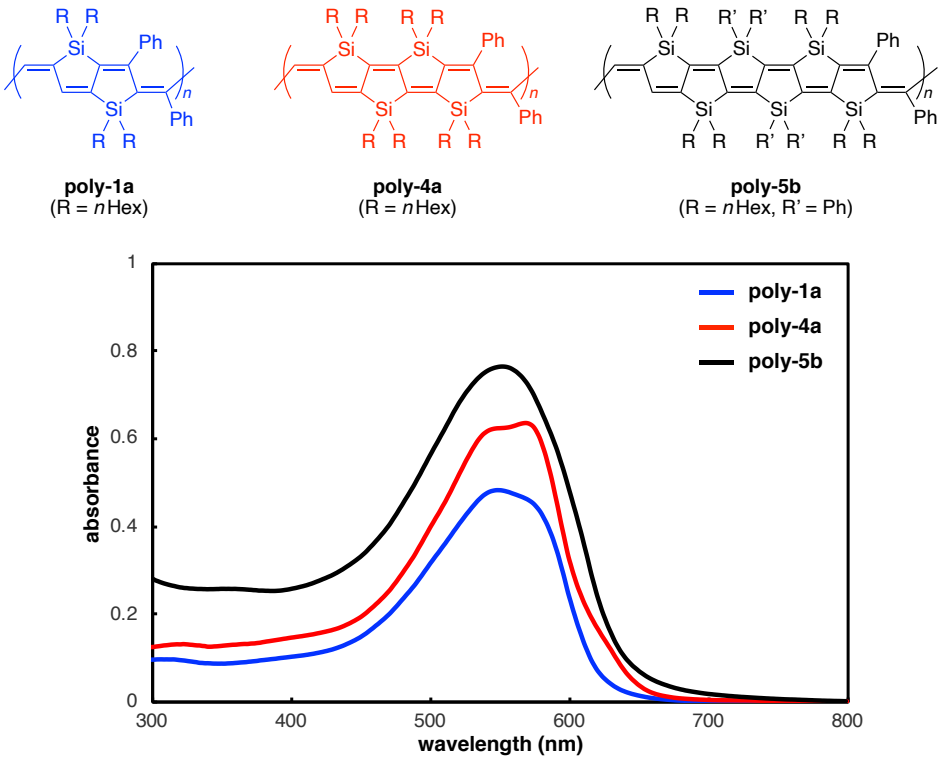

Figure 6. UV-vis spectra of **poly-1a** (blue line; at 1.6 x 10^{-2} g/L), **poly-4a** (red line; at 1.2 x 10^{-2} g/L), and **poly-5b** (black line; at 1.8 x 10^{-2} g/L) in THF at 25 ºC

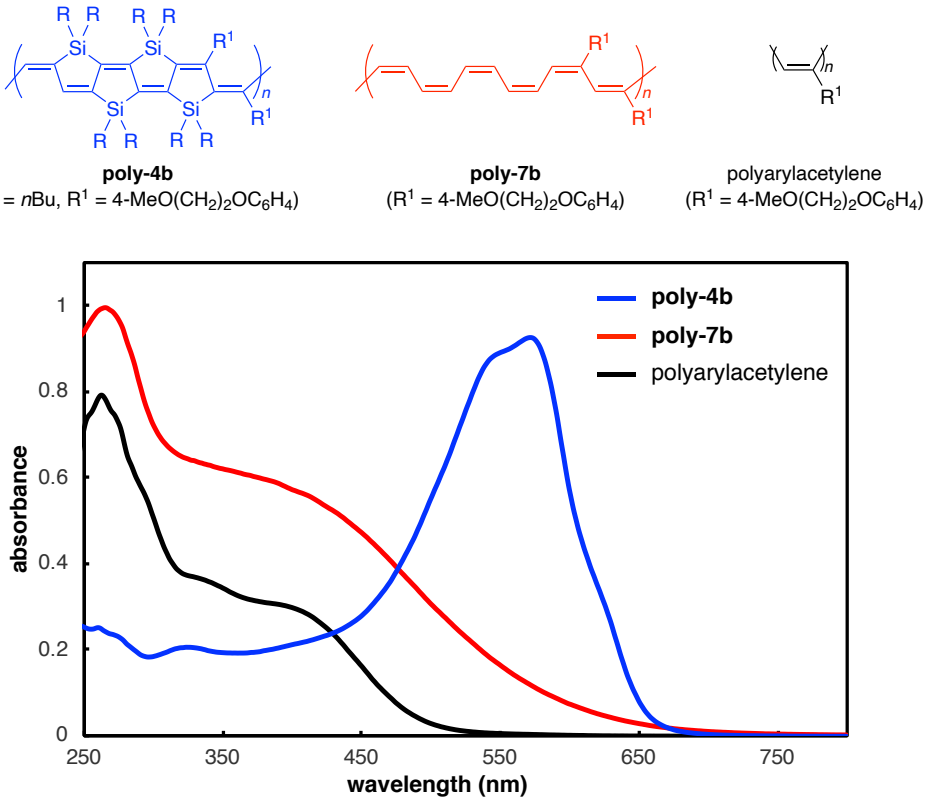

Figure 7. UV-vis spectra of **poly-4b** (blue line; at 2.6 x 10^{-2} g/L), **poly-7** (red line; at 2.2 x 10^{-2} g/L), and polyarylacetylene (aryl = 4-(2-methoxyethoxy)phenyl; black line; at 3.2 x 10^{-2} g/L) in THF at 25 ºC

Electrochemical analysis was conducted by cyclic voltammetry for silicon-bridged **poly-4b** and protodesilylated **poly-7b**. As shown in Figure 8, the oxidation potential of **poly-4b** (E_{ox}^{onset} = 0.75 V) is lower than that of **poly-7b** (E_{ox}^{onset} = 1.25 V), and the reduction potential of **poly-4b** (E_{red}^{onset} = –2.20 V) is higher than that of **poly-7b** (E_{red}^{onset} = –2.35 V). These results indicate that the HOMO–LUMO energy gap is narrower for **poly-4b** compared with **poly-7b**, which is consistent with the UV-vis absorption spectra in Figure 7.

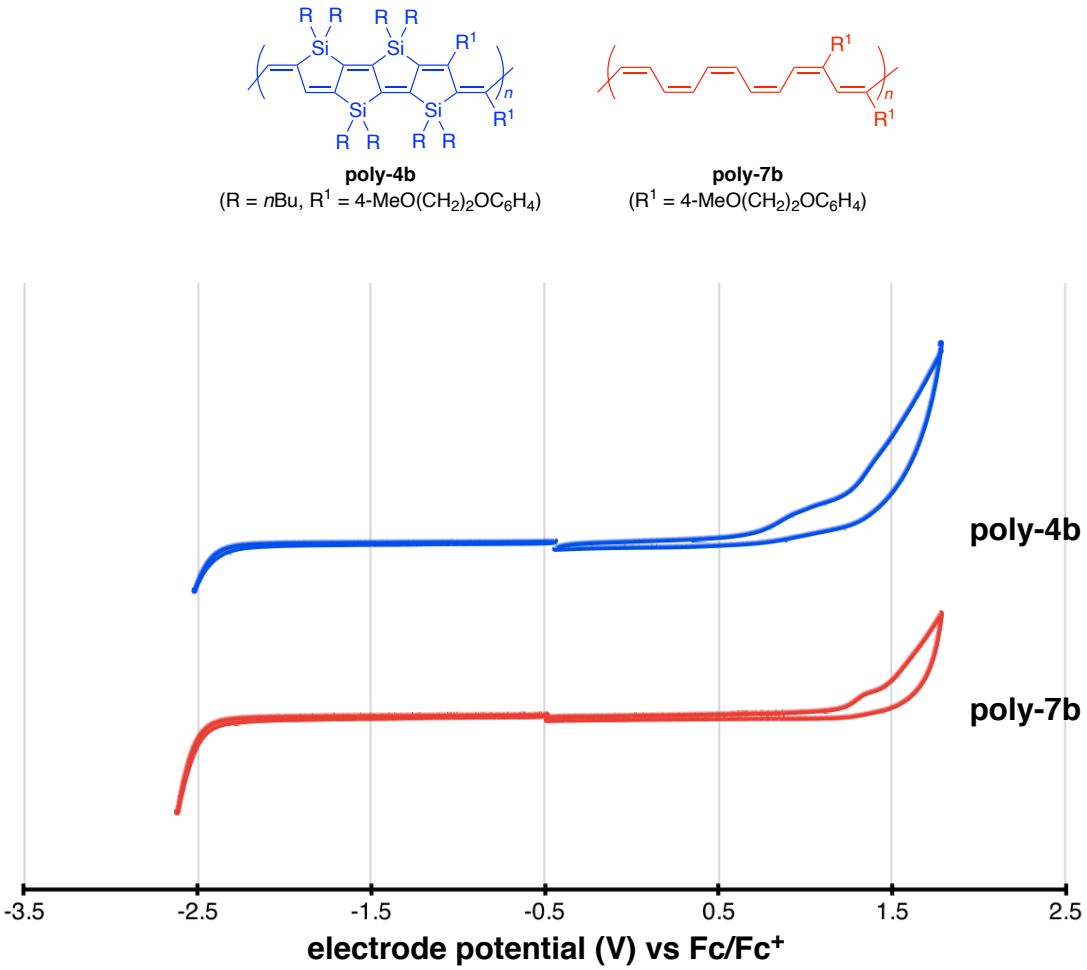

Figure 8. Cyclic voltammograms of **poly-4b** (blue) and **poly-7b** (red) containing 0.1 M (nBu)$_4$NBF$_4$ as the supporting electrolyte, Ag/Ag$^+$ as the reference electrode, glassy carbon as the working electrode, Pt plate as the counter electrode, and a scan rate of 100 mV/s. The oxidation potential and the reduction potential were measured at room temperature under nitrogen in CH_2Cl_2. The potential was externally calibrated against the ferrocene/ferrocenium couple.

The author also examined the electrical conductivity of silicon-bridged **poly-1i** and protodesilylated **poly-6j** as examples (Figure 9-(a)).[19] Electrical conductivity of **poly-1i** and **poly-6j** was determined by measuring the electrical resistance and the film thickness of the polymer thin films, which were prepared by dropping the polymer solution (10 mg/mL in CH_2Cl_2) on the electrode and the films were exposed to iodine vapor for 1 day. For the resistance measurement, two-terminal sensing was used for **poly-1i** and four-

terminal sensing was used for **poly-6j** under floating conditions (Figure 9-(b)). As a result, the conductivity of **poly-1i** and **poly-6j** was found to be 1.0 x 10^{-8} S/cm and 1.3 x 10^{-6} S/cm, respectively. Although the degree of conductivity is not particularly high as semiconductors, these results indicate the possibility of further improvement of conductivity by modification of the main chain structures and/or substituents.

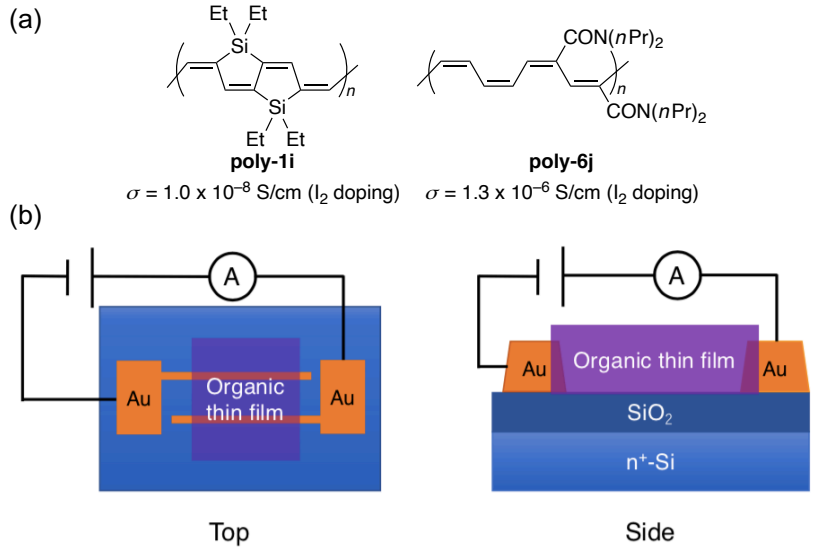

Figure 9. (a) Structures of **poly-1i** and **poly-6j** and their electrical conductivity (b) Illustrations of the set-up for the resistance measurement (left: top view, right: side view)

Finally, it is also worth noting that the stitched polymers obtained in the present study typically showed good thermostability. For example, **poly-1a** and **poly-4b** retained ≥95% of their weights at up to 390 ºC and 389 ºC, respectively, by thermogravimetric analysis.

3.3 Conclusion

The author developed a rhodium-catalyzed stitching polymerization of alkynylsilylacetylenes for the synthesis of π-conjugated polymers with new ladder-type silicon-bridged repeating units. The polymerization proceeded smoothly with high degrees of stitching efficiency and with high molecular weights by employing a Rh/tfb complex as the catalyst under mild conditions. Not only diynes but also triynes and tetraynes could be polymerized under these conditions to give polymers possessing a repeating unit composed of conjugated oligoenes bridged by multiple silicon atoms, which are not easily accessible by existing synthetic methods. The author also demonstrated that the solubility of the polymers could be controlled by introducing appropriate functional groups on the silicon atoms and that sequence-controlled functionalized polyacetylenes could be accessed by protodesilylation of the stitched polymers. The polymers obtained by the present method were found to be highly conjugated, thermally stable, and moderately semiconducting through investigation of their physical properties.

3.4 Experimental Section

General

All air- and moisture-sensitive manipulations were carried out with standard Schlenk techniques under nitrogen. Preparative GPC was performed with JAI LC-9201 or LaboACE LC-5060 equipped with JAIGEL-2HR columns using $CHCl_3$ as an eluent. NMR spectra were recorded on JEOL JNM-ECS400, Agilent Unity-Inova500, or BRUKER AVANCEⅢ700 spectrometer. Size-exclusion chromatography analyses were performed with JASCO-GPC900 equipped with PLgel MIXED-C columns using THF as an eluent and the molecular weights were calibrated against standard polystyrene samples. Absolute molecular weight analyses were performed on Wyatt Technology DAWN HELEOS II multi-angle light scattering instrument. High resolution mass spectra were recorded on JEOL JMS700 spectrometer. Thermogravimetric analyses were performed with SII Exstar TG/DTA6200 under nitrogen atmosphere. UV-vis spectra were recorded on HITACHI U-2900 and JASCO V-770 spectrophotometers. Elemental analysis was performed on YANACO CHN CORDER MT-6. Electrical resistance was measured using two-terminal or four-terminal sensing with Keithley 6430 sourcemeter. Film thickness was measured with OLYMPUS OLS4100 laser microscope. Computations were performed using workstation at Research Center for Computational Science, National Institutes of Natural Sciences, Okazaki, Japan.

THF (Kanto Chemical; dehydrated), CH_2Cl_2 (Kanto Chemical; dehydrated), and MeCN (Wako Chemicals; dehydrated) were degassed by purging nitrogen prior to use. CCl_4 (Wako Chemicals) was dried over $MgSO_4$ and degassed by purging nitrogen prior to use. Diisopropylamine (Wako Chemicals) and triethylamine (Wako Chemicals) were distilled over KOH under vacuum. 1-Bromohexane (Wako Chemicals), iodobenzene (Wako Chemicals), 4-bromobenzyl bromide (TCI), phenylacetylene (Kanto Chemical),

1,5-hexadiyne (TCI), tetradecafluorohexane (Aldrich), dimethylcarbamoyl chloride (Nacalai Tesque), dichlorodiethylsilane (TCI), trichlorosilane (TCI), tetrachlorosilane (TCI), di-*sec*-butylamine (TCI), trichloroisocyanuric acid (TCI), tetrabutylammonium fluoride (Wako Chemicals; trihydrate), *n*BuLi (Kanto Chemical; 1.55–1.59 M solution in hexane), ethynylmagnesium bromide (Aldrich; 0.5 M solution in THF), ethylmagnesium bromide (Kanto Chemical; 0.97 M solution in THF), Mg turnings (Wako Chemicals), iodine (Wako Chemicals), K_2CO_3 (Wako Chemicals), KI (Wako Chemicals), D_2O (ISOTEC), $PdCl_2$ (Tanaka Kikinzoku), and CuI (Kanto Chemical) were used as received. 4-(2-Methoxyethoxy)phenylacetylene,[20-23] (1,2,2-triphenylvinyl)lithium,[24] $[Rh(OH)(cod)]_2$,[25] $Rh(cod)[(\eta^6\text{-}C_6H_5)BPh_3]$,[26] $[RhCl(cod)]_2$,[27] $[RhCl(tfb)]_2$,[28] and $Pd(PPh_3)_4$,[29] were synthesized following the literature procedures.

Representative Procedures:

Dihexyl(phenylethynyl)silylacetylene (1a)

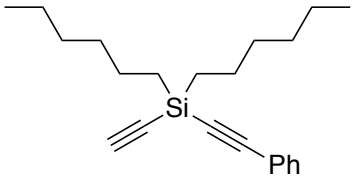

A solution of 1-bromohexane (7.92 g, 48.0 mmol) in THF (20 mL) was added dropwise over 30 min to a suspension of Mg turnings (1.02 g, 42.0 mmol) in THF (20 mL), and the mixture was stirred for 1 h at room temperature. The resulting solution was added slowly over 15 min to trichlorosilane (2.01 mL, 20 mmol) at –78 ºC, and the mixture was stirred for 21 h at –78 ºC. A solution of phenylethynyllithium [generated from phenylacetylene (2.04 g, 20 mmol) and *n*BuLi (13.2 mL, 21 mmol; 1.59 M solution in hexane) in THF (30 mL) at –78 ºC] was then added to it, and the mixture was stirred for 12 h at room temperature. The reaction was quenched with saturated NH_4Claq and

this was extracted with Et_2O. The organic layer was washed with saturated NaClaq, dried over $MgSO_4$, filtered, and concentrated under vacuum. The residue was chromatographed on silica gel with hexane and dried under vacuumed at 40 ºC to afford dihexyl(phenylethynyl)silane as a colorless oil (5.36 g, 17.8 mmol; 89% yield).

^{1}H NMR ($CDCl_3$): δ 7.52-7.43 (m, 2H), 7.37-7.27 (m, 3H), 4.11 (quint, $^3J_{HH}$ = 3.3 Hz, 1H), 1.57-1.23 (m, 16H), 0.89 (t, $^3J_{HH}$ = 6.9 Hz, 6H), 0.83-0.72 (m, 4H). ^{13}C NMR ($CDCl_3$): δ 132.2, 128.8, 128.4, 123.2, 107.3, 90.0, 32.8, 31.7, 24.5, 22.7, 14.3, 12.3.

Dihexyl(phenylethynyl)silane (1.50 g, 4.99 mmol) was added to a suspension of $PdCl_2$ (8.8 mg, 50 μmol) in CCl_4 (10 mL) at room temperature, and the mixture was stirred for 4 h at 40 ºC. The precipitates were filtered off through Celite with THF (3 mL) and the volatiles were removed under vacuum. The residue was dissolved in THF (3 mL) and the volatiles were removed under vacuum. This was repeated again to afford chlorodihexyl(phenylethynyl)silane as a pale yellow oil. Ethynylmagnesium bromide (10.0 mL, 5.00 mmol; 0.5 M solution in THF) was added to it and the mixture was stirred for 2 h at room temperature. The reaction was quenched with saturated NH_4Claq and this was extracted with Et_2O. The organic layer was washed with saturated NaClaq, dried over $MgSO_4$, filtered, and concentrated under vacuum. The residue was chromatographed on silica gel with hexane to afford compound **1a** as a yellow oil (974 mg, 3.00 mmol; 60% yield).

^{1}H NMR ($CDCl_3$): δ 7.54-7.43 (m, 2H), 7.38-7.27 (m, 3H), 2.48 (s, 1H), 1.61-1.21 (m, 16H), 0.89 (t, $^3J_{HH}$ = 6.6 Hz, 6H), 0.85-0.75 (m, 4H). ^{13}C NMR ($CDCl_3$): δ 132.3, 129.0, 128.4, 122.9, 107.0, 94.8, 89.0, 85.9, 32.8, 31.6, 23.7, 22.7, 14.7, 14.3. HRMS (EI) calcd for $C_{22}H_{32}Si$ (M^+) 324.2268, found 324.2268.

Dihexyl(phenylethynyl)silylacetylene (1a-*d*)

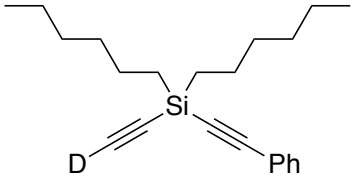

A solution of lithium diisopropylamide [generated from diisopropylamine (310 μL, 2.21 mmol) and *n*BuLi (1.40 mL, 2.23 mmol; 1.59 M solution in hexane) in THF (2.5 mL) at –78 ºC] was added to a solution of compound **1a** (651 mg, 2.01 mmol) in THF (2.5 mL) at –78 ºC, and the resulting solution was stirred for 30 min at –78 ºC. D_2O (2 mL) was added to this solution, and the resulting mixture was warmed to room temperature and stirred for 30 min. This was extracted with Et_2O, dried over Na_2SO_4, filtered, and concentrated under vacuum. The residue was chromatographed on silica gel with hexane to afford compound **1a-*d*** as a colorless oil (343 mg, 1.05 mmol; 53% yield, 98% D).

^{1}H NMR ($CDCl_3$): δ 7.51-7.46 (m, 2H), 7.38-7.27 (m, 3H), 2.48 (s, 0.02H), 1.58-1.45 (m, 4H), 1,45-1.36 (m, 4H), 1.36-1.25 (m, 8H), 0.89 (t, $^3J_{HH}$ = 7.1 Hz, 6H), 0.85-0.77 (m, 4H). ^{13}C NMR ($CDCl_3$): δ 132.3, 129.0, 128.3, 122.8, 107.0, 94.6 (t, $^1J_{CD}$ = 35.0 Hz), 88.9, 85.3 (t, $^2J_{CD}$ = 5.8 Hz), 32.8, 31.6, 23.7, 22.7, 14.7, 14.3. HRMS (EI) calcd for $C_{22}H_{31}DSi$ (M^+) 325.2331, found 325.2331.

3-(Dihexylethynylsilyl)-*N*,*N*-dimethylpropiolamide (1d)

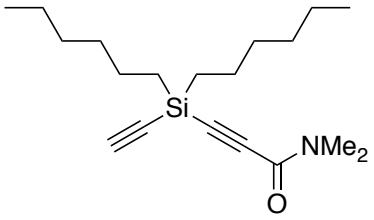

A solution of 1-bromohexane (7.92 g, 48.0 mmol) in THF (10 mL) was added dropwise over 30 min to a suspension of Mg turnings (1.02 g, 42.0 mmol) in THF (30

mL), and the mixture was stirred for 3 h at room temperature. The resulting solution was added slowly over 15 min to trichlorosilane (2.01 mL, 20.0 mmol) at –78 ºC, and the mixture was stirred for 1 h at –78 ºC. Ethynylmagnesium bromide (40.0 mL, 20.0 mmol; 0.5 M solution in THF) was then added to it, and the mixture was stirred for 21 h at room temperature. The reaction was quenched with saturated NH_4Claq and this was extracted with Et_2O. The organic layer was washed with saturated NaClaq, dried over $MgSO_4$, filtered, and concentrated under vacuum. The residue was chromatographed on silica gel with hexane and dried under vacuum at 40 ºC to afford dihexylethynylsilane as a colorless oil (4.12 g, 18.4 mmol; 92% yield).

^{1}H NMR ($CDCl_3$): δ 3.98 (quint, $^3J_{HH}$ = 3.2 Hz, 1H), 2.40 (s, 1H), 1.48-1.19 (m, 16H), 0.89 (t, $^3J_{HH}$ = 6.6 Hz, 6H), 0.78-0.63 (m, 4H). ^{13}C NMR ($CDCl_3$): δ 95.3, 86.0, 32.7, 31.7, 24.3, 22.7, 14.2, 12.0.

Dihexylethynylsilane (1.79 g, 7.97 mmol) was added over 3 min to a suspension of trichloroisocyanuric acid (639 mg, 2.75 mmol) in CH_2Cl_2 (24 mL) at room temperature, and the mixture was stirred for 2 days. The precipitates were filtered off through Celite with THF (5 mL) and the volatile were removed under vacuum. The residue was dissolved in THF (3 mL) and the volatiles were removed again. This was repeated again to afford chlorodihexylethynylsilane as a colorless oil. Ethylnylmagnesium bromide (15.0 mL, 7.50 mmol; 0.5 M solution in THF) was added to it slowly over 5 min and the mixture was stirred for 15 h at room temperature. The reaction was quenched with saturated NH_4Claq and this was extracted with Et_2O. The organic layer was washed with saturated NaClaq, dried over $MgSO_4$, filtered, and concentrated under vacuum. The residue was chromatographed on silica gel with hexane to afford dihexyl(diethynyl)silane as a white solid (1.77 g, 7.12 mmol; 89% yield).

^{1}H NMR ($CDCl_3$): δ 2.46 (s, 2H), 1.53-1.22 (m, 16H), 0.89 (t, $^3J_{HH}$ = 6.9 Hz, 6H), 0.80-0.71 (m, 4H). ^{13}C NMR ($CDCl_3$): δ 95.1, 85.2, 32.8, 31.6, 23.5, 22.7, 14.3, 14.2.

Ethylmagnesium bromide (3.20 mL, 3.10 mmol; 0.97 M solution in THF) was added over 10 min to a solution of dihexyl(diethynyl)silane (745 mg, 3.00 mmol) in THF (6 mL) at room temperature, and this was stirred for 1 h at room temperature. The resulting solution was added to a solution of dimethylcarbamoyl chloride (339 mg, 3.15 mmol) in THF (10 mL) at –78 ºC with the aid of THF (2 mL), and the mixture was warmed to room temperature and stirred for 5 h. The reaction was quenched with saturated NH_4Claq and this was extracted with EtOAc. The organic layer was washed with saturated NaClaq, dried over $MgSO_4$, filtered, and concentrated under vacuum. The residue was chromatographed on silica gel with hexane/EtOAc = 3/1 and further purified by GPC with $CHCl_3$ to afford compound **1d** as a yellow oil. (178 mg, 0.56 mmol; 19% yield).

^{1}H NMR ($CDCl_3$): δ 3.23 (s, 3H), 2.97 (s, 3H), 2.47 (s, 1H), 1.51-1.22 (m, 16H), 0.89 (t, $^3J_{HH}$ = 6.8 Hz, 6H), 0.84-0.74 (m, 4H). ^{13}C NMR ($CDCl_3$): δ 153.7, 97.5, 95.8, 92.0, 84.3, 38.4, 34.2, 32.7, 31.5, 23.5, 22.6, 14.2, 14.0. HRMS (FAB) calcd for $C_{19}H_{34}NOSi$ ($M+H^+$) 320.2404, found 320.2409.

Bis(4-(di-*sec*-butylaminomethyl)phenyl)diethynylsilane (1g)

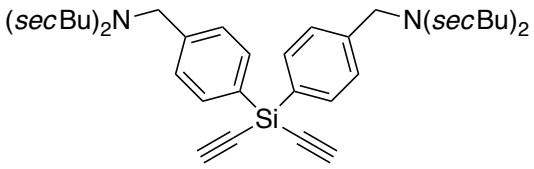

A mixture of 4-bromobenzyl bromide (13.1 g, 52.4 mmol), K_2CO_3 (14.5 g, 105 mmol), KI (434 mg, 2.61 mmol), and di-*sec*-butylamine (9.10 mL, 52.8 mmol) in MeCN (48 mL) was stirred for 23 h at room temperature. The mixture was filtered through a pad of Celite and the solvent was removed under vacuum. The residue was chromatographed on silica

gel with hexane to afford 1-bromo-4-(di-*sec*-butylaminomethyl)benzene as a colorless oil (13.1 g, 43.9 mmol; 84% yield).

^{1}H NMR ($CDCl_3$): δ 7.39 (d, $^3J_{HH}$ = 8.2 Hz, 2H), 7.23 (d, $^3J_{HH}$ = 8.2 Hz, 2H), 3.66 (d, $^2J_{HH}$ = 14.7 Hz, 0.5H), 3.60 (s, 1H), 3.48 (d, $^2J_{HH}$ = 14.7 Hz, 0.5H), 2.65-2.52 (m, 2H), 1.64-1.40 (m, 2H), 1.34-1.12 (m, 2H), 1.00 (d, $^3J_{HH}$ = 6.4 Hz, 3H), 0.99 (d, $^3J_{HH}$ = 6.4 Hz, 3H), 0.85 (t, $^3J_{HH}$ = 7.6 Hz, 3H), 0.84 (t, $^3J_{HH}$ = 7.3 Hz, 3H). ^{13}C NMR ($CDCl_3$): δ 142.1, 141.8, 131.1, 130.3, 130.1, 120.0, 54.3, 53.8, 49.0, 48.7, 29.2, 27.8, 18.1, 16.9, 12.2, 12.1.

A solution of 1-bromo-4-(di-*sec*-butylaminomethyl)benzene (3.58 g, 12.0 mmol) in THF (12 mL) was added dropwise over 1 h to a suspension of Mg turnings (292 mg, 12.0 mmol) in THF (12 mL) at 60 ºC, and the mixture was stirred for 3.5 h at 60 ºC. The resulting solution was added slowly over 10 min to tetrachlorosilane (460 μL, 4.01 mmol) at –78 ºC, and the mixture was stirred for 2.5 h at –78 ºC. This was warmed to room temperature and ethynylmagnesium bromide (24.0 mL, 12.0 mmol; 0.5 M solution in THF) was added to it, and the mixture was stirred for 4 h at room temperature. The reaction was quenched with saturated NH_4Claq and this was extracted with Et_2O. The organic layer was washed with saturated NaClaq, dried over Na_2SO_4, filtered, and concentrated under vacuum. The residue was purified by GPC with $CHCl_3$ to afford compound **1g** as a yellow oil (1.21 g, 2.35 mmol; 59% yield).

^{1}H NMR ($CDCl_3$): δ 7.681 (d, $^3J_{HH}$ = 7.8 Hz, 2H), 7.675 (d, $^3J_{HH}$ = 7.8 Hz, 2H), 7.41 (d, $^3J_{HH}$ = 7.8 Hz, 4H), 3.75 (d, $^2J_{HH}$ = 15.1 Hz, 1H), 3.68 (s, 2H), 3.57 (d, $^2J_{HH}$ = 15.1 Hz, 1H), 2.72 (s, 2H), 2.69-2.57 (m, 4H), 1.63-1.43 (m, 4H), 1.33-1.33 (m, 4H), 1.01 (d, $^3J_{HH}$ = 6.9 Hz, 6H), 0.99 (d, $^3J_{HH}$ = 6.4 Hz, 6H), 0.86 (t, $^3J_{HH}$ = 7.3 Hz, 12H). ^{13}C NMR ($CDCl_3$): δ 146.0, 145.7, 134.68, 134.66, 129.0, 128.9, 128.4, 128.2, 97.0, 84.2, 54.2, 53.8, 49.5, 49.2, 29.2, 27.8, 18.2, 16.9, 12.2, 12.1. HRMS (FAB) calcd for $C_{34}H_{50}N_2Si$ (M^+) 514.3738, found 514.3727.

Diethyldiethynylsilane (1i) (CAS 18292-19-8)

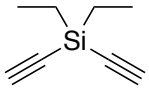

Ethynylmagnesium bromide (42.0 mL, 21.0 mmol; 0.5 M solution in THF) was added to dichlorodiethylsilane (1.57 g, 9.99 mmol) in THF (10 mL) and the mixture was stirred for 4 h at room temperature. The reaction was quenched with saturated NH_4Claq and this was extracted with Et_2O. The organic layer was washed with saturated NaClaq, dried over $MgSO_4$, filtered, and the solvent was distilled off. The residue was chromatographed on silica gel with pentane to afford compound **1i** as a colorless oil (2.29 g, 8.23 mmol; 82% yield, 49 wt% in THF).

^{1}H NMR ($CDCl_3$): δ 2.46 (s, 2H), 1.08 (t, $^3J_{HH}$ = 8.0 Hz, 6H), 0.76 (q, $^3J_{HH}$ = 8.1 Hz, 4H). ^{13}C NMR ($CDCl_3$): δ 95.2, 84.5, 7.0, 6.0.

1-Phenyl-1,5-hexadiyne (3) (CAS 37124-88-2)

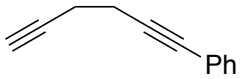

Triethylamine (2.78 mL, 20.0 mmol), 1,5-hexadiyne (1.25 g, 16.0 mmol), and THF (8.0 mL) were successively added to a mixture of $Pd(PPh_3)_4$ (231 mg, 0.200 mmol), CuI (76.2 mg, 0.400 mmol), and iodobenzene (1.63 g, 8.00 mmol) in THF (4.0 mL) at room temperature, and the resulting mixture was stirred for 46 h at room temperature. The precipitates were filtered off through a pad of silica gel with Et_2O and the solvents were removed under vacuum. The residue was chromatographed on silica gel with hexane and further purified by GPC with $CHCl_3$ to afford compound **3** as a pale yellow (450 mg, 2.68 mmol; 33% yield).

^{1}H NMR ($CDCl_3$): δ 7.44-7.37 (m, 2H), 7.32-7.26 (m, 3H), 2.69-2.60 (m, 2H), 2.54-2.46 (m, 2H), 2.05 (t, $^{4}J_{HH}$ = 2.8 Hz, 1H). ^{13}C NMR ($CDCl_3$): δ 131.7, 128.3, 128.0, 123.7, 88.1, 82.8, 81.7, 69.5, 19.7, 19.0.

Dihexyl(dihexyl(phenylethynyl)silylethynyl)silylacetylene (4a)

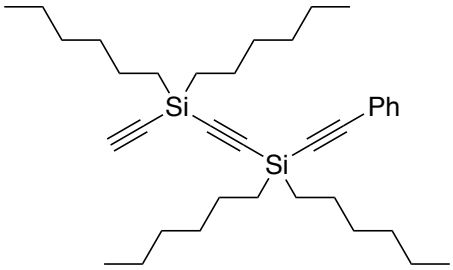

A solution of lithium diisopropylamide [generated from diisopropylamine (1.11 mL, 7.87 mmol) and *n*BuLi (5.00 mL, 7.75 mmol; 1.55 M solution in hexane) in THF (8 mL) at –78 °C] was added to a solution of dihexylethynylsilane (1.79 g, 7.97 mmol) in THF (2 mL) at –78 ºC, and the resulting mixture was stirred for 1.5 h at –78 ºC to afford a solution of dihexylsilylethynyllithium. Separately, dihexyl(phenyethynyl)silane (2.36 g, 7.85 mmol) was added to a suspension of $PdCl_2$ (13.3 mg, 75.0 μmol) in CCl_4 (15 mL) at room temperature, and the mixture was stirred for 2 h at room temperature. The precipitates were filtered off through Celite with CCl_4 (5 mL) and the volatiles were removed under vacuum. The residue was dissolved in THF (2 mL) and the volatiles were removed under vacuum. This was repeated again and the residue was dissolved THF (10 mL) and cooled to –78 ºC. The solution of dihexylsilylethynyllithium generated above was added to it at –78 ºC, and the resulting mixture was warmed to room temperature and stirred for 1 h. The reaction was quenched with saturated NH_4Claq and this was extracted with Et_2O. The organic layer was washed with saturated NaClaq, dried over $MgSO_4$, filtered, and concentrated under vacuum. The residue was chromatographed on silica gel

with hexane to afford dihexyl(dihexyl(phenylethynyl)silylethynyl)silane as a yellow oil (2.81 g, 5.37 mmol; 68% yield).

^{1}H NMR ($CDCl_3$): δ 7.55-7.43 (m, 2H), 7.37-7.27 (m, 3H), 3.98 (quint, $^{3}J_{HH}$ = 3.4 Hz, 1H), 1.58-1.22 (m, 32H), 0.95-0.84 (m, 12H), 0.83-0.76 (m, 4H), 0.75-0.67 (m, 4H). ^{13}C NMR ($CDCl_3$): δ 132.3, 128.9, 128.3, 123.1, 111.8, 111.7, 106.7, 89.5, 32.8, 32.7, 31.7, 24.5, 23.8, 22.74, 22.73, 14.9, 14.3, 12.1.

Dihexyl(dihexyl(phenylethynyl)silylethynyl)silane (2.64 g, 5.05 mmol) was added to a suspension of $PdCl_2$ (8.8 mg, 50 μmol) in CCl_4 (10 mL) at room temperature, and the mixture was stirred for 10 h at 60 ºC. Additional $PdCl_2$ (8.8 mg, 50 μmol) was added to it and the mixture was further stirred for 12 h at 60 ºC. The precipitates were filtered off through Celite with CCl_4 (3 mL) and the volatiles were removed under vacuum. The residue was dissolved in THF (2 mL) and the volatiles were removed under vacuum. This was repeated again to afford chlorodihexyl(dihexyl(phenylethynyl)silylethynyl)-silane as a yellow oil. Ethynylmagnesium bromide (10.5 mL, 5.25 mmol; 0.5 M solution in THF) was added to it at room temperature and the mixture was stirred for 5 h at room temperature. The reaction was quenched with saturated NH_4Claq and this was extracted with Et_2O. The organic layer was washed with saturated NaClaq, dried over $MgSO_4$, filtered, and concentrated under vacuum. The residue was chromatographed on silica gel with hexane and further purified by GPC with $CHCl_3$ to afford compound **4a** as a yellow oil (1.56 g, 2.85 mmol; 56% yield).

^{1}H NMR ($CDCl_3$): δ 7.54-7.45 (m, 2H), 7.37-7.27 (m, 3H), 2.44 (s, 1H), 1.61-1.22 (m, 32H), 0.98-0.85 (m, 12H), 0.85-0.71 (m, 8H). ^{13}C NMR ($CDCl_3$): δ 132.3, 128.9, 128.3, 123.1, 111.6, 110.3, 106.8, 94.8, 89.3, 85.5, 32.8, 31.69, 31.65, 23.8, 23.6, 22.74, 22.72, 14.8, 14.5, 14.3, 14.2. HRMS (EI) calcd for $C_{36}H_{58}Si_2$ (M^+) 546.4072, found 546.4067.

Dihexyl(dihexyl(dihexyl(phenylethynyl)silylethynyl)silylethynyl)silylacetylene (5a)

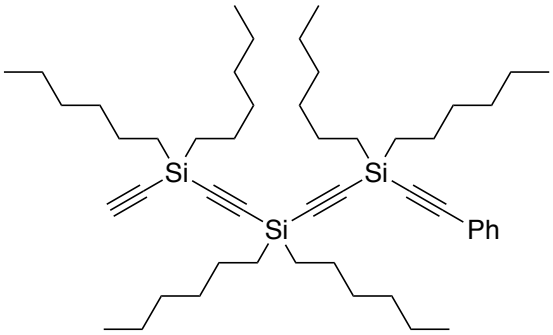

A solution of lithium diisopropylamide [generated from diisopropylamine (740 μL, 5.24 mmol) and *n*BuLi (3.30 mL, 5.25 mmol; 1.59 M solution in hexane) in THF (5 mL) at –78 °C] was added to a solution of dihexylethynylsilane (1.19 g, 5.30 mmol) in THF (5 mL) at –78 ºC, and the resulting solution was stirred for 20 min at –78 ºC to afford a solution of dihexylsilylethynyllithium. Separately, dihexylethynylsilane (1.19 g, 5.30 mmol) was added to a suspension of trichloroisocyanuric acid (425 mg, 1.83 mmol) in CH_2Cl_2 (20 mL) at room temperature, and the mixture was stirred for 2 h at room temperature. The precipitates were filtered off through Celite with THF (5 mL) and the volatiles were removed under vacuum. The residue was dissolved in THF (2 mL) and the volatiles were removed under vacuum. This was repeated again and the residue was dissolved in THF (5 mL) and cooled to –78 ºC. The solution of dihexylsilylethynyllithium generated above was added to it at –78 ºC, and the resulting mixture was warmed to room temperature and stirred for 13 h. The reaction was quenched with saturated NH_4Claq and this was extracted with Et_2O. The organic layer was washed with saturated NaClaq, dried over $MgSO_4$, filtered, and concentrated under vacuum. The residue was chromatographed on silica gel with hexane to afford dihexyl(dihexyl(ethynyl)silylethynyl)silane as a colorless oil (1.64 g, 3.67 mmol; 69% yield).

^{1}H NMR ($CDCl_3$): δ 3.97 (quint, $^{3}J_{HH}$ = 3.4 Hz, 1H), 2.43 (s, 1H), 1.55-1.20 (m, 32H), 0.89 (t, $^{3}J_{HH}$ = 6.6 Hz, 12H), 0.79-0.62 (m, 8H). ^{13}C NMR ($CDCl_3$): δ 112.2, 110.8, 94.7, 85.5, 32.8, 32.7, 31.70, 31.65, 24.4, 23.6, 22.7, 14.5, 14.2, 12.0.

A solution of lithium diisopropylamide [generated from diisopropylamine (220 μL, 1.56 mmol) and *n*BuLi (980 μL, 1.56 mmol; 1.59 M solution in hexane) in THF (1.5 mL) at –78 °C] was added to a solution of dihexyl(phenylethynyl)silylacetylene (488 mg, 1.50 mmol) in THF (1.5 mL) at –78 ºC, and the resulting solution was stirred for 20 min at –78 ºC to afford a solution of dihexyl(phenylethynyl)silylethynyllithium. Separately, dihexyl(dihexyl(ethynyl)silylethynyl)silane (670 mg, 1.50 mmol) was added to a suspension of trichloroisocyanuric acid (137 mg, 0.589 mmol) in CH_2Cl_2 (6 mL) at room temperature, and the mixture was stirred for 13 h at room temperature. The precipitates were filtered off through Celite with THF (3 mL) and the volatiles were removed under vacuum. The residue was dissolved in THF (1 mL) and the volatiles were removed under vacuum. This was repeated again and the residue was dissolved in THF (3 mL) and cooled to –78 ºC. The solution of dihexyl(phenylethynyl)silylethynyllithium generated above was added to it at –78 ºC, and the resulting mixture was stirred for 15 h at room temperature. The reaction was quenched with saturated NH_4Claq and this was extracted with Et_2O. The organic layer was washed with saturated NaClaq, dried over $MgSO_4$, filtered, and concentrated under vacuum. The residue was chromatographed on silica gel with hexane and further purified by GPC with $CHCl_3$ to afford to compound **5a** as a yellow oil (657 mg, 0.854 mmol; 57% yield).

^{1}H NMR ($CDCl_3$): δ 7.51-7.45 (m, 2H), 7.36-7.26 (m, 3H), 2.42 (s, 1H), 1.57-1.21 (m, 48H), 0.95-0.83 (m, 18H), 0.83-0.70 (m, 12H). ^{13}C NMR ($CDCl_3$): δ 132.3, 128.9, 128.3, 123.1, 111.30, 111.28, 110.6, 110.3, 106.7, 94.8, 89.4, 85.5, 32.83, 32.79, 31.7,

31.6, 23.8, 23.7, 23.6, 22.8, 22.7, 14.8, 14.6, 14.4, 14.3. HRMS (EI) calcd for $C_{50}H_{84}Si_3$ (M^+) 768.5875, found 768.5880.

Analytical Data for Other Monomers:

Diethyl(4-(2-methoxy)ethoxyphenylethynyl)silylacetylene (1b)

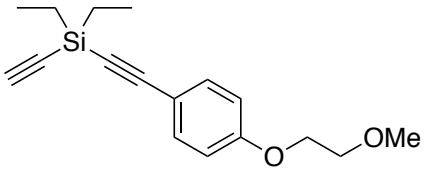

^{1}H NMR ($CDCl_3$): δ 7.42 (d, $^3J_{HH}$ = 8.7 Hz, 2H), 6.85 (d, $^3J_{HH}$ = 8.7 Hz, 2H), 4.12 (t, $^3J_{HH}$ = 4.8 Hz, 2H), 3.75 (t, $^3J_{HH}$ = 4.8 Hz, 2H), 3.45 (s, 3H), 2.47 (s, 1H), 1.12 (t, $^3J_{HH}$ = 7.8 Hz, 6H), 0.80 (q, $^3J_{HH}$ = 7.8 Hz, 4H).^{13}C NMR ($CDCl_3$): δ 159.4, 133.9, 115.1, 114.6, 107.2, 94.7, 86.7, 85.4, 71.0, 67.5, 59.4, 7.3, 6.5. HRMS (FAB) calcd for $C_{17}H_{22}O_2Si$ (M^+) 286.1384, found 286.1384.

Dihexyl(1-pentynyl)silylacetylene (1c)

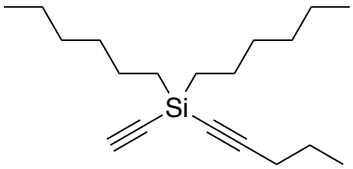

^{1}H NMR ($CDCl_3$): δ2.42 (s, 1H), 2.23 (t, $^3J_{HH}$ = 7.1 Hz, 2H), 1.55 (sext, $^3J_{HH}$ = 7.1 Hz, 2H), 1.51-1.22 (m, 16H), 0.99 (t, $^3J_{HH}$ = 7.3 Hz, 3H), 0.89 (t, $^3J_{HH}$ = 6.9 Hz, 6H), 0.78-0.64 (m, 4H). ^{13}C NMR ($CDCl_3$): δ 109.9, 94.2, 86.4, 79.4, 32.8, 31.6, 23.7, 22.7, 22.1, 22.0, 14.8, 14.2, 13.5. HRMS (EI) calcd for $C_{19}H_{34}Si$ (M^+) 290.2424, found 290.2427.

Di(2-ethylhexyl)diethynylsilane (1e)

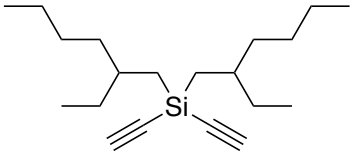

^{1}H NMR ($CDCl_3$): δ 2.48 (s, 2H), 1.65 (sept, $^{3}J_{HH}$ = 6.2 Hz, 2H), 1.47-1.20 (m, 16H), 0.90 (t, $^{3}J_{HH}$ = 6.4 Hz, 6H), 0.86 (t, $^{3}J_{HH}$ = 7.3 Hz, 6H), 0.77 (d, $^{3}J_{HH}$ = 6.9 Hz, 4H). ^{13}C NMR ($CDCl_3$): δ 95.2, 86.2, 35.5, 35.4, 28.8, 28.6, 23.1, 19.8, 14.3, 10.8. HRMS (EI) calcd for $C_{20}H_{36}Si$ (M^+) 304.2581, found 304.2582.

Dihexyl(trimethylsilylethynyl)silylacetylene (1f)

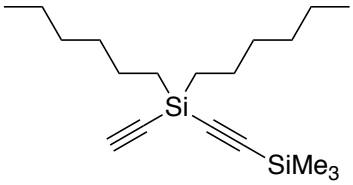

^{1}H NMR ($CDCl_3$): δ 2.43 (s, 1H), 1.51-1.22 (m, 16H), 0.89 (t, $^{3}J_{HH}$ = 6.9 Hz, 6H), 0.77-0.68 (m, 4H), 0.18 (s, 9H). ^{13}C NMR ($CDCl_3$): δ 116.7, 108.1, 94.7, 85.8, 32.7, 31.6, 23.6, 22.7, 14.5, 14.2, –0.10. HRMS (EI) calcd for $C_{19}H_{36}Si_2$ (M^+) 320.2350, found 320.2359.

Diethynyldi(3,3,4,4,5,5,6,6,6-nonafluorohexyl)silane (1h)

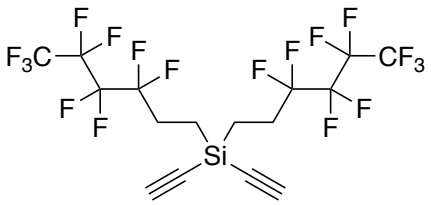

^{1}H NMR ($CDCl_3$): δ 2.62 (s, 2H), 2.36-2.16 (m, 4H), 1.14-0.99 (m, 4H). ^{13}C NMR ($CDCl_3$): δ 98.1, 81.4, 25.5 (t, $^{2}J_{CF}$ = 23.5 Hz), 4.3. Carbons having fluorine atoms were

not observed under our measurement conditions. Anal. Calcd for $C_{16}H_{10}F_{18}Si$: C, 33.58; H,1.76. Found: C, 33.53, H, 1.61.

3-(Dihexylethynylsilyl)-*N*,*N*-dipropylpropiolamide (1j)

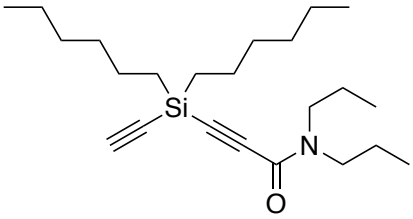

^{1}H NMR ($CDCl_3$): δ 3.50 (t, $^3J_{HH}$ = 7.3 Hz, 2H), 3.37-3.26 (m, 2H), 2.46 (s, 1H), 1.71-1.53 (m, 4H), 1.53-1.21 (m, 16H), 1.00-0.84 (m, 12H), 0.83-0.73 (m, 4H). ^{13}C NMR ($CDCl_3$): δ 153.5, 98.0, 95.6, 90.8, 84.2, 50.9, 46.5, 32.7, 31.5, 23.5, 22.6, 22.2, 20.7, 14.1, 14.0, 11.4, 11.2. HRMS (EI) calcd for $C_{23}H_{41}NOSi$ (M^+) 375.2952, found 375.2954.

Dihexyl(2-phenylethyl)silylacetylene (2a)

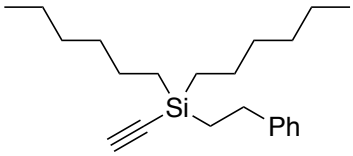

^{1}H NMR ($CDCl_3$): δ 7.28 (t, $^3J_{HH}$ = 7.8 Hz, 2H), 7.21 (d, $^3J_{HH}$ = 7.3 Hz, 2H), 7.17 (t, $^3J_{HH}$ = 7.1 Hz, 1H), 2.76-2.68 (m, 2H), 2.41 (s, 1H), 1.43-1.21 (m, 16H), 1.04-0.96 (m, 2H), 0.89 (t, $^3J_{HH}$ = 7.1 Hz, 6H), 0.68-0.60 (m, 4H). ^{13}C NMR ($CDCl_3$): δ 145.0, 128.5, 128.0, 125.8, 94.7, 87.9, 33.2, 31.6, 30.1, 23.9, 22.7, 15.4, 14.3, 13.2. HRMS (EI) calcd for $C_{22}H_{36}Si$ (M^+) 328.2581, found 328.2583.

Dihexylvinylsilylacetylene (2b)

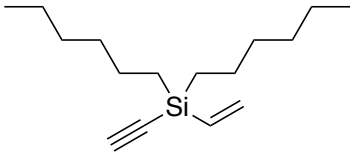

^{1}H NMR ($CDCl_3$): δ 6.13-6.01 (m, 2H), 5.97-5.86 (m, 1H), 2.43 (s, 1H), 1.46-1.20 (m, 16H), 0.88 (t, $^{3}J_{HH}$ = 6.9 Hz, 6H), 0.75-0.64 (m, 4H). ^{13}C NMR ($CDCl_3$): δ 134.4, 134.2, 95.0, 86.9, 33.1, 31.7, 23.7, 22.7, 14.2, 13.5. HRMS (EI) calcd for $C_{16}H_{30}Si$ (M^+) 250.2111, found 250.2114.

Dihexylphenylsilylacetylene (2c)

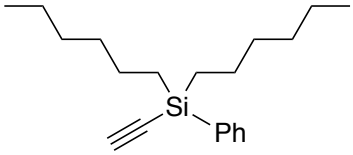

^{1}H NMR ($CDCl_3$): δ 7.65-7.59 (m, 2H), 7.42-7.33 (m, 3H), 2.53 (s, 1H), 1.48-1.19 (m, 16H), 0.93-0.81 (m, 10H). ^{13}C NMR ($CDCl_3$): δ 135.0, 134.4, 129.6, 128.0, 95.7, 87.0, 33.1, 31.6, 23.8, 22.7, 14.2, 14.0. HRMS (EI) calcd for $C_{20}H_{32}Si$ (M^+) 300.2268, found 300.2269.

Dibutyl(dibutyl(4-(2-methoxy)ethoxyphenylethynyl)silylethynyl)silylacetylene (4b)

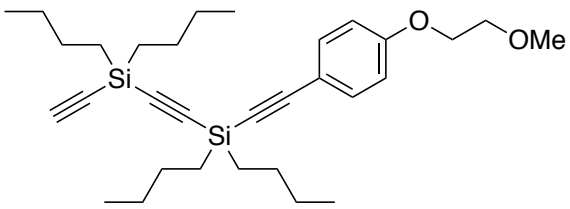

^{1}H NMR ($CDCl_3$): δ 7.41 (d, $^{3}J_{HH}$ = 8.7 Hz, 2H), 6.85 (d, $^{3}J_{HH}$ = 8.7 Hz, 2H), 4.12 (t, $^{3}J_{HH}$ = 4.6 Hz, 2H), 3.75 (t, $^{3}J_{HH}$ = 4.6 Hz, 2H), 3.45 (s, 3H), 2.44 (s, 1H), 1.55-1.35 (m, 16H), 0.97-0.87 (m, 12H), 0.83-0.72 (m, 8H). ^{13}C NMR ($CDCl_3$): δ 159.3, 133.8, 115.4,

114.6, 111.9, 110.0, 106.9, 94.8, 87.6, 85.5, 71.0, 67.5, 59.4, 26.12, 26.08, 26.0, 25.9, 14.6, 14.2, 13.9, 13.8. HRMS (EI) calcd for $C_{31}H_{48}O_2Si_2$ (M^+) 508.3193, found 508.3194.

Dihexyl(diphenyl(dihexyl(phenylethynyl)silylethynyl)silylethynyl)silylacetylene (5b)

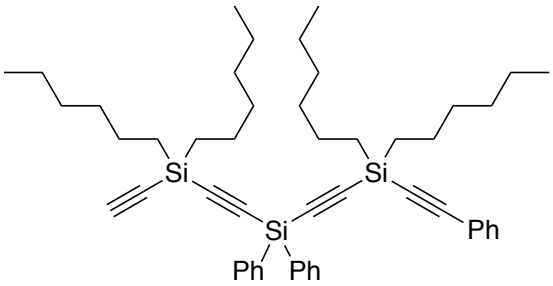

^{1}H NMR ($CDCl_3$): δ 7.76 (d, $^3J_{HH}$ = 6.4 Hz, 2H), 7.52-7.46 (m, 2H), 7.45-7.28 (m, 9H), 2.45 (s, 1H), 1.62-1.18 (m, 32H), 0.98-0.75 (m, 20H). ^{13}C NMR ($CDCl_3$): δ 135.0, 132.5, 132.3, 130.4, 129.0, 128.4, 128.1, 123.0, 114.4, 113.3, 108.7, 108.1, 107.1, 95.2, 89.0, 85.1, 32.8, 32.7, 31.7, 31.6, 23.8, 23.6, 22.72, 22.68, 14.7, 14.4, 14.29, 14.26. HRMS (EI) calcd for $C_{50}H_{68}Si_3$ (M^+) 752.4623, found 752.4627.

General Procedure for Table 2, Table 3 (Entries 1 and 3), Table 4, Table 5 (Entries 1 and 2), and Equations 1–3.

Triethylamine (10.4 μL, 74.6 μmol) and THF (0.3 mL) were added to a solution of $[RhCl(tfb)]_2$ (2.7 mg, 7.5 μmol Rh) in THF (0.2 mL). This was stirred for 5 min at –10 ºC and monomer **1**, **3**, **4**, or **5** (0.250 mmol) was added with the aid of THF (0.5 mL). The mixture was stirred for 22 h at –10 ºC and warmed to room temperature. This was added dropwise to stirring MeOH (50 mL) with the aid of CH_2Cl_2 (5.0 mL), and the precipitates that formed were collected by filtration and the solid thus obtained was dried under vacuum to afford **poly-1**, **poly-3**, **poly-4**, or **poly-5**.

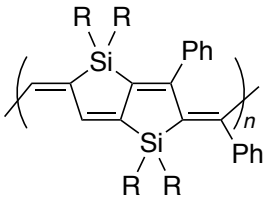

R = *n*Hex

Table 2, Entry 1. Purple solid. 96% yield (77.7 mg). T_d = 390 ºC (5% weight loss). The same polymerization was conducted using 1.00 mmol of monomer **1a** and the reaction progress (by ^{1}H NMR against an internal standard (1,4-dimethoxybenzene)) and the molecular weight of the polymer component (by SEC against a polystyrene standard) were checked to confirm the chain-growth nature of this stitching polymerization: M_n = 25000, M_w/M_n = 1.7 at 16% conversion; M_n = 32000, M_w/M_n = 1.7 at 31% conversion; M_n = 66000, M_w/M_n = 1.8 at 59% conversion.

^{1}H NMR (400 MHz in $CDCl_3$)

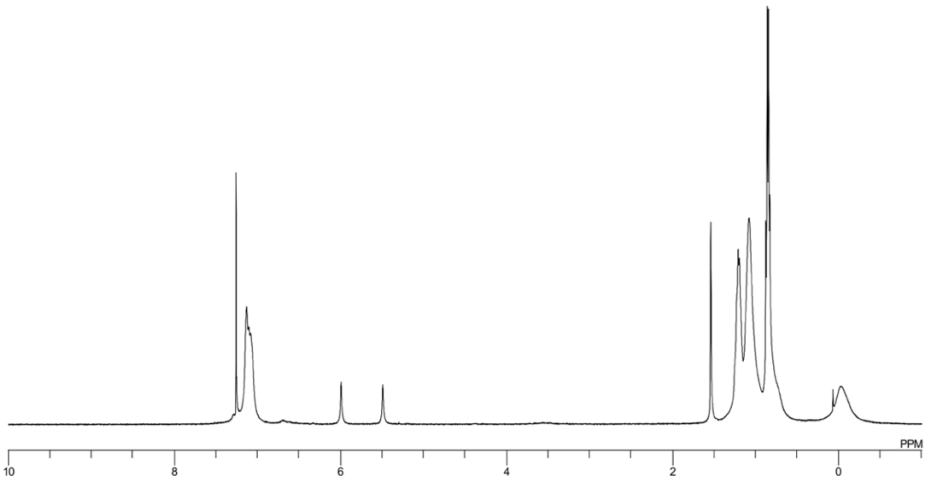

Inverse gated ^{13}C NMR (176 MHz in $CDCl_3$)

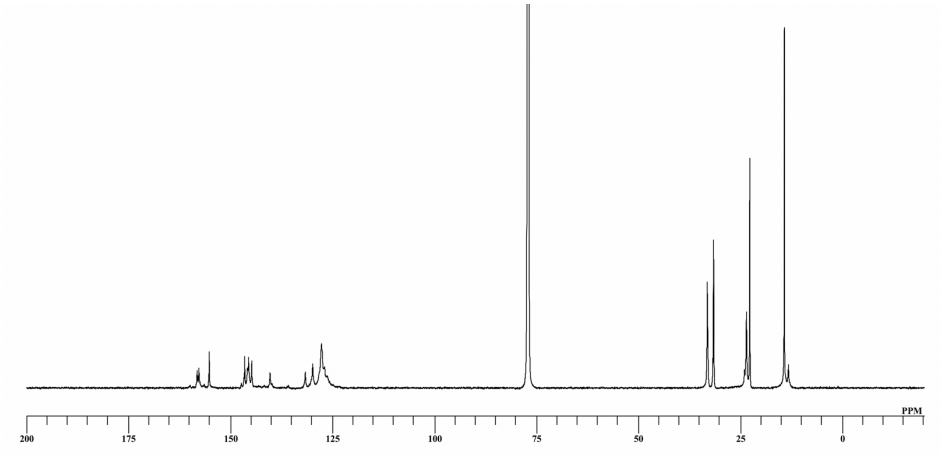

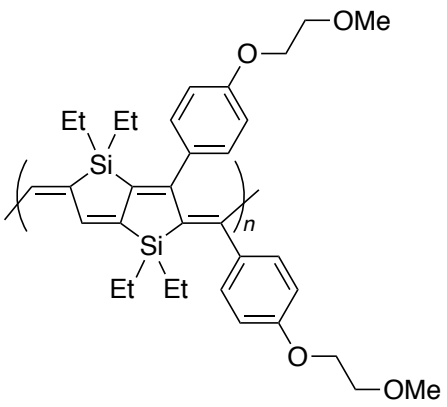

Table 2, Entry 2. Purple solid. 88% yield (505 mg).The polymerization was conducted on a 2.00 mmol scale. T_d = 355 ºC (5% weight loss).

^{1}H NMR (400 MHz in $CDCl_3$)

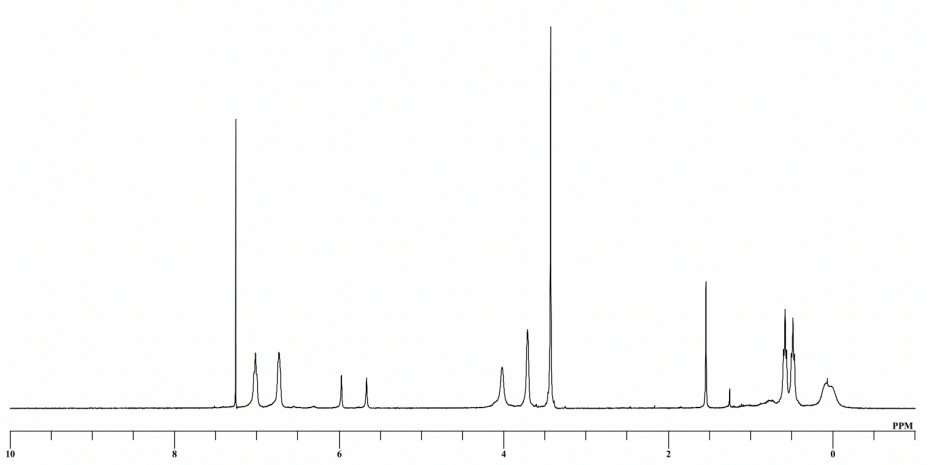

^{13}C NMR (101 MHz in $CDCl_3$)

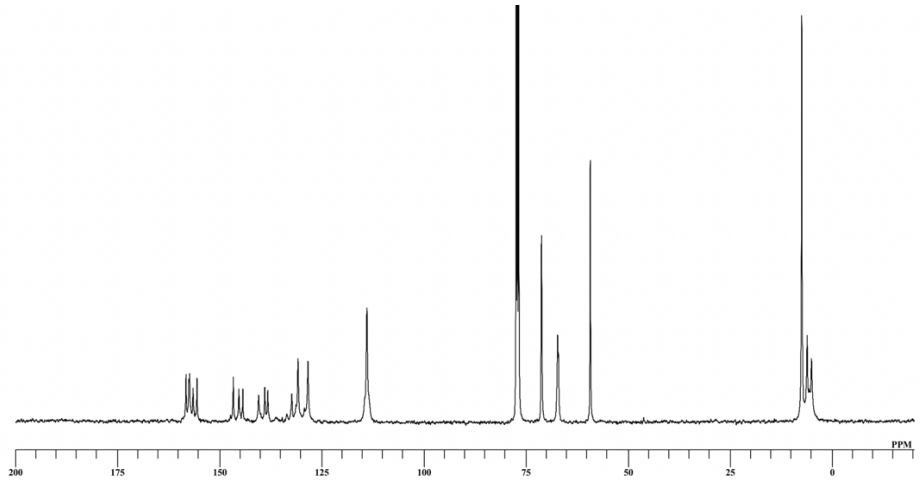

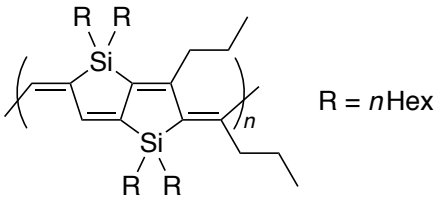

Table 2, Entry 3. Red solid. 92% yield (67.1 mg). 6 mol% Rh of $[RhCl(tfb)]_2$ and 60 mol% of triethylamine were used. T_d = 336 ºC (5% weight loss).

^{1}H NMR (400 MHz in $CDCl_3$)

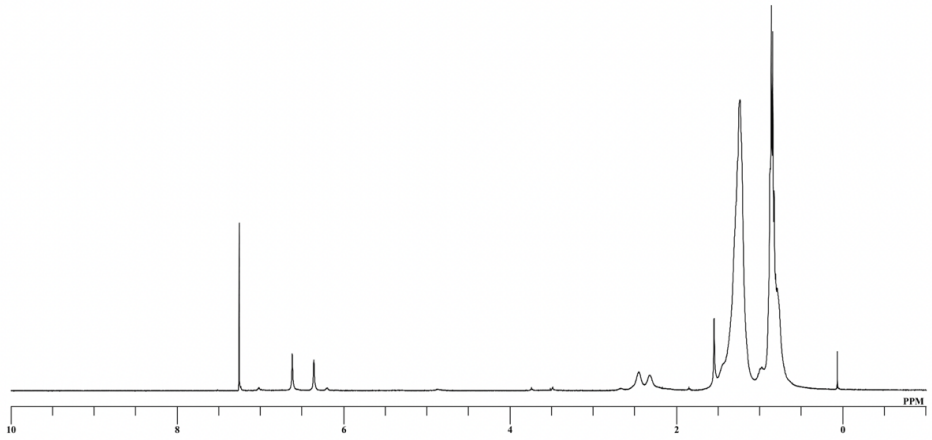

^{13}C NMR (101 MHz in $CDCl_3$)

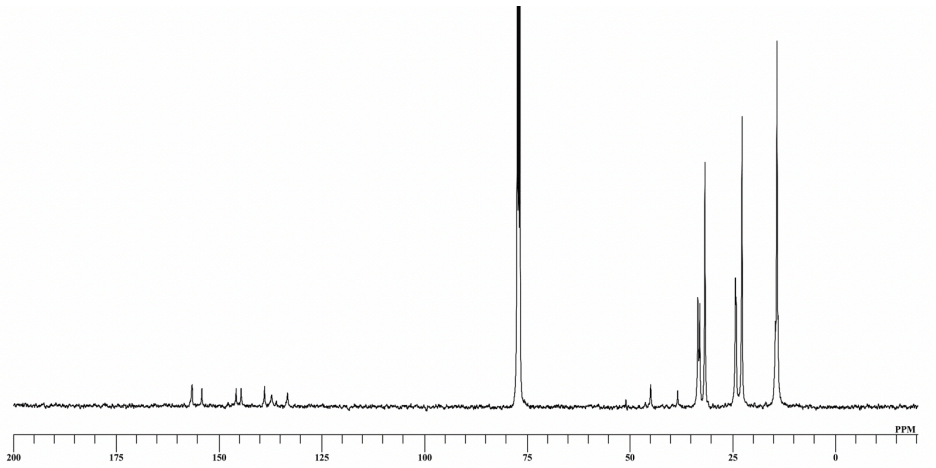

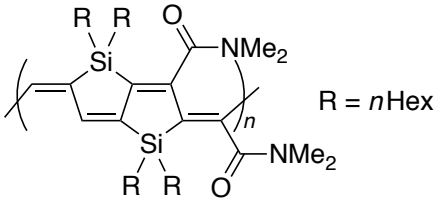

Table 2, Entry 4. Purple solid. 82% yield (65.6 mg). 6 mol% Rh of $[RhCl(tfb)]_2$ and 60 mol% of triethylamine were used. T_d = 322 ºC (5% weight loss).

^{1}H NMR (498 MHz in $CDCl_3$)

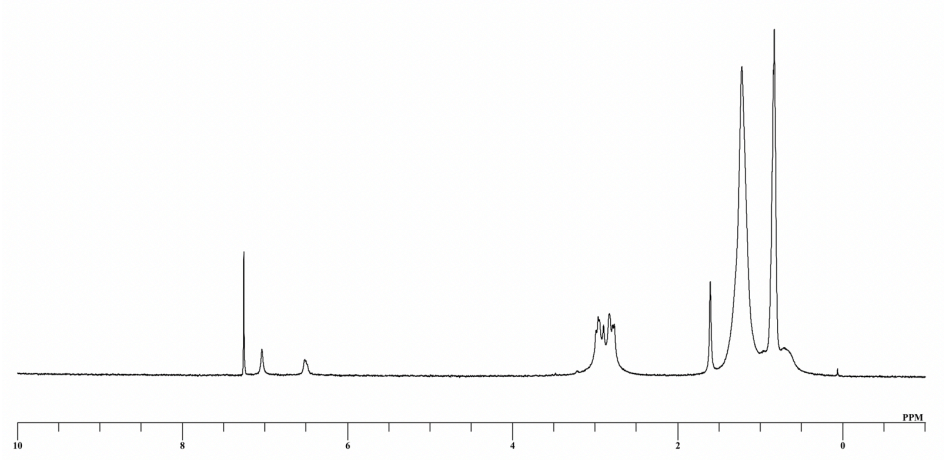

^{13}C NMR (101 MHz in $CDCl_3$)

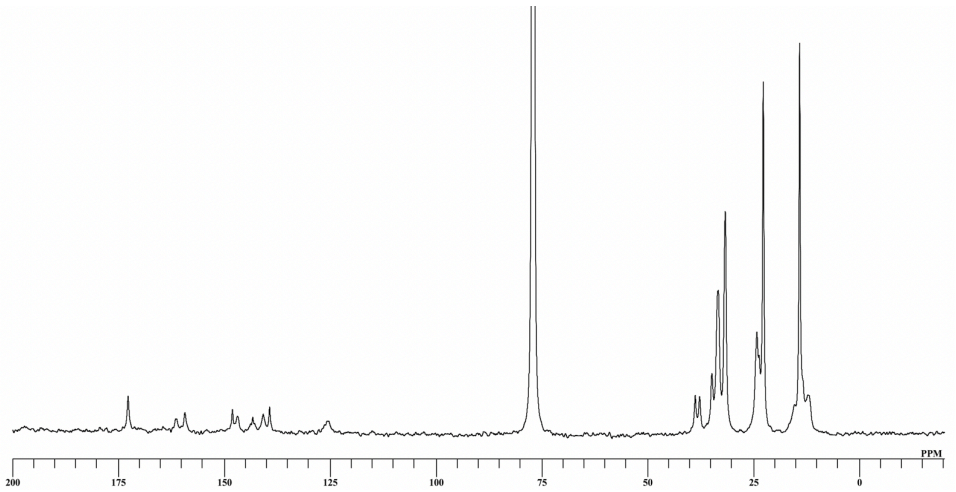

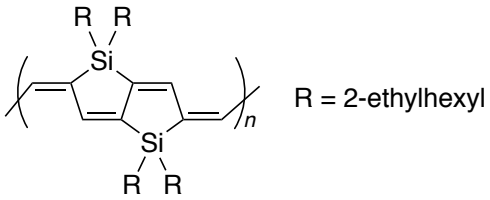

Table 2, Entry 5. Purple solid. 95% yield (72.4 mg). 6 mol% Rh of $[RhCl(tfb)]_2$ and 60 mol% of triethylamine were used at 20 ºC. T_d = 370 ºC (5% weight loss).

^{1}H NMR (400 MHz in $CDCl_3$)

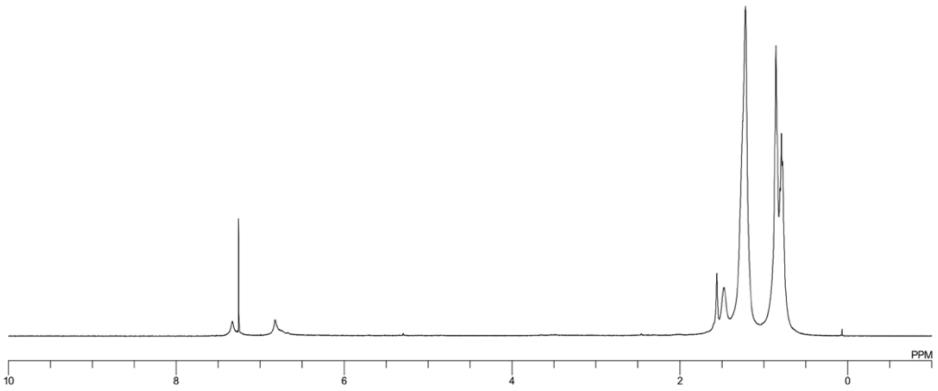

^{13}C NMR (101 MHz in $CDCl_3$)

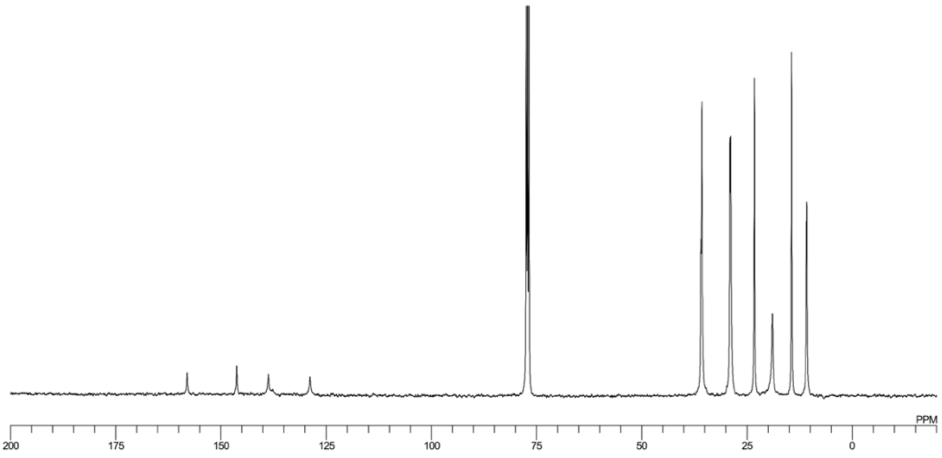

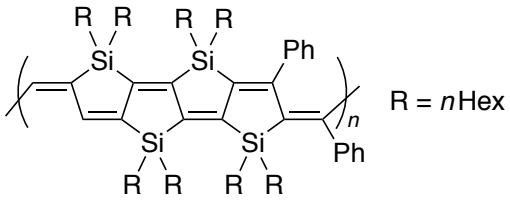

Table 4, Entry 1. Purple solid. 78% yield (105 mg). 6 mol% Rh of $[RhCl(tfb)]_2$ and 60 mol% of triethylamine were used. T_d = 329 ºC (5% weight loss).

^{1}H NMR (400 MHz in $CDCl_3$)

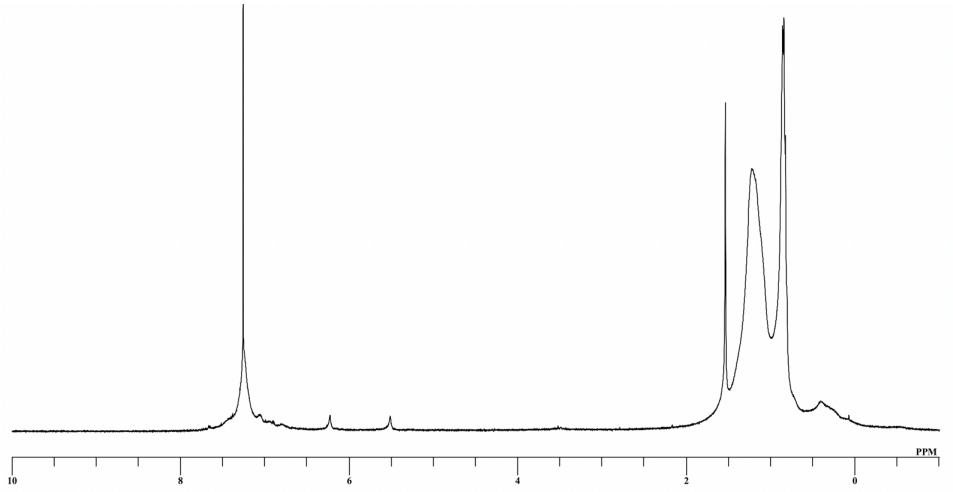

Inverse gated ^{13}C NMR (176 MHz in $CDCl_3$)

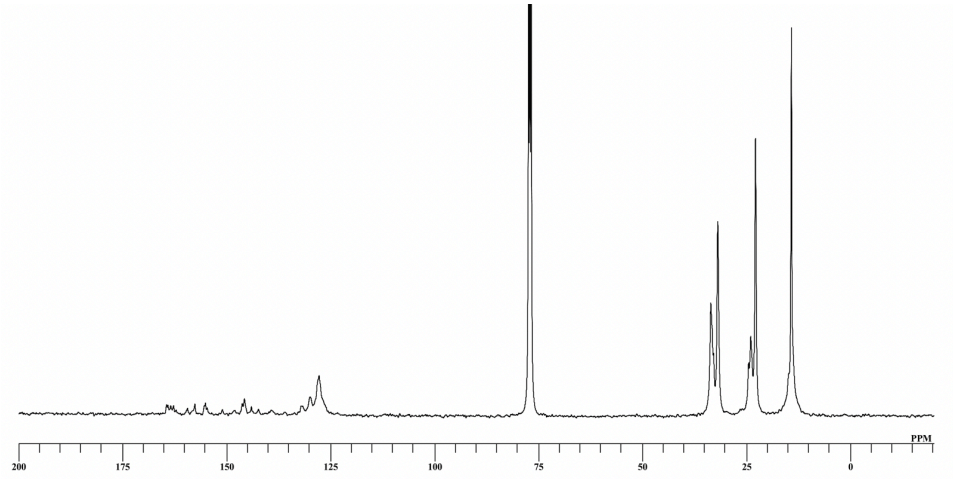

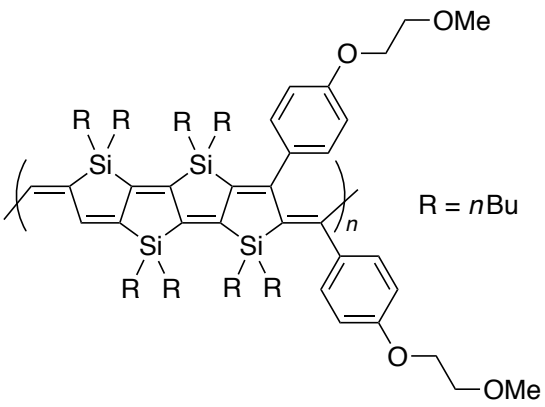

Table 4, Entry 3. Purple solid. 93% yield (485 mg). The polymerization was conducted on a 1.00 mmol scale and 6 mol% Rh of $[RhCl(tfb)]_2$ and 60 mol% of triethylamine were used. T_d = 389 ºC (5% weight loss).

^{1}H NMR (400 MHz in $CDCl_3$)

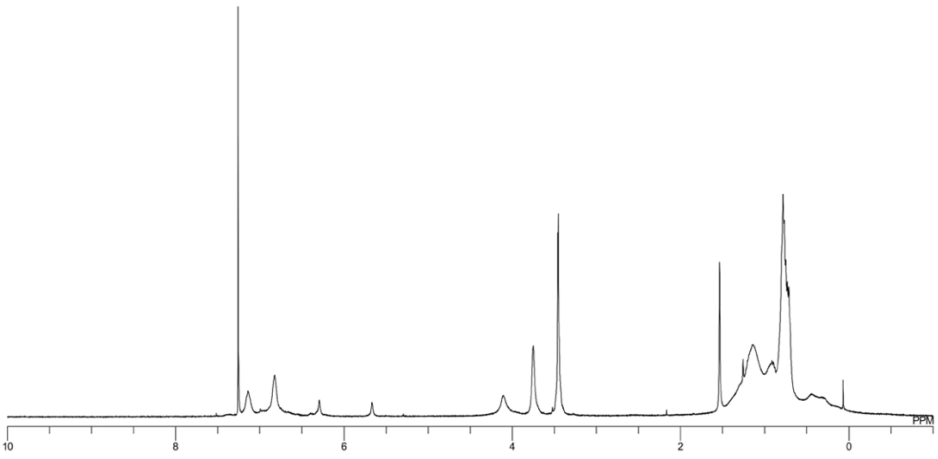

^{13}C NMR (101 MHz in $CDCl_3$)

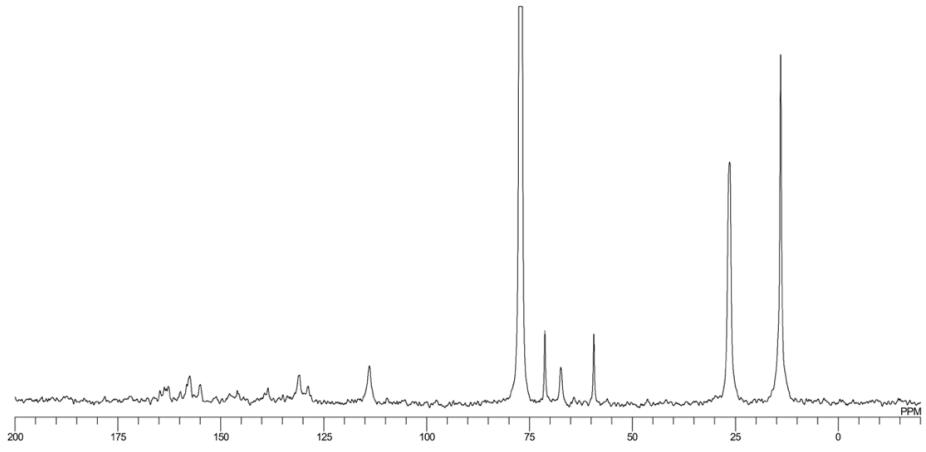

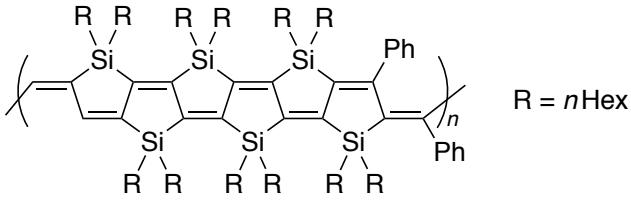

Table 5, Entry 1. Purple solid. 79% yield (76.3 mg). The polymerization was conducted on a 0.125 mmol scale and 20 mol% Rh of $[RhCl(tfb)]_2$ and 200 mol% of triethylamine were used. Incorporation efficiency of internal alkynes (83%) was estimated by the area ratio of sp^2 carbon peaks, sp carbon peaks, and sp^3 carbon peaks of the quantitative ^{13}C NMR spectrum. T_d = 287 ºC (5% weight loss).

^1H NMR (400 MHz in $CDCl_3$)

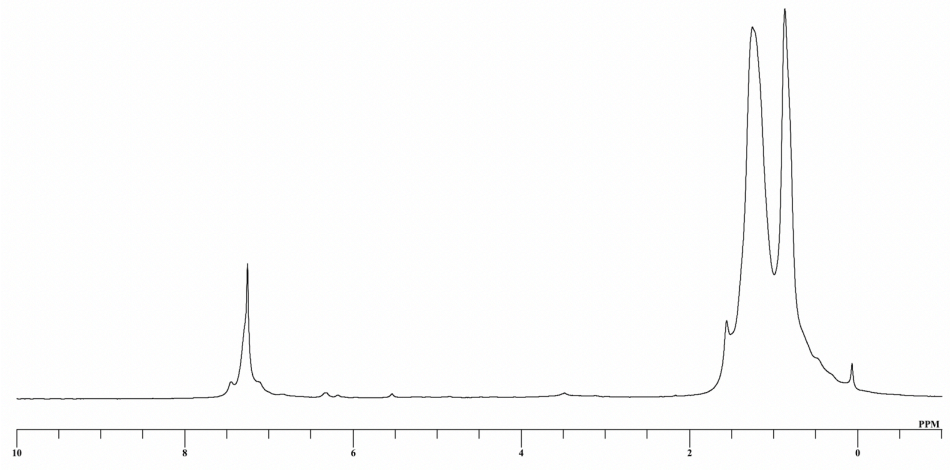

Inverse gated ^{13}C NMR (176 MHz in $CDCl_3$)

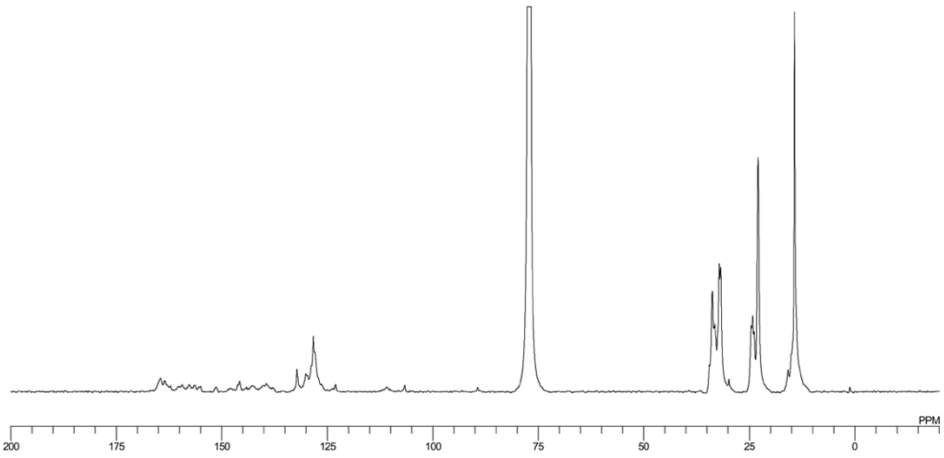

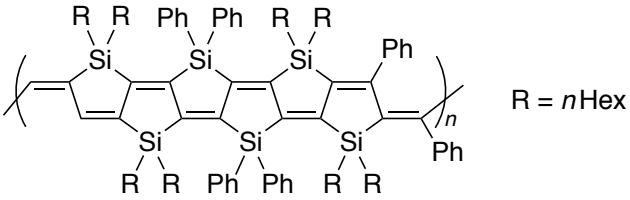

Table 5, Entry 2. Purple solid. 89% yield (84.2 mg). The polymerization was conducted on a 0.125 mmol scale and 20 mol% Rh of $[RhCl(tfb)]_2$ and 200 mol% of triethylamine were used. Incorporation efficiency of internal alkynes (97%) was estimated by the area ratio of sp^2 carbon peaks, sp carbon peaks, and sp^3 carbon peaks of the quantitative ^{13}C NMR spectrum. T_d = 282 ºC (5% weight loss).

^1H NMR (400 MHz in $CDCl_3$)

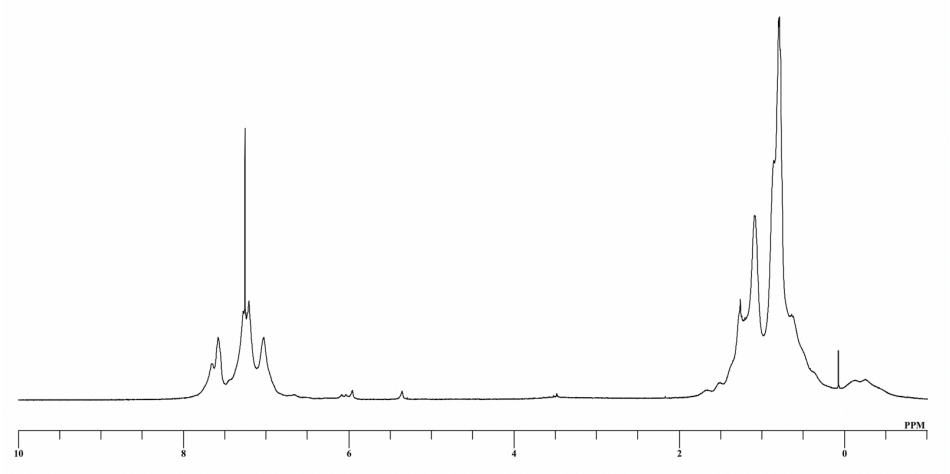

Inverse gated ^{13}C NMR (176 MHz in $CDCl_3$)

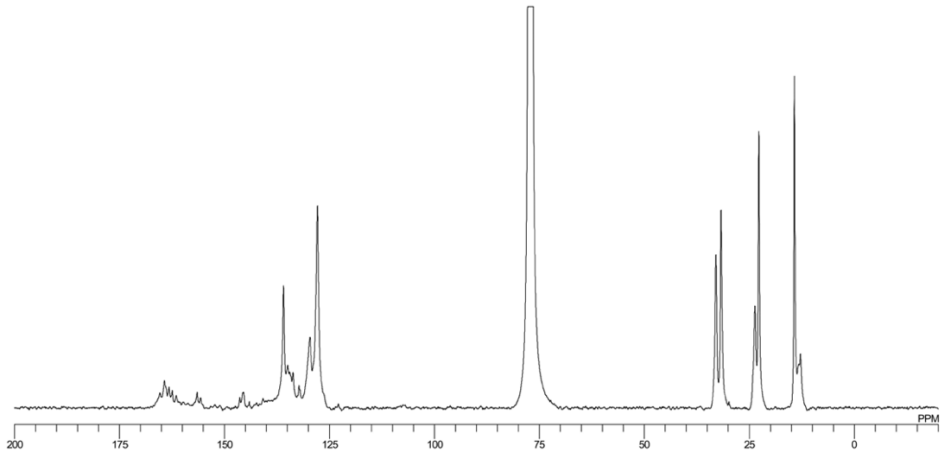

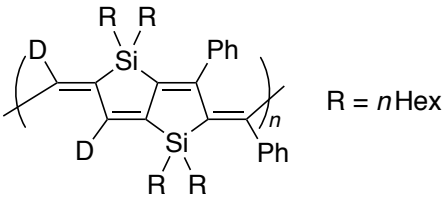

Table 6, Entry 2. Purple solid. 90% yield (73.3 mg).

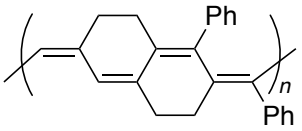

Equation 1. Red solid, 98% yield (75.2 mg). The polymerization was conducted on a 0.500 mmol scale. T_d = 253 ºC (5% weight loss).

^{1}H NMR (400 MHz in $CDCl_3$)

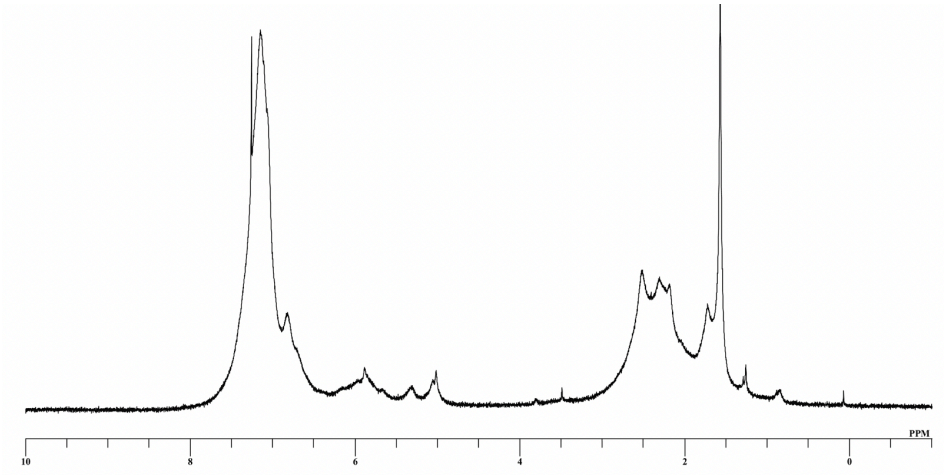

^{13}C NMR (101 MHz in $CDCl_3$)

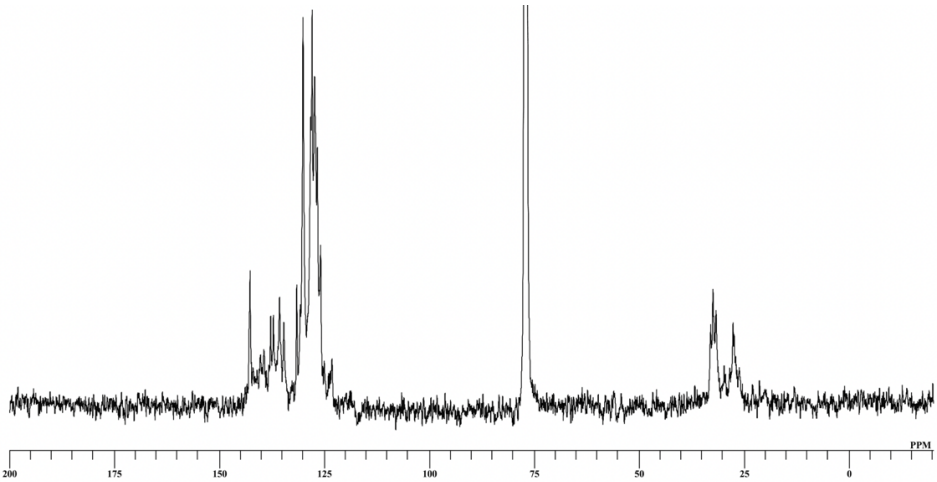

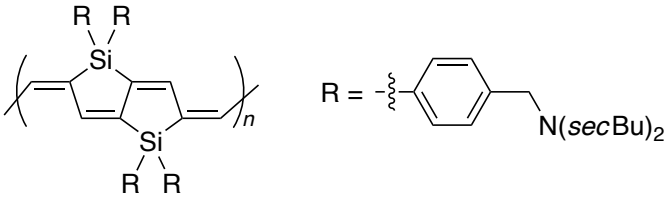

Equation 2. Purple solid. 70% yield (89.6 mg). 6 mol% Rh of $[RhCl(tfb)]_2$ and 60 mol% of triethylamine were used at 20 ºC. T_d = 260 ºC (5% weight loss).

^1H NMR (400 MHz in $CDCl_3$)

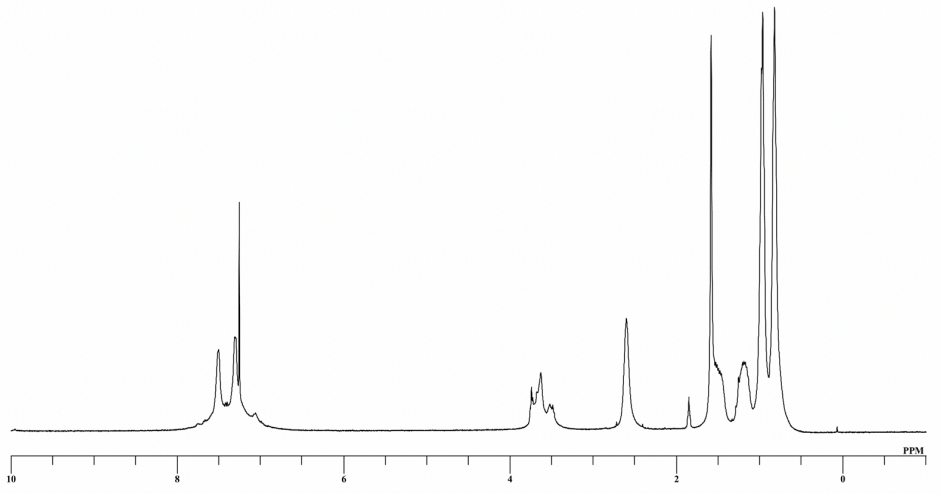

^{13}C NMR (101 MHz in $CDCl_3$)

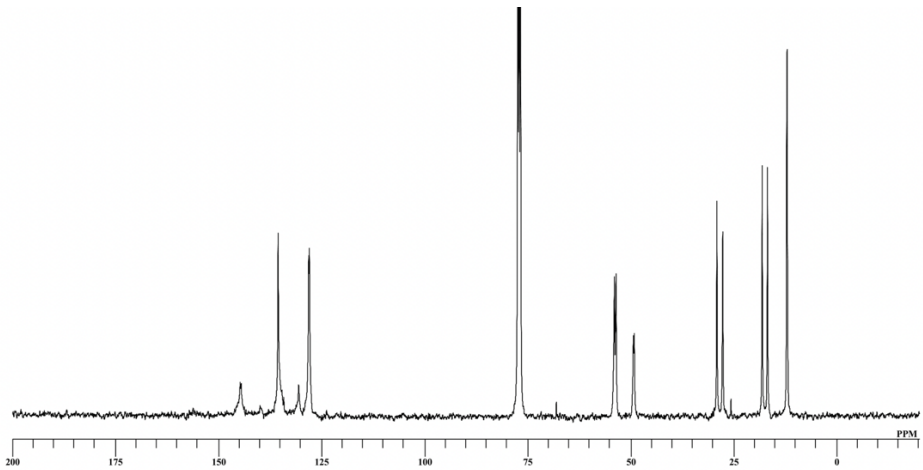

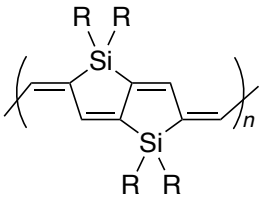

R = $(CH_2)_2(CF_2)_3CF_3$

Equation 3. Purple-red solid. 98% yield (140 mg). 12 mol% Rh of $[RhCl(tfb)]_2$ and 120 mol% of triethylamine were used at 60 ºC. Molecular weights were not determined due to the poor solubility in THF. T_d = 238 ºC (5% weight loss).

^{1}H NMR (498 MHz in $CDCl_3$)

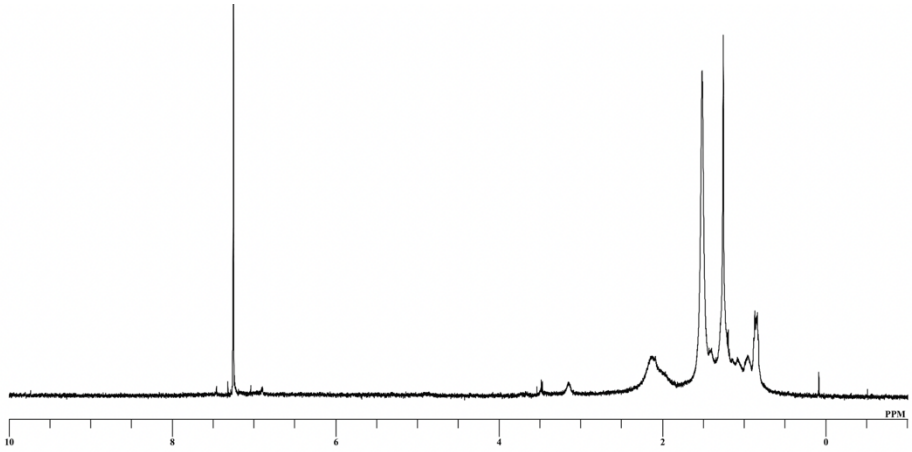

^{13}C NMR (101 MHz in $CDCl_3/C_6F_6$)

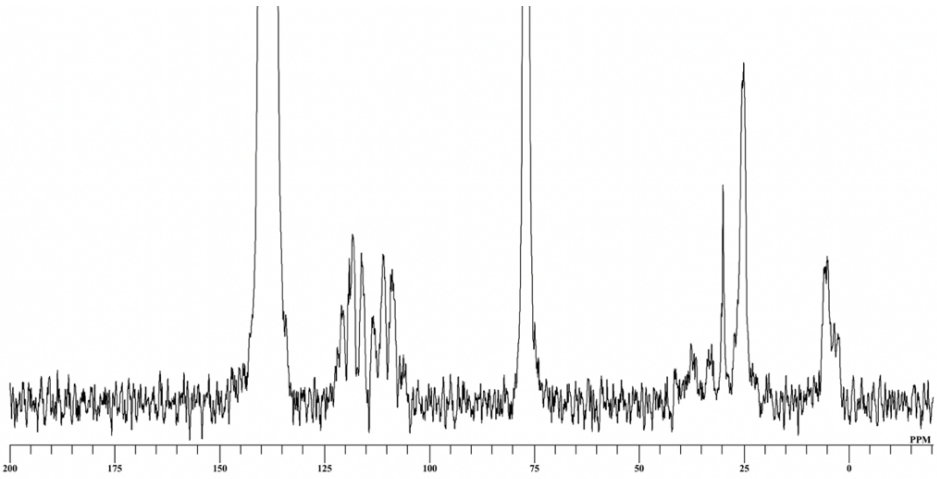

Procedure for Table 6 (Entries 3 and 4)

(1,2,2-Triphenylvinyl)lithium (112 μL, 11.2 μmol; 0.10 M solution in toluene) and

THF (0.3 mL) were added to a solution of $[RhCl(tfb)]_2$ (2.7 mg, 7.5 μmol Rh) in THF (0.2 mL). This was stirred for 5 min at –10 ºC and monomer **1a** or **1a-*d*** (0.250 mmol) was added with the aid of THF (0.5 mL). The mixture was stirred for 22 h at –10 ºC and warmed to room temperature. This was added dropwise to stirring MeOH (50 mL) with the aid of CH_2Cl_2 (5.0 mL), and the precipitates that formed were collected by filtration and the solid thus obtained was dried under vacuum to afford **poly-1a** or **poly-1a-*d***.

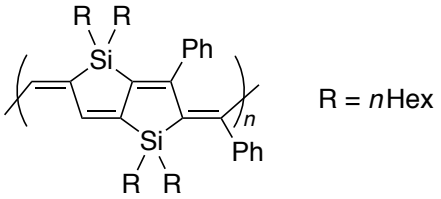

Entry 3. Purple solid. 82% yield (66.8 mg).

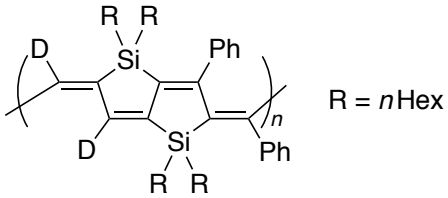

Entry 4. Purple solid. 90% yield (73.8 mg).

Procedure for Equation 4

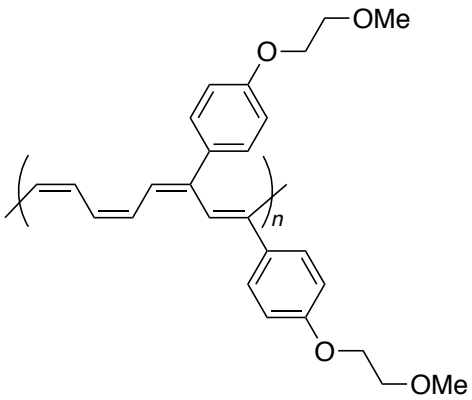

A solution of tetrabutylammonium fluoride (394 mg, 1.25 mmol; trihydrate) in THF (10 mL) was added to a solution of **poly-1b** (143 mg) in THF (10 mL), and the mixture

was stirred for 22 h at 60 ºC. After cooled to room temperature, this was washed with H_2O and extracted with toluene. The organic layer was concentrated and this was added dropwise to stirring MeOH (50 mL) with the aid of CH_2Cl_2 (5 mL), and the precipitates that formed were collected by filtration. The resulting solid was dissolved in CH_2Cl_2 (5 mL) and this was added dropwise to stirring hexane (50 mL) with the aid of CH_2Cl_2 (5 mL). The precipitates that formed were collected by filtration and the solid thus obtained was dried under vacuum to afford **poly-6b** as a red solid (85.3 mg; 84% yield). The desilylation efficiency (95%) was estimated by the ^{1}H NMR spectrum. T_d = 327 ºC (5% weight loss).

^{1}H NMR (400 MHz in $CDCl_3$)

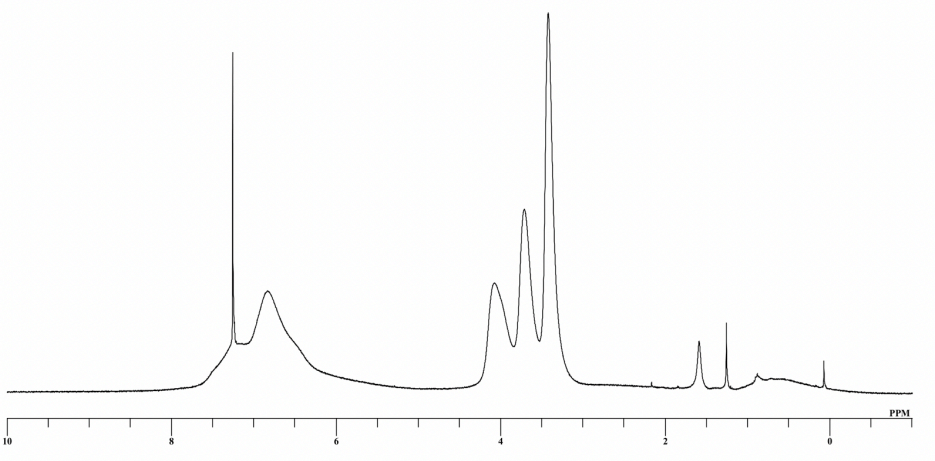

^{13}C NMR (101 MHz in $CDCl_3$)

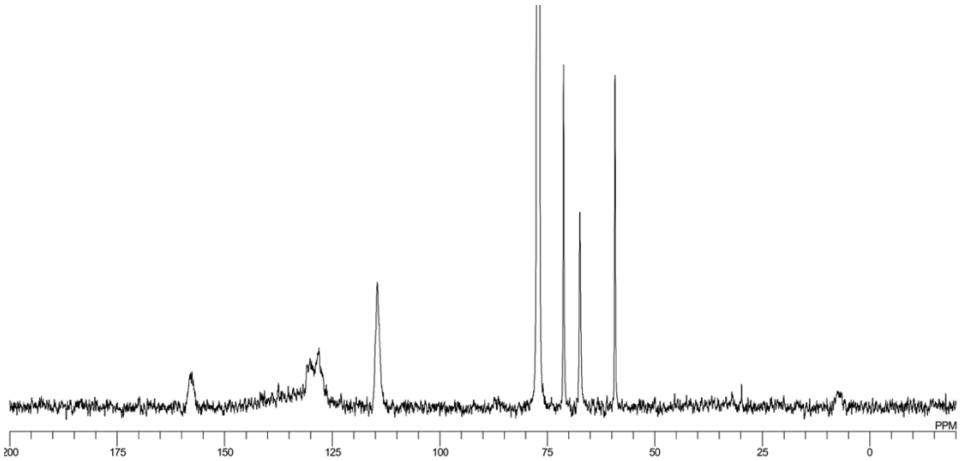

Procedure for Equation 5

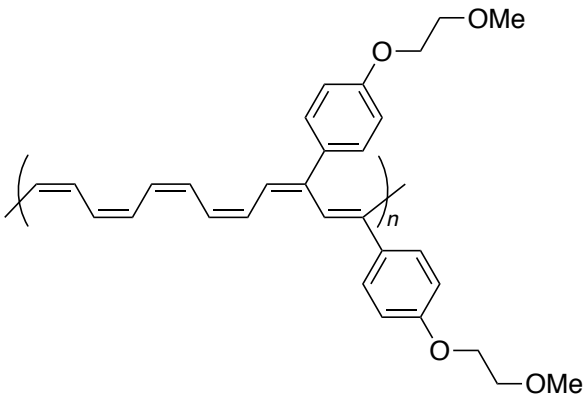

A solution of tetrabutylammonium fluoride (789 mg, 1.25 mmol; trihydrate) in THF (10 mL) was added to a solution of **poly-4b** (262 mg) in THF (10 mL), and the mixture was stirred for 22 h at 60 ºC. After cooled to room temperature, this was washed with H_2O and extracted with toluene. The organic layer was concentrated and this was added dropwise to stirring MeOH (50 mL) with the aid of CH_2Cl_2 (5 mL), and the precipitates that formed were collected by filtration. The resulting solid was dissolved in CH_2Cl_2 (5 mL) and this was added dropwise to stirring hexane (50 mL) with the aid of CH_2Cl_2 (5 mL). The precipitates that formed were collected by filtration and the solid thus obtained was dried under vacuum to afford **poly-7b** as a dark red solid (109 mg; 95% yield). The desilylation efficiency (94%) was estimated by the ^{1}H NMR spectrum. T_d = 275 ºC (5% weight loss).

^{1}H NMR (498 MHz in $CDCl_3$)

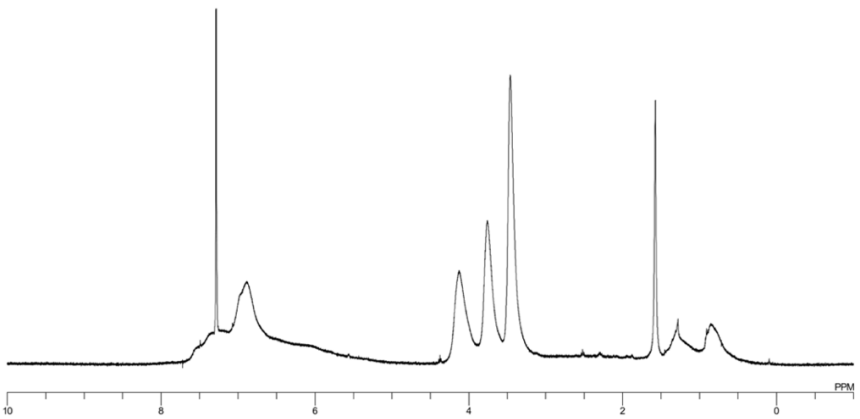

^{13}C NMR (101 MHz in $CDCl_3$)

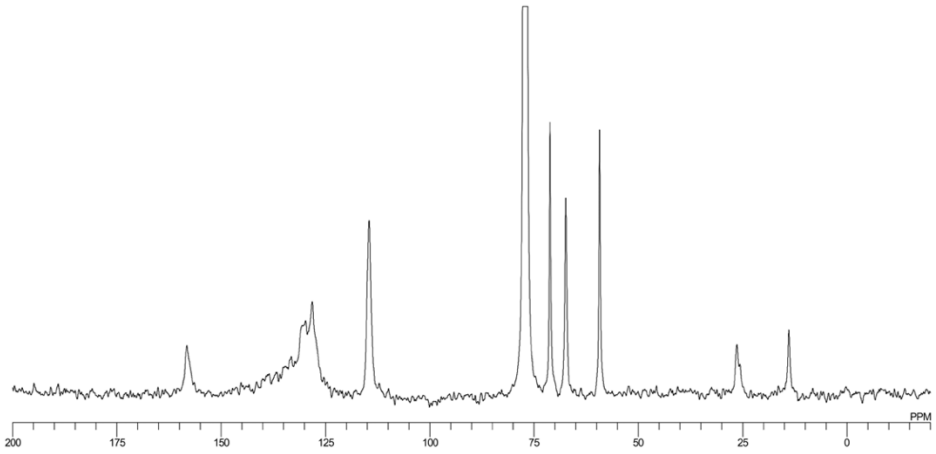

Procedure for Polyphenylacetylene.

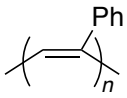

Phenylacetylene (102 mg, 1.00 mmol) and THF (2.0 mL) were added to a solution of $[Rh(OH)(cod)]_2$ (3.4 mg, 15 μmol Rh) in THF (2.0 mL), and the mixture was stirred for 22 h at 60 ºC. This was added dropwise to stirring MeOH (50 mL) with the aid of CH_2Cl_2 (5.0 mL), and the precipitates that formed were collected by filtration and the solid thus obtained was dried under vacuum to afford polyphenylacetylene as a yellow solid (81.4 mg; 80% yield, M_n = 24000, M_w/M_n = 1.8). T_d = 258 ºC (5% weight loss).

^1H NMR (400 MHz in $CDCl_3$)

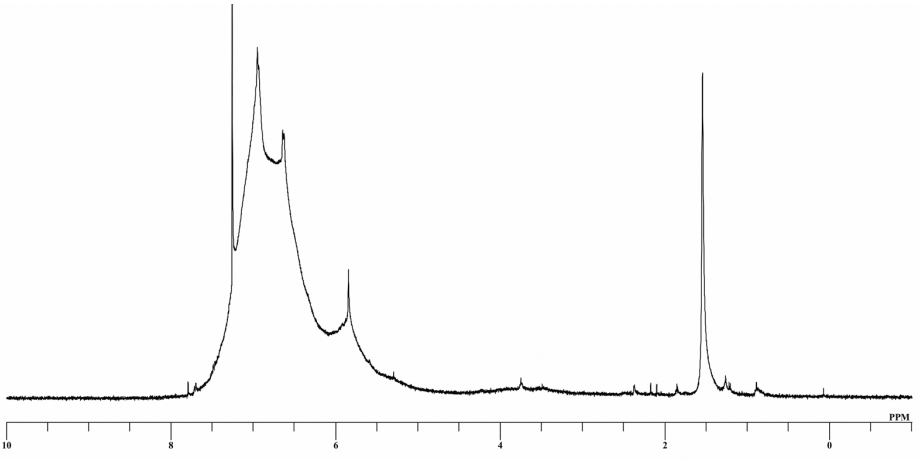

^{13}C NMR (101 MHz in $CDCl_3$)

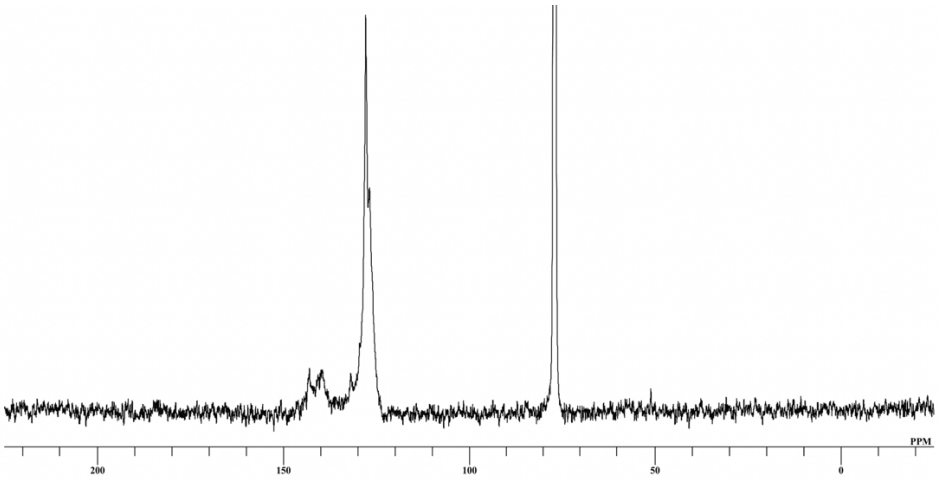

Procedure for Poly(4-(2-methoxyethoxy)phenyl)acetylene.

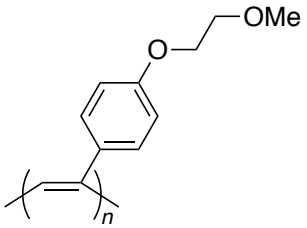

4-(2-Methoxyethoxy)phenylacetylene (88.0 mg, 0.500 mmol) and THF (1.0 mL) were added to a solution of $[Rh(OH)(cod)]_2$ (3.4 mg, 15 mmol Rh) in THF (1.0 mL), and the mixture was stirred for 2 days at room temperature. This was added dropwise to stirring MeOH (50 mL) with the aid of CH_2Cl_2 (5.0 mL), and the precipitates that formed were collected by filtration and the solid thus obtained was dried under vacuum to afford poly(4-(2-methoxyethoxy)phenyl)acetylene as a yellow solid (73.5 mg; 84% yield, M_n = 44000, M_w/M_n = 2.0). T_d = 307 ºC (5% weight loss).

^{1}H NMR (400 MHz in $CDCl_3$)

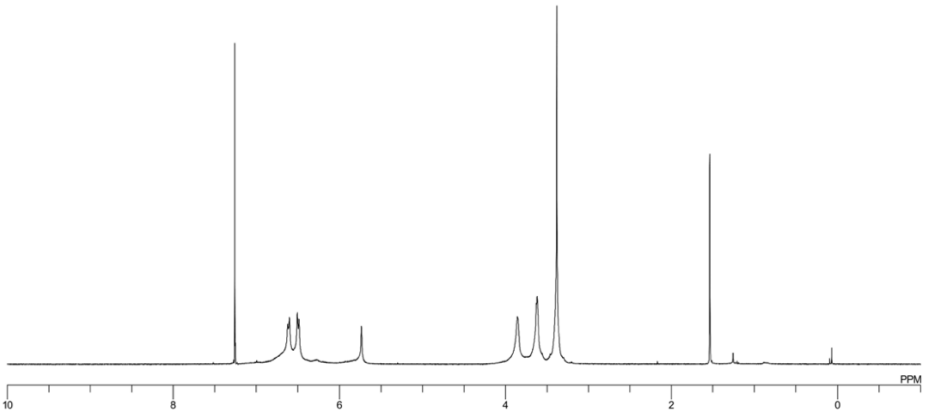

^{13}C NMR (101 MHz in $CDCl_3$)

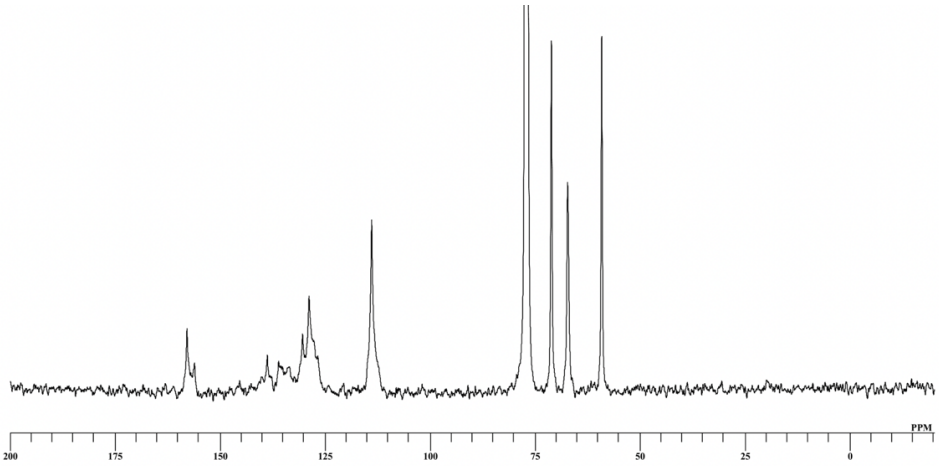

Procedure for Poly-1i.

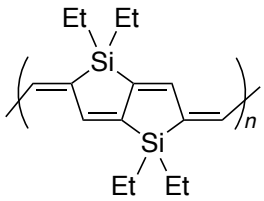

(1,2,2-Triphenylvinyl)lithium (600 μL, 60.0 μmol; 0.10 M solution in toluene) and THF (0.3 mL) were added to a solution of $[RhCl(tfb)]_2$ (10.9 mg, 30.0 μmol Rh) in THF (0.2 mL). This was stirred for 5 min at room temperature and monomer **1i** (34.0 mg, 0.250 mmol) was added with the aid of THF (0.5 mL). The mixture was stirred for 22 h at room temperature, and this was added dropwise to stirring MeOH (50 mL) with the aid of

CH_2Cl_2 (5.0 mL). The precipitates that formed were collected by filtration and the solid thus obtained was dried under vacuum to afford **poly-1i** as a purple solid (32.0 mg; 94% yield, M_n = 3300, M_w/M_n = 2.5). T_d = 188 ºC (5% weight loss).

^{1}H NMR (400 MHz in $CDCl_3$)

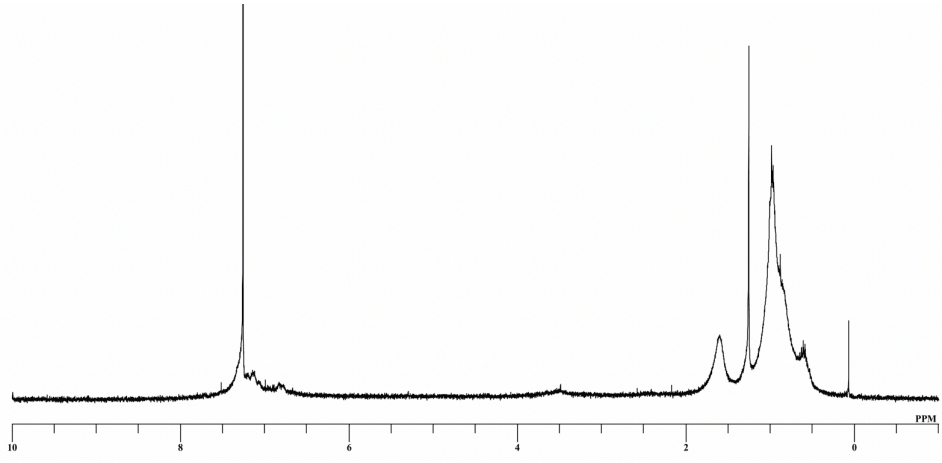

^{13}C NMR (101 MHz in $CDCl_3$)

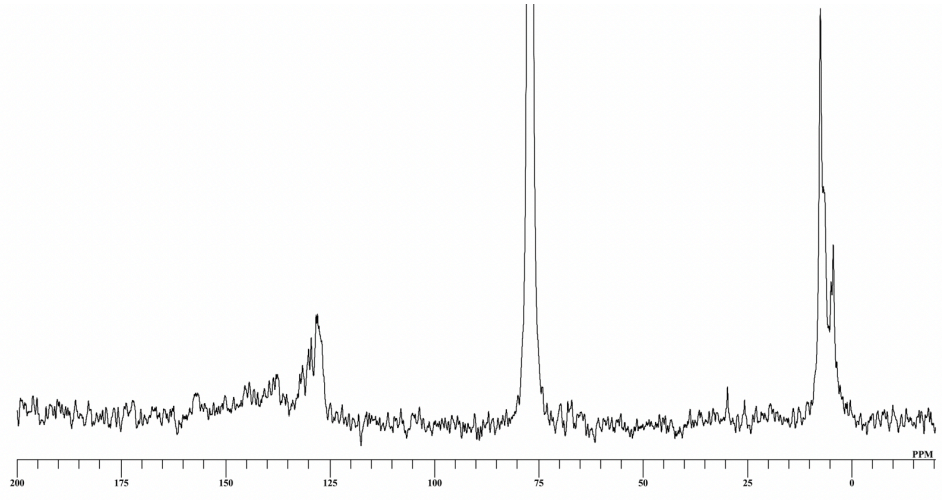

Procedure for Poly-6j.

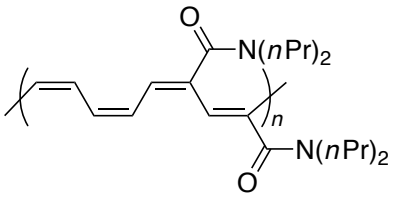

Triethylamine (41.8 μL, 300 μmol) and THF (1.2 mL) were added to a solution of $[RhCl(tfb)]_2$ (10.9 mg, 30.0 μmol Rh) in THF (0.8 mL). This was stirred for 5 min at 20 ºC and monomer **1j** (376 mg, 1.00 mmol) was added with the aid of THF (2.0 mL). The mixture was stirred for 22 h at 20 ºC and this was added dropwise to stirring MeOH (50 mL) with the aid of CH_2Cl_2 (5.0 mL). The precipitates that formed were collected by filtration and the solid thus obtained was dried under vacuum to afford **poly-1j** as a purple solid (291 mg; 78% yield, M_n = 33000, M_w/M_n = 1.9).

A solution of tetrabutylammonium fluoride (197 mg, 0.625 mmol; trihydrate) in THF (5 mL) was added to a solution of **poly-1j** (93.9 mg) in THF (5 mL), and the mixture was stirred for 22 h at 60 ºC. After cooled to room temperature, this was washed with H_2O and extracted with toluene. The organic layer was concentrated and this was added dropwise to stirring hexane (50 mL) with the aid of CH_2Cl_2 (5 mL). The precipitates that formed were collected on Celite with hexane, and this was dissolved in CH_2Cl_2 and concentrated under vacuum to afford **poly-6j** as a dark red solid (40.1 mg; 83% yield, M_n = 6000, M_w/M_n = 2.4). T_d = 201 ºC (5% weight loss).

^{1}H NMR (400 MHz in $CDCl_3$)

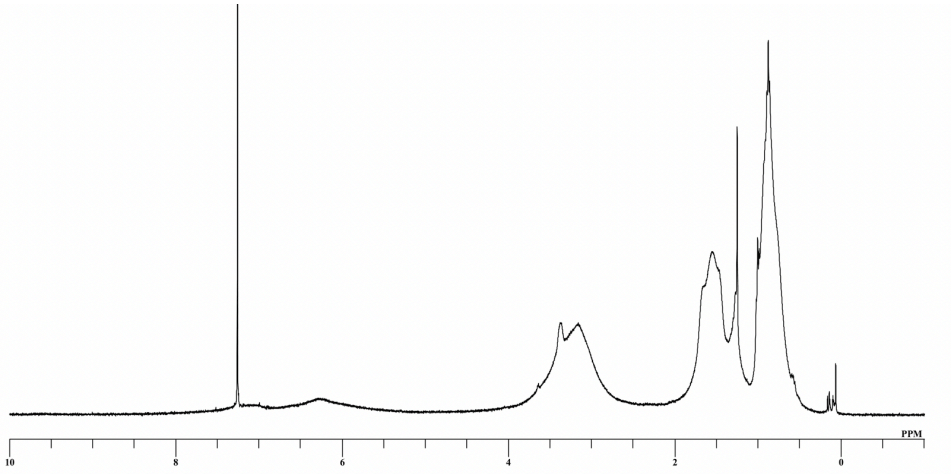

^{13}C NMR (101 MHz in $CDCl_3$)

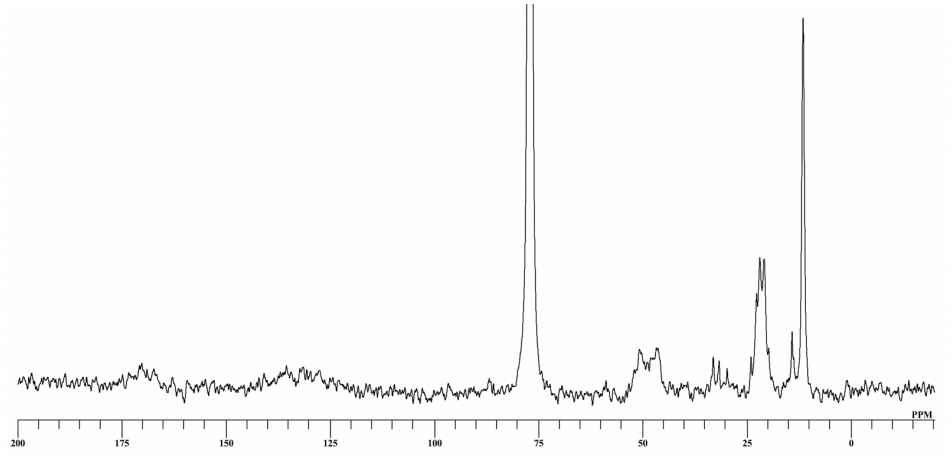

3.6 References

[1] For reviews: (a) Tan, N. S. L.; Lowe, A. B. *Angw. Chem., Int. Ed.* **2020**, *59*, 5008–5021. (b) Shiotsuki, M.; Sanda, F.; Masuda, T. *Polym. Chem.* **2011**, *2*, 1044–1058. (c) Liu, J.; Lam, J. W. Y.; Tang, B. Z. *Chem. Rev.* **2009**, *109*, 5799–5867. (d) Masuda, T. *J. Polym. Sci. Part A: Polym. Chem.* **2007**, *45*, 165–180. (e) Aoki, T.; Kaneko, T.; Teraguchi, M. *Polymer* **2006**, *47*, 4867–4892. (f) Mayershofer, M. G.; Nuyken, O.. *J. Polym. Sci. Part A: Polym. Chem.* **2005**, *43*, 5723–5747.

[2] (a) Yang, W.; Tabata, M.; Kobayashi, S.; Yokota, K.; Shimizu, A. *Polym. J.* **1991**, *23*, 1135–1138. (b) Kishimoto, Y.; Eckerle, P.; Miyatake, T.; Ikariya, T.; Noyori, R. *J. Am. Chem. Soc.* **1994**, *116*, 12131–12132. (c) Kishimoto, Y.; Itou, M.; Miyatake, T.; Ikariya, T.; Noyori, R. *Macromolecules* **1995**, *28*, 6662–6666. (d) Kishimoto, Y.; Miyatake, T.; Ikariya, T.; Noyori, R. (e) Katayama, H.; Yamamura, K.; Miyaki, Y.; Ozawa, F. Stereoregular. *Organometallics* **1997**, *16*, 4497–4500. (f) Misumi, Y.; Masuda, T.. *Macromolecules* **1998**, *31*, 7572–7573. (g) Misumi, Y.; Kanki, K.; Miyake, M.; Masuda, T. *Macromol. Chem. Phys.* **2000**, *201*, 2239–2244. (h) Saeed, I.; Shiotsuki, M.; Masuda, T. *Macromolecules* **2006**, *39*, 8567–8573. (i) Saeed, I.; Shiotsuki, M.; Masuda, T. *Macromolecules* **2006**, *39*, 8977–8981. (j) Onishi, N.; Shiotsuki, M.; Sanda, F.; Masuda, T. *Macromolecules* **2009**, *42*, 4071–4076. (k) Jiménez, M. V.; Pérez-Torrente, J. J.; Bartolomé, M. I.; Vispe, E.; Lahoz, F. J.; Oro, L. A. *Macromolecules* **2009**, *42*, 8146–8156. (l) Agony, M.; Jiménez, M. V.; García-Orduña, P.; Oro, L. A.; Vispe, E.; Pérez-Torrente, J. J.. *Organometallics* **2019**, *38*, 1991–2006. (m) Tan, N. S. L.; Nealon, G. L.; Moggach, S. A.; Lynam, J. M.; Ogden, M. I.; Massi, M.; Lowe, A. B. *Macromolecules* **2021**, *54*, 6191–6203.

[3] Kishimoto, Y.; Eckerle, P.; Miyatake, T.; Kainosho, M.; Ono, A.; Ikariya, T.; Noyori, R. *J. Am. Chem. Soc.* **1999**, *121*, 12035–12044. (b) Ke, Z.; Abe, S.; Ueno, T.;

Morokuma, K. *J. Am. Chem. Soc.* **2011**, *133*, 7926–7941. (c) Angoy, M.; Jiménez, M. V.; Modrego, F. J.; Oro, L. A.; Passarelli, V.; Pérez-Torrente, J. J. *Organometallics* **2018**, *37*, 2778–2794.

[4] (a) Yashima, E.; Maeda, Y.; Okamoto, Y. *J. Am. Chem. Soc.* **1998**, *120*, 8895–8896. (b) Goto, H.; Zhang, H. Q.; Yashima, E. *J. Am. Chem. Soc.* **2003**, *125*, 2516–2523. (c) Aoki, T.; Kaneko, T.; Maruyama, N.; Sumi, A.; Takahashi, M.; Sato, T.; Teraguchi, M. *J. Am. Chem. Soc.* **2003**, *125*, 6346–6347. (d) Sanda, F.; Araki, H.; Masuda, T. *Macromolecules* **2004**, *37*, 8510–8516. (e) Fukushima, T.; Takachi, K.; Tsuchihara, K. *Macromolecules* **2006**, *39*, 3103–3105. (f) Cheuk, K. K. L.; Lam, J. W. Y.; Li, B. S.; Xie, Y.; Tang, B. Z. *Macromolecules* **2007**, *40*, 2633–2642. (g) Liu, L.; Zang, Y.; Hadano, S.; Aoki, T.; Teraguchi, M.; Kaneko, T.; Namikoshi, T. *Macromolecules* **2010**, *43*, 9268–9276. (h) Luo, X.; Deng, J.; Yang, W. *Angew. Chem., Int. Ed.* **2011**, *50*, 4909–4912. (i) Rodríguez, R.; Quiñoá, E.; Riguera, R.; Freire, F. *J. Am. Chem. Soc.* **2016**, *138*, 9620–9628.

[5] (a) Qu, J.; Suzuki, Y.; Shiotsuki, M.; Sanda, F.; Masuda, T. *Polymer* **2007**, *48*, 4628–4636. (b) Sugano, S.; Kouzai, H. *Bull. Chem. Soc. Jpn.* **2016**, *89*, 27–32.

[6] (a) Goto, H.; Nimori, S.; Akagi, K. *Synth. Met.* **2005**, *155*, 576–587. (b) Mizuta, K.; Hiraga, N.; Koga, T.; Yamabuki, K.; Onimura, K.; Oishi, T. *Polym. J.* **2011**, *43*, 141–146. (c) Hu, T.; Kong, H.; Chen, L.; Chen, Y.; Li, F.; Zha, D.. *J. Therm. Anal. Calorim.* **2011**, *105*, 995–1006.

[7] For a review: (a) Aoki, T.; Kaneko, T. *Polym. J.* **2005**, *37*, 717–735. For selected examples: (b) Kaneko, T.; Yamamoto, K.; Asano, M.; Teraguchi, M.; Aoki, T. *J. Membrane Sci.* **2006**, *278*, 365–372. (c) Kaneko, T.; Sato, K.; Uchiya, Y.; Teraguchi, M.; Aoki, T. *Int. J. Polym. Sci.* **2012**, 974204. (d) Wang, J.; Li, J.; Aoki, T.; Kaneko, T.; Teraguchi, M.; Shi, Z.; Jia, H. *Macromolecules* **2017**, *50*, 7121–7136. (e) Zang,

Y.; Aoki, T.; Kaneko, T.; Teraguchi, M.; Ma, L.; Jia, H.; Miao, F. *Polymer* **2018**, *156*, 66–70.

[8] (a) Cataldo, F. *Polym. Int.* **1993**, *30*, 375–379. (b) Kakuchi, T.; Kamimura, H.; Matsunami, S.; Yokota, K.; Tsuda, K. *Macromolecules* **1995**, *28*, 658–660. (c) Ichikawa, Y.; Nishimura, T.; Hayashi, T. *Organometallics* **2011**, *30*, 2342–2348.

[9] For reviews: (a) Ohshita, J. Conjugated *Macromol. Chem. Phys.* **2009**, *210*, 1360–1370. (b) Wong, W. W. H.; Hooper, J. F.; Holmes, A. B. *Aust. J. Chem.* **2009**, *62*, 393–401. (c) Chen, J.; Cao, Y. *Macromol. Rapid Commun.* **2007**, *28*, 1714–1742. See also: (d) McDearmon, B.; Page, Z. A.; Chabinyc, M. L.; Hawker, C. J. *J. Mater. Chem. C* **2018**, *6*, 3564–3572. (e) Wu, J.-S.; Cheng, S.-W.; Cheng, Y.-J.; Hsu, C.-S. *Chem. Soc. Rev.* **2015**, *44*, 1113–1154. (f) McCulloch, I.; Ashraf, R. S.; Biniek, L.; Bronstein, H.; Combe, C.; Donaghey, J. E.; James, D. I.; Nielsen, C. B.; Schroeder, B. C.; Zhang, W. *Acc. Chem. Res.* **2012**, *45*, 714–722. (g) Facchetti, A. *Chem. Mater.* **2011**, *23*, 733–758.

[10] Ikeda, S.; Shintani, R. *Angew. Chem., Int. Ed.* **2019**, *58*, 5734–5738.

[11] For a rhodium-catalyzed step-growth polymerization of 1,2-diethynyldisilanes: (a) Ohshita, J.; Furumori, K.; Ishikawa, M.; Yamanaka, T. *Organometallics* **1989**, *8*, 2084–2085. (b) Ishikawa, M. *Pure. Appl. Chem.* **1991**, *63*, 851–854.

[12] Polymerization of silylacetylenes were reported under molybdenum, tungsten, niobium, or tantalum catalysis: (a) Voronkov, M. G.; Pukhnarevich, V. B.; Sushchinskaya, S. P.; Annenkova, V. Z.; Annenkova, V. M.; Andreeva, N. J. *J. Polym. Sci.: Polym. Chem. Ed.* **1980**, *18*, 53–57. (b) Gal, Y.-S.; Choi, S.-K. *J. Polym. Sci. Part A: Polym. Chem.* **1987**, *25*, 2323–2326.

[13] No polymerization proceeded even at 60 °C for these monomers.

[14] (a) Shintani, R.; Iino, R.; Nozaki, K. *J. Am. Chem. Soc.* **2016**, *138*, 3635–3638. (b) Shintani, R.; Misawa, N.; Tsuda, T.; Iino, R.; Fujii, M.; Yamashita, K.; Nozaki, K. *J. Am. Chem. Soc.* **2017**, *139*, 3861–3867.

[15] Chain transfer could also take place during the stitching reaction, which would lead to an incompletely stitched unit.

[16] Electropositive nature of the silicon substituent could destabilize the α-silyl-substituted alkenylrhodium species and it may undergo decomposition before the subsequent intermolecular alkyne insertion.

[17] (a) Yashima, E.; Maeda, Y.; Okamoto, Y. A. *Chem. Lett.* **1996**, 955–956. (b) Maeda, K.; Takeyama, Y.; Sakajiri, K.; Yashima, E. *J. Am. Chem. Soc.* **2004**, *126*, 16284–16285. (c) Yuan, W. Z.; Zhao, H.; Shen, X. Y.; Mahtab, F.; Lam, J. W. Y.; Sun, J. S.; Tang, B. Z. *Macromolecules* **2009**, *42*, 9400–9411.

[18] For reviews on fluorous chemistry: (a) Vincent, J.-M. *Chem. Commun.* **2012**, *48*, 11382–11391. (b) Cametti, M.; Crousse, B.; Metrangolo, P.; Milani, R.; Resnati, G. *Chem. Soc. Rev.* **2012**, *41*, 31–42. (c) Berger, R.; Resnati, G.; Metrangolo, P.; Weber, E.; Hulliger, J. *Chem. Soc. Rev.* **2011**, *40*, 3496–3508.

[19] For recent reviews on semiconducting polymers: (a) Guo, X.; Facchetti, A. *Nat. Mater.* **2020**, *19*, 922–928. (b) Chen, J.; Yang, K.; Zhou, X.; Guo, X. *Chem. Asian J.* **2018**, *13*, 2587–2600. (c) Lee, E. K.; Lee, M. Y.; Park, C. H.; Lee, H. R.; Oh, J. H. *Adv. Mater.* **2017**, *29*, 1703638. For examples of semiconducting substituted polyacetylenes: (d) Furlani, A.; Napoletano, C.; Paolesse, R.; Russo, M. V. *Synth. Met.* **1987**, *21*, 337–342. (e) Leclerc, M.; Prud'homme, R. E. *Macromolecules* **1987**, *20*, 2153–2159. (f) Zhou, S.; Hong, H.; He, Y.; Yang, D.; Jin, X.; Qian, R.; Masuda, T.; Higashimura, T. *Polymer* **1992**, *33*, 2189–2193. (g) Gruber, A. S.; Boiteux, G.; de Souza, R. F.; de Souza, M. O. *Polym. Bull.* **2002**, *47*, 529–537. (h) Krebs, F. C.;

Jørgensen, M. *Polym. Bull.* **2003**, *50*, 359–366. (h) Gal, Y. S.; Lim, K. T.; Shim, S. Y.; Kim, S. H.; Koh, K.; Jang, S. H.; Jin, S. H. *Synth. Met.* **2005**, *154*, 169–172. (i) Mori, A.; Kubota, C.; Fujita, K.; Hayashi, M.; Ogura, T.; Suzuki, T.; Okano, K.; Funahashi, M.; Horie, M. *Macromolecules* **2020**, *53*, 1171–1179.

[20] Wang, F.; Lan, M.; To, W.-P.; Li, K.; Lok, C.-N.; Wamg, P.; Che, C.-M. *Chem. Commun***. 2016**, *52*, 13273–13276.

[21] Veliks, J.; Tseng, J.-C.; Arias, K.; Weisshar, F.; Linden, A.; Siegel, J. S. *Chem. Sci.* **2014**, *5*, 4317–4327.

[22] Lu, Y.; Suzuki, T.; Zhang, W.; Moore, J. S.; Marinas, B. J. *Chem. Mater.* **2007**, *19*, 3194–3204.

[23] Kazakova, A. K.; Konev, A. S. Zorin, I. M.; Poshekhonov, I. S.; Korzhikov-Vlakh, V. A.; Khlebnikov. A. F. *Org. Biomol. Chem.* **2019**, *17*, 9864–9873.

[24] Saeed, I.; Shiotsuki, M.; Masuda, T. *Macromolecules* **2006**, *39*, 8567–8573.

[25] Uson, R.; Oro, L.A.; Cabeza, J. A. *Inorg. Synth*. **1985**, *23*, 126–130.

[26] Schrock, R. R.; Osborn, J. A. *Inorg. Chem.* **1970**, *9*, 2339–2343.

[27] Giordano, G.; Crabtree, R. H. *Inorg. Synth.* **1979**, *19*, 218–220..

[28] Shintani, R.; Misawa, N.; Tsuda, T.; Iino, R.; Fujii, M.; Yamashita, K.; Nozaki, K. *J. Am. Chem. Soc*. **2017**, *139*, 3861–3867.

[29] Coulson, D. R.; Satek, L. C.; Grim, S. O. *Inorg. Synth.* **1972**, *13*, 121–124.

List of Publications

Publications

1. “Rhodium-Catalyzed Stitching Polymerization of 1,5-Hexadiynes and Related Oligoalkynes”

   Sho Ikeda, Ryo Shintani.

   Angew. Chem., Int. Ed. **2019**, *58*, 5734–5738.

2. “Rhodium-Catalyzed Stitching Polymerization of Alkynylsilylacetylenes”

   Sho Ikeda, Yuki Hanamura, Hirokazu Tada, Ryo Shintani.

   J. Am. Chem. Soc. **2021**, *143*, 19559–19566.

Acknowledgement

The studies presented in this thesis are the summaries of the author's work carried out during 2017–2022 at Graduate School of Engineering Science, Osaka University.

The author would first like to express his deepest appreciation to Professor Dr. Ryo Shintani for his invaluable guidance and continuous encouragement throughout this work. He owes his deepest appreciation to Associate Professor Dr. Akihiro Shimizu for his helpful suggestions and insightful comments.

The author would next like to appreciate Professor Dr. Kazushi Mashima and Professor Dr. Ichiro Hisaki for their fruitful advice for this dissertation.

The author wishes to thank Professor Dr. Hirokazu Tada for collaboration work on measurements of conductivities, Professor Dr. Shigeru Yamago and Assistant Professor Dr. Yangtian Lu for MALS analysis, Mr. Hitoshi Haneoka for NMR analysis and Ms. Rika Miyake for HRMS analysis.

The author also appreciates the entire Shintani group. He would like to thank Ms. Shoko Ueno and Ms. Yuko Inaba for their kind assistance throughout his stay in Shintani group. He gives special thanks to all the past and current members in Shintani group for sharing a tough and enjoyable laboratory life.

The author acknowledges financial support from the Japan Society for the Promotion of Science (JSPS) Research Fellowship for Young Scientists (DC2) from April, 2020 unitl March, 2022.

Finally, his deepest thanks go to his parents for their warm and continuous supports and encouragement throughout my life.

March, 2022

Sho Ikeda